DEPARTAMENTO DE CIÊNCIAS DA VIDA

FACULDADE DE CIÊNCIAS E TECNOLOGIA
UNIVERSIDADE DE COIMBRA

The role of GRIM-19 and interacting proteins in human tumours

Dissertação apresentada à Universidade de Coimbra para cumprimento dos requisitos necessários à obtenção do grau de Mestre em Biologia Celular e Molecular, realizada sob a orientação científica do Professor Doutor Valdemar Máximo (Faculdade de Medicina da Universidade do Porto e IPATIMUP) e orientação académica do

Marcelo José Marques Correia

2011

ACKNOWLEDGEMENTS

During the last few months while I performed my laboratory work for this Master thesis, I had some good and bad moments. Fortunately, everything happened for the best, with the support of several people, inside or outside the laboratory, and to whom I would like to express my gratitude.

Firstly I would like to thank Dr. Valdemar Máximo, my "professor" and supervisor who accepted me in his group and gave me all the support and help that I needed. Above all, he is the person who gave me the opportunity to perform the laboratory work needed for the conclusion of this project.

I would also like to thank Dr. Paula Soares, who is the Cancer Biology group leader. "Paulinha" is a wonderful person who takes care of the daily activities and well-functioning of the group, creating a fantastic group atmosphere.

To Professor Manuel Sobrinho-Simões, I thank for the opportunity to perform my experiments in IPATIMUP, a great institute that is continuously forming new brilliant and more than capable scientists to the new challenges that will found in their future.

I would like to thank to the people who helped me directly in the laboratory work. Adriana, I thank you for your help with the samples and all of the work that you had with me. André Silva and Joana Torres, thank you for teaching and sharing your laboratory skills with me. And all the members of Cancer Biology group for their help in all kind of stuff. Besides all the help with the work, they were all great friends.

Although not belonging to the group, I also want to thank Dr. Paula Silva for her fantastic help with some technical problems and to Dr. Carla Oliveira and Patrícia Oliveira for their help with the bioinformatics procedures.

To my parents, my sister and my girlfriend I thank for all the patience through all these years with me and all the support they have given me.

ABSTRACT

Background: Oxyphylic or oncocytic tumours are composed exclusively or predominantly by oxyphylic or oncocytic cells, characterized by their consistent excessive mitochondrial number, structurally and functionally abnormal. Hürthle cell tumours (HCT) are a particular group of tumours of the thyroid gland with these features. The genetic alterations underlying the etiopathogenesis of oncocytic tumours remains to be clarified, although recent data suggest that mitochondrial DNA (mtDNA) complex I disruptive mutations may be involved. *GRIM-19* (*Gene associated with Retinoid Interferon-induced Mortality - 19*) is a novel tumour suppressor gene that is involved in interferon-β (IFN- β) and retinoic acid(RA)-induced cell death pathway and is also a subunit of mitochondrial respiratory chain (MRC) complex I. STAT3 (Signal Transducer and Activator of Transcription 3) is involved in embryonic development, cell growth and anti-apoptosis and is one of the GRIM-19 interacting proteins, participating in IFN/RA-induced cell death mediated by GRIM-19 and being inhibited by it. In 2005, Máximo *et al.* [1] reported *GRIM-19* mutations in HCT and proposed that *GRIM-19* might have an important role in HCT tumourigenesis and possibly in oncocytic tumours of other organs, such as renal cell oncocytoma. Recently, it has been reported that GRIM-19 expression was low or even absent in renal cell carcinomas, revealing its importance in kidney tumourigenesis.

Objectives: In the present study, we intended to assess GRIM-19 expression and cellular location, by immunohistochemistry analysis, in a series of thyroid tumours with and without Hürthle cells, and also in a series of kidney tumours (attempting to the oncocytic histotype) to clarify the role of GRIM-19 in tumourigenesis and in oncocytic phenotype development. We also aimed to correlate GRIM-19 and STAT3 expression,

cellular location and activation in order to clarify if STAT3 in tumourigenesis is under GRIM-19 regulation.

Results: We observed that GRIM-19 is downregulated in Hürthle cell tumours, but not in non-Hürthle cell tumours, independently of the histotype and of the benign or malignant nature of the tumours. In kidney, GRIM-19 is downregulated, in general, in all tumour histotypes (oncocytomas and non-oncocytomas). Furthermore, we did not observe any correlation between GRIM-19 expression and STAT3 activation.

Conclusions: We can conclude that in thyroid tumours GRIM-19 is specifically downregulated in HCT, corroborating the idea that MRC complex I impairment is a feature of oncocytic tumours of the thyroid. However, in kidney tumours, it seems that GRIM-19 is not related with oncocytic phenotype, as in thyroid, but with tumourigenesis in general. GRIM-19 expression and STAT3 activation are not correlated as we expected, suggesting that, in tumourigenesis, STAT3 activation through phosphorylation is not regulated by GRIM-19.

Relevance: This study shows GRIM-19 as the first nuclear DNA complex I protein downregulated in HCT, supporting the assumption that mitochondrial complex I dysfunction is involved in the etiopathogenesis of oncocytic tumours, at least in thyroid. Moreover, our data also suggests that GRIM-19 may have a more comprehensive role in kidney tumourigenesis

KEY WORDS

GRIM-19; oncocytic tumours; thyroid tumours; renal cell tumours; STAT3.

RESUMO

Background: Os tumores oxifílicos ou oncocíticos são compostos exclusivamente ou predominantemente por células oxifílicas ou oncocíticas, caracterizadas pelo seu consistente e elevado número de mitocôndrias, estrutural e funcionalmente aberrantes. Os tumores de células Hürthle (TCH) são um grupo particular de tumores da glândula da tireóide que apresentam estas características. As alterações genéticas que estão na base da etiopatogénese dos tumores oncocíticos continuam ainda por esclarecer, embora dados recentes sugiram que mutações disruptivas em subunidades do complexo I mitocondrial codificadas pelo ADN mitocondrial (ADNmt) possam estar envolvidas. O gene *GRIM-19* (*Gene 19 associado com a mortalidade induzida por ácido retinóico e interferão*) é um supressor tumoral que está envolvido na cascata de morte celular induzida pelo interferão-β (IFN) e ácido retinóico (RA), sendo também uma subunidade do complexo I da cadeia respiratória mitocondrial (CRM). STAT3 (transdutor de sinal e activador da transcrição 3) está envolvido no desenvolvimento embrionário, no crescimento celular e em mecanismos anti-apoptóticos e é uma das proteínas que interagem com GRIM-19, participando na morte celular induzida por IFN/RA mediada pela proteína GRIM-19 e sendo também inibido por esta. Em 2005, Máximo e colaboradores [1] descreveram pela primeira vez mutações do gene *GRIM-19* nos TCH, propondo que o *GRIM-19* pode ter um papel importante na tumorigénese dos TCH e, possivelmente, em tumores oncocíticos de outros órgãos, como por exemplo em oncocitomas renais. Recentemente foi demonstrado que a expressão da proteína GRIM-19 está reduzida ou até mesmo ausente em carcinomas de células renais, revelando a sua importância na tumorigénese renal.

Objectivos: Com o presente estudo, pretendeu-se avaliar a expressão e localização celular da proteína GRIM-19, através de análise imunohistoquímica, numa série de tumores da tireóide com e sem células de Hürthle, e também numa série de tumores

renais (focando o histotipo oncocítico) para esclarecer o papel da GRIM-19 na tumorigénese e no desenvolvimento do fenótipo oxifílico. Também se pretende correlacionar a proteína GRIM-19 e a expressão, localização celular e activação de STAT3 a fim de esclarecer se STAT3 está sob regulação de GRIM-19.

Resultados: Observámos que a GRIM-19 tem uma expressão diminuída nos tumores de células de Hürthle, mas não em tumores não-Hürthle, independentemente do seu histotipo e da natureza benigna ou maligna dos tumores. No rim, a GRIM-19 tem a sua expressão reduzida em todos os histotipos tumorais (oncocitomas e não oncocitomas). Além disso, não observámos uma correlação entre a expressão da proteína GRIM-19 e a activação de STAT3.

Conclusões: Podemos concluir que nos tumores da tireóide, GRIM-19 está especificamente subexpresso nos TCH, corroborando a ideia de que danos no complexo I do CRM é uma característica dos tumores oncocíticos da tireóide. No entanto, nos tumores renais, parece que a GRIM-19 não está relacionada com o fenótipo oncocítico, como acontece na tireóide, mas com a tumorigénese em geral. A proteína GRIM-19 e a activação de STAT3 não estão correlacionados como esperado, sugerindo que, na tumorigénese, a activação através de regulação da fosforilação de STAT3 não é regulado pela GRIM-19.

Relevância: Este estudo mostra a GRIM-19 como a primeira subunidade do complexo I codificada pelo ADN nuclear subexpressa nos TCH, sustentando a hipótese de que a disfunção do complexo I da mitocôndria está envolvida na etiopatogénese dos tumores oncocíticos, pelo menos em tireóide. Além disso, os nossos dados também sugerem que a GRIM-19 pode ter um papel mais abrangente na tumourigénese renal.

PALAVRAS-CHAVE

GRIM-19; tumores oncocíticos; tumores da tireóide; Tumores de células renais; STAT3.

INDEX

ABBREVIATIONS

ATC – Anaplastic thyroid carcinoma

ATP – Adenosine triphosphate

Bcl-2 - B-cell lymphoma protein 2

BHD - Birt-Hogg-Dubé

CCRCC – Clear cell RCC

CDKN2a – Cyclin-dependent kinase inhibitor 2A

cDNA – Complementary DNA

COPD – Chronic obstructive pulmonary disease

CromRCC – Chromophobe RCC

DAB - 3,3' Diaminobenzidine

DNA – Deoxyribonucleic acid

EDTA - Ethylenediaminetetraacetic acid

EGFR – Epidermal growth factor receptor

ETC – Electron transport chain

FH – Fumarate hydrolase

FTA – Follicular thyroid adenoma

FTC – Follicular thyroid carcinoma

FVPTC – Follicular variant of papillary carcinoma

GRIM – Gene associated with Retinoid-Interferon-Induced Mortality

GRIM-19 – Gene associated with Retinoid-Interferon-Induced Mortality 19

HCMV – Human Cytomegalovirus

HE - Haematoxylin and Eosin Staining

HHV8 – Human herpesvirus 8

HLRCC – Hereditary leiomyomatosis and renal cell cancer

HPRC – Hereditary papillary renal carcinoma

HPV-16 – Human papillomavirus type 16

HCT – Hürthle cell tumours

HtrA2 – HtrA serine peptidase 2

IAP – Inhibitor of apoptosis protein

ICAM-1 – Intercellular adhesion molecule 1

IFN – Interferon

IHC – Immunohistochemistry

JAK-STAT – Janus tyrosine kinases – signal-transduction activators of transcription

KS – Kaposi's sarcoma

MMP-2 – Matrix metalloproteases 2

MRC – Mitochondrial respiratory chain

mRNA – Messenger RNA

mtDNA – mitochondrial DNA

nDNA – nuclear DNA

NF-kB - nuclear factor kappa beta

NOD2 – Nucleotide oligomerization domain 2

NSCLC – Non-small cell lung cancer

OLFM4 (GW112) – Olfactomedin 4

OXPHOS – Oxidative phosphorylation

PBS – Phosphate buffered saline

PCR – Polymerase Chain reaction

PRCC - Papillary RCC

PTC - Papillary thyroid carcinoma

PTEN – Phosphatase and tensin homolog

p-STAT3 – Phosphorylated STAT3

p-STAT3 ser727 – Phosphprylation in residue serine at position 727 of STAT3

p-STAT3 Tyr705 – Phosphprylation in residue tyrosine at position 705 of STAT3

qRT-PCR – Real Time Polymerase Chain Reaction

RA – Retinoic acid

RAR – Retinoic acid receptors

RCC – Renal cell carcinoma

RCT – Renal cell tumours

RNA – Ribonucleic acid

ROnc – Renal oncocytoma

ROS – Reactive oxygen species

RT-PCR – Reverse Transcriptase – Polymerase Chain Reaction

SDHA – Succinate dehydrogenase complex, subunit A

SDS-PAGE – Sodium dodecyl sulfate polyacrylamide gel electrophoresis

Ser727 – Serine residue at position 727

shRNA – Short hairpin RNA

STAT3 - Signal Transducer and Activator of Transcription 3

TAD – Transactivation domain

TCO - Thyroid tumours with cell oxyphilia gene

Tyr705 – Tyrosine residue at position 705

WB – Western blot

VEGF – Vascular endothelial growth factor

VHL - Von Hippel-Lindau

vIRF – Viral interferon regulatory factors

XIAP – X-linked inhibitor of apoptosis protein

Y2H – Yeast two-hybrid assay

LITERATURE REVIEW

GRIMs (Genes associated with Retinoid-Interferon-Induced Mortality)

Apoptosis is a type of programmed cell death essential during organism development and homeostasis, in balance with proliferation and differentiation of cells, being a crucial mechanism for elimination of damaged or undesirable cells. This mechanism has two main pathways, the extrinsic and the intrinsic, that in presence of various death stimuli, both involving caspase activation, leads to the cleavage of multiple intracellular substrates [2] - (see [3] for a review). The B-cell lymphoma protein 2 (Bcl-2), caspases and inhibitors of apoptosis proteins (IAPs) are proteins involved in these two pathways and form the "central death engine" [4]. Several exogenous factors control this machinery. One of them are cytokines, but the mechanism involved is poorly understood [4].

Interferons (IFNs) are a family of cytokines which are involved in regulation of antiviral, antitumour and immune response in vertebrates. [5, 6].

Retinoids are vitamin A derivates that can induce differentiation and inhibit proliferation [7, 8]. All-trans-retinoic acid (RA) is one type of retinoids that binds to specific nuclear receptors (retinoic acid receptors – RAR) and activates transcription of several genes [8-10].

It was demonstrated that there is a crosstalk between IFN and RA growth-suppressive pathways, despite their different mechanisms of action. Several experiments also demonstrated that the combination of interferons and retinoids synergistically inhibits tumour cell growth and tumour angiogenesis in comparison to each one alone, as referred by Kalvakolanu *et al*. (2010) [4, 5].

In 1998, Hofman *et al*. [5] verified that IFN/RA combination induces cell death in human breast carcinoma cells. However, when the authors examined if this induced cell death was due to alterations in the activity or in the expression of IFN-stimulated gene products, that until that moment were known to be responsible for growth arrest and apoptosis, they verified that none of them were involved. The authors have also detected no alterations in p53 tumour suppressor neither in Bcl-2 or Bcl-2–associated X protein (BAX). The authors supposed that there might be other gene(s) associated with IFN/RA induced cell death. Using an antisense knockout technique, the authors isolated 14 episomes, several of them identified for the first time and thus these genes being responsible for IFN/RA-induced cell death, clones that expresses the antisense mRNA

(in presence of death inducer –IFN/RA) survived and the genes were identified. Hofman *et al*. named these genes as *Genes associated with Retinoid-IFN-induced Mortality* (*GRIMs*) [5].

Kalvakolanu [11] referred that the isolation of several *GRIM*s suggests the existence of a coordinated network of factors that are required to activate IFN-β/RA-induced cell death. Therefore, inhibition of only one of them could be sufficient to block cell death pathway [11]. Based on this, his group suggested a model (Figure 1), where IFN/RA activates the "GRIM Engine" that activates the "Central Death Engine".

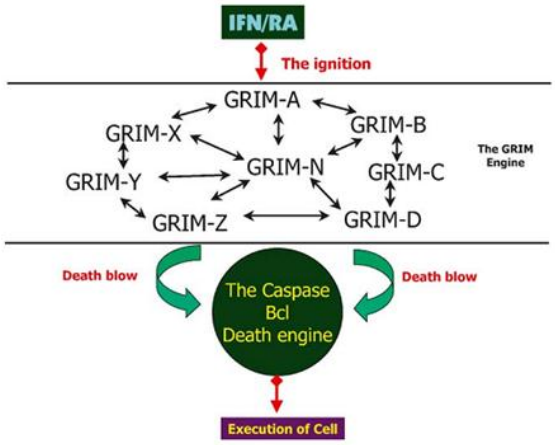

Figure 1 - Proposed model for the involvement of *GRIMs* in cell death regulation. IFN/RA initiates the "GRIM Engine" that leads to "Central Death Engine". Adapted from [11].

With these studies, GRIM-19 was demonstrated to be involved in IFN/RA-induced cell death. Although it may be involved in other pathways involving other ligands and other biochemical processes in normal cells. GRIMs were suggested to be: (1) novel tumour suppressors, (2) useful biomarkers for evaluation of clinical responses to treatments, (3) targets for therapy when its expression is altered [11].

A novel gene: *GRIM-19*

In 2000, using an antisense knockout technique, Angell *et al*. [9] discovered GRIM-*19*, a novel cell death-regulatory gene induced by IFN-β and RA combination. The authors verified that the antisense *GRIM-19* was able to confer a strong growth

advantage to cells when exposed to the combination of IFN-β and RA treatment (Figure 2) [9].

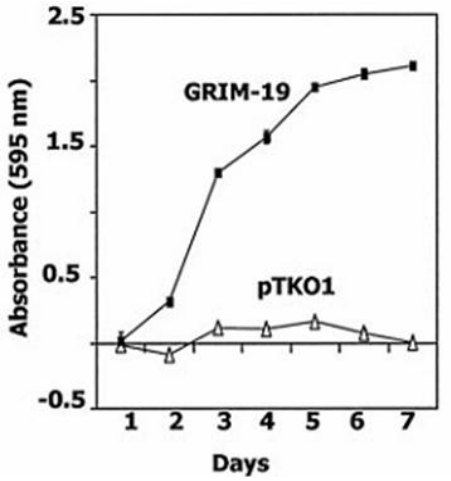

Figure 2 - HeLa cells transfected with an empty vector (pTKO1) and the vector with an antisense *GRIM-19* (GRIM-19) were treated with IFN-β and RA and a growth-assay was performed. The cells transfected with the antisense GRIM-19 become resistant to death induced by IFN/RA (adapted from [9]).

To reiterate these death-regulatory functions, overexpression of *GRIM-19* was able to reduce cell viability, while cells expressing moderate levels of *GRIM-19* were significantly more susceptible to cytotoxic effect of IFN/RA. GRIM-19 seemed to induce apoptosis under IFN/RA combination [9].

GRIM-19 mRNA is highly expressed in human heart, skeletal muscle, liver, kidney and placenta. In contrast, it has the lowest expression in human lung, peripheral blood leukocytes, spleen, thymus and colon. GRIM-19 protein intracellular locations were also elucidated by Angell *et al*. It was possible to see GRIM-19 protein primarily in the nucleus, but it was also seen as a punctuate staining in cytoplasm [9].

In the same year it was published another paper that described the chromosomal location of human *GRIM-19*. Chidambaram *et al*. [7] revealed that *GRIM-19* is located in human chromosome 19p13.1 – 13.2. Human chromosome 19p13.2 locus was associated with genes that can suppress prostate and thyroid tumour cell growth [12, 13], so *GRIM-19* was suggested to be one candidate tumour-suppressor gene [7].

GRIM-19, a mitochondrial complex I subunit

Mitochondrial biology

The name mitochondrion was introduced in 1898 by Benda and comes from the Greek "mitos" (thread) and "chondros" (granule), referring to the appearance of these structures during spermatogenesis [14]. Currently, the origin of mitochondria is still not clear, but it is believed that they arose from an endosymbiotic relationship between a glycolytic proto-eukaryotic cell and an oxidative bacterium [15].

Mitochondria are semi-autonomous organelles that are traditionally associated with energy production required for cellular metabolism, producing most of the cellular ATP (adenosine-5′-triphosphate) via the oxidative phosphorylation (OXPHOS). However, they have also an essential role in cell death regulation [15, 16].

Structurally, the mitochondrion is unusual since it contains two membranes (inner and outer membranes) that separate two distinct compartments: the intermembrane space and the internal matrix (Figure 3) [17]. The inner membrane is highly folded into cristae, which encloses complexes of the electron transport chain (ETC) and the ATP synthase that controls the basic rates of cellular metabolism [17]. The outer membrane contains porins that forms large aqueous channels through the lipid bilayer, which makes it be permeable to all molecules of 5000 Daltons or less, including small proteins. Such molecules can enter into the intermembrane space, but most of them cannot pass the impermeable inner membrane that has transport proteins which are more selective [18].

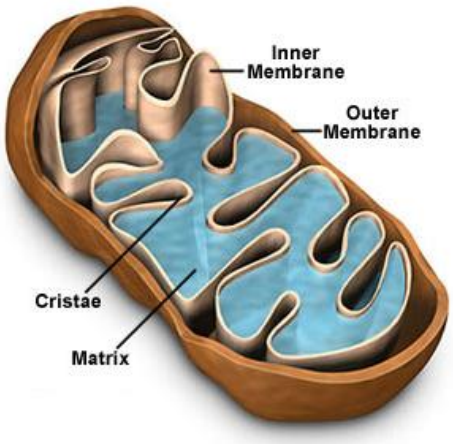

Figure 3 – Mitochondrial morphological characteristics (adapted from [19]).

Mitochondria possess their own genome which encodes some machinery necessary for their replication, transcription, translation and protein assembly [15, 20]. Mitochondria have about two to ten molecules of their own DNA, the mitochondrial DNA (mtDNA). This 16.5 kb circular double-stranded molecule encodes 22 transfer RNAs (tRNAs) and 12S and 16S ribosomal RNA (rRNA), as well as 13 proteins (ND1, ND2, ND3, ND4, ND4L, ND5, ND6, CytB, COI, COII, COIII, ATPase6 and ATPase8) that are part of the mitochondrial respiratory chain (MRC) and OXPHOS system (Figure 4) [16, 21]. Despite having their own DNA, they are not independent from the nuclear DNA (nDNA) because most mitochondrial proteins are encoded by nDNA which are imported into mitochondria [15]. The nDNA encodes at least 76 OXPHOS proteins, required for the mitochondrial metabolic pathways, and all of the enzymes required for mitochondrial biogenesis including mtDNA polymerase γ (POLG), RNA polymerase, mtDNA transcription factors and ribosomal proteins, among others [22].

Energy metabolism

Mitochondria are responsible for about 90% of the ATP production in the cell through OXPHOS which is an oxygen-dependent process. It is achieved by a series of well-coordinated protein complexes – the MRC [16, 23]. The metabolic requirement of the cell is in base of the number of mitochondria in the cell [19].

The complete OXPHOS system is located within the inner membrane and is composed by five multi-subunit enzymes formed from gene products of 76 nuclear and 13 mitochondrial genes [23]. These multi-enzymatic complexes are designated and composed by: (1) Complex I (nicotinamide and reduced adenine dinucleotide (NADH): ubiquinone oxidoreductase) is assembled by 45 polypeptides, 7 (ND1–4, 4L, 5, and 6) encoded by mtDNA; (2) Complex II (succinate: ubiquinone oxidoreductase) by 4 nDNA polypeptides; (3) Complex III (uniquinone: ferricytochrome c oxidoreductase) by 11 polypeptides, 1 (cytochrome-b) encoded by mtDNA; (4) Complex IV (ferricytochrome c: oxygen oxidoreductase) by 13 polypeptides, 3 [cytochrome c oxidase (CO I–III)] encoded by mtDNA; (5) Complex V (ATP synthase) by 16 polypeptides, 2 (ATP6 and 8) encoded by mtDNA [22-24]. The first four complexes (complex I-IV) are designated as MRC complexes and complex V – ATP Synthase –, as its name say, is responsible for ATP synthesis [24].

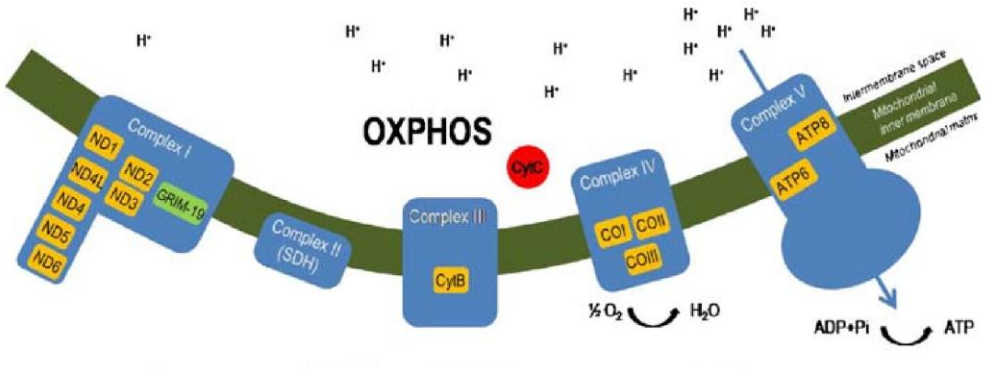

Figure 4 – OXPHOS system. There are represented some proteins encoded by mtDNA (yellow boxes) and GRIM-19 subunit (green box) that are present in each complex (adapted from [16]).

In addition, the cell can also produce ATP through glycolysis, a process that does not require oxygen, although it is less efficient than OXPHOS [16]. Each time there is a decrease in oxygen levels or an OXPHOS deficiency, it leads to a shift from OXPHOS to glycolysis.

Mitochondrial complex I

Currently, it is known that mitochondrial complex I (mitochondrial NADH: ubiquinone oxidoreductase) is composed by two arms: one at the surface of the lipid bilayer and the other that protrudes from the membrane and is named subcomplex 1λ and is composed by 15 subunits [25]. Fearnley *et al.* [25], isolated the subunits of bovine mitochondrial complex I and subcomplex 1λ by sodium dodecyl sulfate polyacrylamide gel electrophoresis (SDS-PAGE) and analysed by peptide mass fingerprinting to confirm the subunit composition of subcomplex 1λ. The authors confirmed the presence of 14 previously known subunits, but they also observed the presence of a fifteenth band that did not correspond to any known subunit of the subcomplex 1λ (Figure 5). The authors, based on nomenclature for mitochondrial complex I, named this new subunit as B16.6 [25].

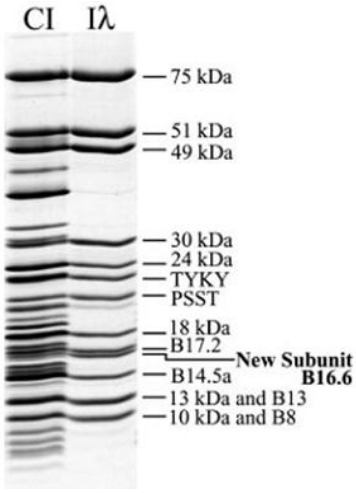

Figure 5 – Subunit composition of the bovine complex I (CI) and subcomplex Iλ (Iλ) from mitochondrial respiratory chain. It is possible to visualize the new subunit identified, the B16.6 (adapted from [25]).

Based in the amino acid sequence, the authors concluded that B16.6 subunit corresponds to the bovine homolog of the GRIM-19 human protein, with 83% of identity. Taking in account the previous study of Angell *et al*. [9], the authors suggested that the punctuate staining in the cytoplasm observed, possibly correspond to a mitochondrial localization [9, 25]. This location of GRIM-19 on mitochondria was confirmed later by other authors [26-28].

Hu *et al*. [26] developed and characterized three monoclonal antibodies against GRIM-19 and verified that GRIM-19 is present both in the nucleus and in the cytoplasm, supposedly in mitochondrial complex I [26]. One year later, Murray *et al*. confirmed GRIM-19 as a complex I protein [27].

Huang *et al*. [28] re-examined the localization of GRIM-19 in various cell types and verified that its primary localization is on mitochondria as a complex I component. The authors proposed that stronger immunofluorescence staining in the nucleus of GRIM-19 observed in previous reports should be due to nonspecific reactions of the antibodies with nuclear proteins or possibly GRIM-19 could be able to be released from mitochondria and translocate to other cellular compartments under certain conditions [28]. Moreover, the authors verified that homozygous deletion of *GRIM-19* causes early embryonic lethality within day 9.5. These non-expressing *GRIM-19* blastocysts had retarded growth and its mitochondria had abnormal structure, morphology and

distribution in the cell. The researchers have also showed that *GRIM-19* elimination destroyed the mitochondrial complex I assembly and the electron transport activity and was indirectly responsible for defects in the assembly of other complexes resulting in mitochondrial failure [28].

Recently, GRIM-19 was newly reported as being present in nucleus, mitochondria and cytoplasm [29, 30]. The clear localization of GRIM-19 is still in discussion. It is now clear that GRIM-19 is located in mitochondria, but its localization in cytoplasm (not specifically in mitochondria) or in nucleus is still controversial.

With these studies, it is possible to conclude that GRIM-19 fulfil two roles in the cell: (1) is involved in IFN/RA-induced cell death and (2) is a subunit of mitochondrial complex I.

GRIM-19 interactions

There are several studies in which the authors found and confirmed some partners of GRIM-19 involved in growth suppression, briefly described in the next paragraphs [31-36].

Signal Transducer and Activator of Transcription 3 (**STAT3**) is the most important protein showed to interact with GRIM-19 and has the most relevance to this work because it was described as being involved in carcinogenesis. For that reason, STAT3 will be mentioned after in a distinct topic.

GW112, also named Olfactomedin (**OLFM4**) is a protein that is usually overexpressed in human tumours. It was found as a GRIM-19 partner in IFN-β/RA mediated cell death, attenuating this induced apoptosis from 82.5±3.6% in cells transfected with GRIM-19 to 20.8±4.4% in cells co-transfected with GRIM-19 and GW112/OLFM4. GW112/OLFM4 was also capable to attenuate GRIM-19 apoptosis-related genes (PIG12, GADD153 and c-Abl) expression [31]. Using an adenovirus vector to express *GRIM-19* (*Ad-GRIM-19*) in SGC-7901 cells (gastric cancer cell line) it was observed a decrease of GW112 and nuclear factor kappa beta (NF-kB) binding capacity [32]. NF-kB is a regulator of GW112/OLFM4 expression, once it has the ability to bind to its promoter region [37]. Infection with *Ad-GRIM-19* inhibited tumour cell adhesion, migration and invasion *in vitro* and metastasis *in vivo*, which can be explained by the decrease of the release of vascular endothelial growth factor (VEGF),

urokinase-type plasminogen activator (u-PA) and matrix metalloproteases 2 and 9 (MMP-2 and MMP-9). *GRIM-19* seems to act as an upstream regulator of GW112/OLFM4 blocking NF-kB binding activity and metastasis in gastric cancer [32].

HtrA2 degrades X-linked inhibitor of apoptosis protein (XIAP), one type of IAP that is able to block caspase-9, relieving its activity [38]. This protein (HtrA2) was shown to interact with GRIM-19. HtrA2 and GRIM-19 for itself were sufficient to induce resistance to cell death induced by IFN/RA. The treatment leaded to GRIM-19 and HtrA2 release from mitochondria. GRIM-19—HtrA2 interaction induced high levels of apoptosis that was synergistically enhanced by IFN/RA treatment. Degradation of XIAP by HtrA2 increased significantly by GRIM-19, which leaded to increased caspase-9 activation. vIRF, that also bins to GRIM-19 and inhibits apoptosis [33], is capable of disable GRIM-19—HtrA2 interactions and inhibit destruction of XIAP by IFN/RA [34].

Cell cycle inhibitor **CDKN2A (p16^{Ink4a})**, inhibitor of cyclin-dependent kinase 4 (Cdk4) is other GRIM-19 interacting protein [35]. Some genes responsible for cell-cycle progression induced by E2F1 (transcription factor that is critical to cell cycle development) are inhibited by p16 which prevents cyclin D – CDK4 association. Recently, it was reported that GRIM-19 also have this effect. Co-expression of these two proteins (p16 and GRIM-19) synergistically inhibited the expression of these genes responsible for cell-cycle progression. GRIM-19 was been shown to enhance the association between p16 and CDK4. This interaction was reverted with GRIM-19 depletion [35]. It was the first work that demonstrated the suppressive role of GRIM-19 in cell growth and also referred its involvement in other pathways required for cell cycle control.

NODs (nucleotide oligomerization domains) are a family of intracellular bacterial receptors that recognize bacterial invasion that utilize RIP2/RICK and induce NF-kB activation by a not well understood pathway [39]. It was demonstrated the interaction between **NOD2** and GRIM-19 by yeast two-hybrid assay (Y2H) and co-immunoprecipitation. When GRIM-19 expression was evaluated in tissues with inflammatory bowel disease (Crohn's disease and ulcerative colitis) it was observed that in involved areas from mucosa of this two diseases, the mRNA levels of GRIM-19 were low. Other observation was that infection with invasive bacteria (*Salmonella Typhimurium*) upregulated GRIM-19 mRNA levels, while non-invasive bacteria (*E. coli*) had no effect. The authors also verified that Caco-2 cells transiently expressing

GRIM-19 had fewer invasions by the invasive bacteria types. These observations suggested that GRIM-19 is required for pathogen invasion regulation [36].

Seo *et al.* (2002) demonstrated, with an Y2H assay, GRIM-19 as a novel vIRF interacting protein. The authors verified that this specific interaction can block GRIM-19 ability to induce apoptosis after IFN/RA treatment and also, observed that Human papillomavirus type 16 (HPV-16) E6 protein of the high risk strains binds to GRIM-19 [33]. GRIM-19 is thus a target of viruses to avoid cell death and to allow them to replicate into the cell.

As referred by Máximo *et al*. in 2008 [40], different locations of GRIM-19 observed in several studies may reflect the different roles of GRIM-19 in cell biology, as part of mitochondria respiratory chain and as part of IFN/RA-induced cell death pathway. Its interactions, with various proteins may also reflect GRIM-19 different roles [40].

STAT3

STATs (Signal Transducers and Activators of Transcription) are key mediators of cytokine signalling by surface receptors that results in JAK (Janus Kinase) – STAT pathway activation and induces the expression of ligand-dependent genetic programs that determine the biological response to a stimulus [41]. STAT3 is one STAT family member that is involved in embryonic development [42], cell growth and anti-apoptosis [43]. Usually, STAT3 is tightly regulated by feedback inhibitors, but its constitutive activation has been documented and directly contributes to oncogenesis in cells transformed by viruses, oncogenes and autocrine growth factors [41, 44] and it was seen in tumours [41, 45, 46]. STAT3 is responsible for the expression of some genes involved in cell proliferation like cyclins B1 and D1, cdc2, c-myc, and antiapoptotic proteins like Bcl-X_L, Bcl-2 and Mcl-1, $p21^{WAF1/CIP1}$ [41].

In general, STATs (and in particular STAT3) are predominantly in a latent state in cytoplasm. When a ligand binds to the extracellular domain of the cytokine receptors and activates them, the intracellular receptor associated Janus Kinase (JAK) is activated by autophosphorylation. It leads to phosphorylation of tyrosine residue (Tyr705) in monomeric and unphosphorylated STAT3, which becomes active and ready to dimerize by the SH2 domains from each one. The dimerization is essential for STAT3 activity

because allows its translocation to the nucleus where it exerts its biological function, through the DNA binding [41, 47, 48]. Another phosphorylation, on serine residue (Ser727), has also been shown to be important to STAT3 activation, but its relevance is not completely clear. Some studies pointed that phosphorylation at this serine residue (Ser727) is fundamental to the optimal transcriptional activation of STAT3 after tyrosine residue (Tyr705) phosphorylation [49, 50], while others, such Bowman and co-workers showed a repressive effect associated in certain conditions [41]. Other studies showed that Ser727 phosphorylation can be essential for STAT3 signalling, once its blockage can block this signalling [41, 51, 52]. There are also some studies indicating that Ser727 phosphorylation may result in STAT3 signalling activation independently of Tyr705 phosphorylation under certain conditions [53-55]. More recently, STAT3 was described to be present in mitochondria and the Ser727 phosphorylation was reported to be important to this localization, independently of the function in the nucleus [56].

As shown, STAT3 activation and function lead to a lot of questions. More studies are required to really understand this issue.

Lufei *et al* [57], and Zhang *et al*. [44] described STAT3 and GRIM-19 as interacting proteins. By, yeast two hybrid assays (Y2H), Lufei *et al*. [57] identified GRIM-19 as specific STAT3 interacting protein (is specific to STAT3; do not interact with STAT1 or STAT5), this interaction was also demonstrated *in vivo* and *in vitro* [57]. Zhang *et al*. [44] using the same technique to identify other GRIM-19 protein partners, confirmed the GRIM-19/STAT3 interaction. The authors, also, confirmed that GRIM-19 interacts specifically with STAT3, but not with other STATs (1, 2 and 5a STAT family members). After IFN/RA treatment (inducers of GRIM-19 expression), more STAT3 was co-immunoprecipitated with GRIM-19 in comparison with unstimulated cells, which was supposed to be caused by an increase of GRIM-19 expression (Figure 6) [44].

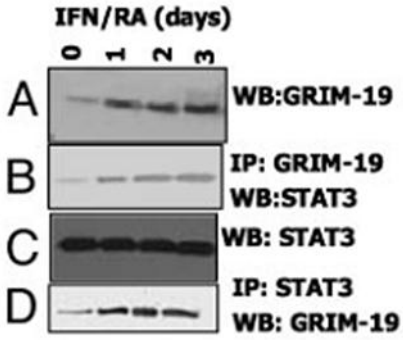

Figure 6 – Endogenous GRIM-19 binds to STAT3 in a time dependent correlation with IFN/RA treatment (adapted from [44]).

Accordingly to Zhang *et al.* [44] STAT3 is negatively regulated by GRIM-19. Although, it does not inhibit STAT3 activation, nuclear translocation, neither does it have DNA binding capacity. The researchers determined that GRIM-19 regulates the binding of STAT3 to the transactivation domain (TAD) and blocks its activity, being serine 727 residue required. This residue was confirmed as critical for the interaction since they verified that the binding capacity is almost lost (95% reduction) in a S727A mutant [44].

In contrast, Lufei *et al*. [57] reported that GRIM-19 binds to the coiled-coil, DNA binding and linker domains of STAT3. They observed that, in unstimulated cells, STAT3 was distributed in cytoplasm and nucleus, but in cells co-expressing GRIM-19 the majority of STAT3 disappeared from these locals and formed dot-like dense structures at the nuclear periphery, co-localised with GRIM-19. Thus, the authors concluded that this perinuclear aggregates block STAT3 nuclear translocation and this might be the way how GRIM-19 inhibits STAT3 activity [57]. Zhang *et al*. [44] contra-argued saying that Lufei *et al*. conclusions were based in STAT3 and GRIM-19 overexpression in cells, being necessary to take in consideration the possibility that interactions can be mediated through the heterodimerization of mutant and endogenous STAT3 [44]. Kalvakolanu also refuted the inhibitory effect of GRIM-19 in STAT3 activity by nuclear translocation blockage referring that STAT3 phosphorylation, nuclear translocation and DNA binding are not different in cells overexpressing GRIM-19 [11]. Apart from these contradictory ideas, it is important to refer that Zhang *et al*. [44] also verified that TAD alone is insufficient for the interaction and so, other secondary low-affinity sites may be required for interaction with GRIM-19.

These two studies are contradictory in two aspects: (1) primary domains of STAT3/GRIM-19 binding and (2) way how GRIM-19 blocks STAT3 activity. However, both studies identified STAT3 as a participant in GRIM-19 death-inducing pathway and GRIM-19 as a novel inhibitor of STAT3.

However, GRIM-19 role in oncogenic cell proliferation and its effects in a constitutively active STAT3 condition and cellular transformation were not clarified. Trying to understand this, Kalakonda *et al*. [58] used a cellular system that expressed a constitutively activated STAT3 that was sufficient to induce oncogenic transformation in PC3 cells, a human prostatic cell line. When GRIM-19 vector was introduced and cells expressed it, colony formation by these cells decreased, which was also observed in other cancer cell lines. GRIM-19 could overcome cellular transformation caused by STAT3 constitutively activated and suppressed the expression of endogenous genes involved in cell growth control. Studies *in vivo* also showed that GRIM-19 was able to inhibit tumour formation [58].

Nallar *et al.* [30] identified a motif in N-terminus of GRIM-19 which is responsible for STAT3 repression. The N-terminus was determined to be essential for GRIM-19 antitumoural function. When the authors promoted its deletion, they observed that the capacity of this mutated GRIM-19 to suppress growth was lower than the wild-type GRIM-19. A motif of four amino acids: glutamic acid, aspartate, methionine and proline – QDMP, which has similar structure with some viral proteins, was demonstrated to be the major responsible for GRIM-19 function in cell growth and motility inhibition, once mutations in this motif suppressed this functions of wild-type GRIM-19 in cells [30]. Interestingly, a tumour-derived mutation described by our group [1], located at N-terminus (lysine converted to an asparagine in amino acid 5 – K5N) was also unable of inhibit colony formation in soft-agar and limit cell growth [30].

It was recently reported that STAT3 is present in mitochondria and has a regulatory function in OXPHOS, particularly in MRC complexes I and II [56]. Based in previous studies reporting GRIM-19 interaction with STAT3 [44, 57] and GRIM-19 effects on MRC [25, 28] the authors supposed that STAT3 might also co-localize with GRIM-19 in mitochondria. Using an SDS-PAGE the researchers observed that it is the case, although in a smaller quantity comparing to the cytosol fraction. Using STAT3 knockout cells ($STAT3^{-/-}$) it was shown that STAT3 is essential for complexes I and II activity, since their activity decreased significantly in these cells and STAT3a (a STAT3 isoform) restoration were able to restore the activity of these complexes [56]. Later,

other study confirmed this mitochondrial STAT3 localization and showed that it is important for Ras-dependent cellular transformation [59]. STAT3 was demonstrated as being essential to Ras (H-RasV12) induced cell growth, since, in STAT3 deficient cells, growth was impaired compared with cells expressing STAT3. Only Ser727 and C-terminus was required to the cooperation between Ras and STAT3 in cell growth advantage. It was also confirmed, *in vivo*, that mitochondrial STAT3 is essential for Ras-transformed cells growth. Another interesting result from this study is the STAT3 involvement in mitochondrial function. STAT3 deficient cells show mitochondrial dysfunction, with a particularly decrease in the activity of complex II and ATP synthase, while transformed cells increased fermentation process of energy production. It appears that mitochondrial STAT3 contributes to Ras-dependent transformation leading to higher activity of complexes II and V but, at same time, leading to an energy production shift from OXPHOS to fermentation (a cancer hallmark) [59].

GRIM-19 in cancer

Alchanati *et al*. [60] in an attempt to define molecular alterations in renal cell carcinoma (RCC) revealed, using mass spectrometry, that GRIM-19 expression is completely or almost lost (93% of cases) in these tumours. A complete lack of GRIM-19 expression was observed in four of the eleven cases (36%), and very weak expression in six (55%) was observable by western blot, confirming GRIM-19 loss. These results were also confirmed by immunohistochemistry, which revealed loss of expression of GRIM-19 in all types of RCC studied (Clear cell, papillary and chromophobe). The authors also showed that this loss of expression occurs also, with a lower frequency, in urogenital cancers. GRIM-19 downregulation observed in RCC has been shown to be due to a loss of mRNA expression that seems to harbour no mutations. This result suggests another level of regulation like epigenetic mechanisms, namely DNA hypermethylation and/or histone deacetylation that can interfere with the accessibility of the transcription machinery to DNA [60]. However, this hypothesis had never been tested and promoter characterization and other studies have to be done to address this issue. It was been shown, using a RCC cell line, that the inhibition of GRIM-19 leads to an enhancement of cell growth, whereas GRIM-19 overexpression enhanced cell death. Cells expressing antisense GRIM-19, which were injected into

nude mice, seem to have a greater potential to form tumours with a growth rate substantially higher, comparing with cells transfected with empty vector. This effect was due to an increased expression of STAT3 regulated genes, at least in some part, suggesting that the novel GRIM-19 tumour suppressor activity (this was the first work to attribute this designation to this protein) may be modulated by inhibition of STAT3 [60].

It was been shown that GRIM-19 is involved in mitochondrial complex I assembly, and subsequently in mitochondrial electron transport, and in IFN/RA-induced cell death [25]. The first study concerning GRIM-19 mutations was made by Máximo *et al*. [1], in 2005. The authors studied a series of thyroid tumours, including 26 Hürthle cell tumours and 20 non-Hürthle cell carcinoma, and blood donor samples. They detected three missense mutations in sporadic Hürthle cell carcinoma, one germline mutation in a Hürthle cell papillary carcinoma and none mutations in non-Hürthle cell carcinomas and in blood samples [1]. This was the first nuclear gene that has been associated with Hürthle cell tumours and the authors suggested that *GRIM-19* might be involved in oxyphilic tumours pathogenesis [1]. Alchanati *et al*. [60] found one new mutation in one single case of their series [60]. However, the oncocytic tumours of the kidney were not included in this study. The observations of Máximo *et al.* [1] in oncocytic tumours of the thyroid would be interesting to study in other oncocytic tumours of other organs to confirm if GRIM-19 is a key for the oncocytic development of these tumours or if it is important only in the HCT.

Another study revealed an alternative splicing form of *GRIM-19* incorporating intron 3, which appears to be a RCC tumour-specific isoform. From 23 samples, 14 possessed the mutant transcript, being 10 of them Clear Cell Carcinomas, suggesting that this isoform could be linked with this renal tumour histotype. Beside the fact that the protein was not observed in the tissues, it was expressed when transfected into *HeLa* cells, which not allows to conclude if the non-expression is due to instability of the protein or to the alternative splicing in tumours [61]. It is interesting to note that this histotype (Clear Cell Carcinomas) is the one with the higher loss of GRIM-19 expression observed by Alchanati *et al.* [60].

A recent study performed by Gong *et al.* [62] in order to investigate the expression of GRIM-19 and STAT3 in human colorectal tissues, demonstrated that GRIM-19 expression was lower in tumour samples compared to normal colorectal tissues and it was closely related with STAT3 expression, showing a negative

correlation between GRIM-19, STAT3 and phosphorylated STAT3 expression. Although GRIM-19 mRNA expression was lower in tumour samples, no genetic mutations were observed [62].

In primary human prostate carcinomas, Zhang *et al*. [63] showed loss of GRIM-19 expression associated with STAT3 increased expression by an immunohistochemical assay. The authors also constructed a STAT3-specific short hairpin RNA (shRNA – a RNA interference molecule) that reduced STAT3 expression in prostate cancer PC-3M cells and it, in the presence of GRIM-19, inhibited STAT-3-dependet genes and suppresses cell growth in a synergistic way. Both GRIM-19 restoration and STAT shRNA treatment were able to block metastasis as observed by suppressing metalloprotease 2 (MMP-2) activity (known to promote metastasis) and inhibiting infiltration of the tumour into muscle or lymph node [63].

Another confirmation of GRIM-19 involvement in cancer was observed in human cervical cancer, the most common gynaecologic neoplasm in women. Zhou (Y) *et al*. [64] demonstrated that GRIM-19 expression was extremely reduced in these tumours compared with control normal cervical samples and this was associated with increased STAT3 activity, demonstrated by the upregulation of STAT3 target genes, such as Cyclin B1, Bcl-2-L1 and also STAT3 in tumours. The restoration of GRIM-19 levels in *HeLa* cells was able to re-establish the control over STAT3-dependent gene expression and tumour growth, *in vivo*. GRIM-19 expression suppressed the expression of VEGF, MMP-2 and MMP-9 [64].

GRIM-19 involvement in lung tumour cases was reported by Zhou (A) *et al*. [29]. In non-small cell lung cancer (NSCLC), GRIM-19 was significantly lower (24.3%) than in normal lung tissues. In association with Alchanati *et al.* and Gong *et al*. findings, these data, confirm GRIM-19 as a new tumour suppressor gene [29, 60, 62]. The authors also observed that GRIM-19 expression correlates with clinicophatologic factors of lung cancer (positive rate of GRIM-19 in clinical stages I and II was higher than in stages III and IV or NSCLC). It was also observed that in normal lung tissues GRIM-19 is primarily located in cytoplasm, but in lung cancer tissues it is predominantly located in the nucleus, corroborating the idea that GRIM-19 translocates from cytoplasm to nucleus in a STAT3 related process in carcinogenesis [29].

Table I - Summary of studies which evaluated GRIM-19 expression and correlation with STAT3 in several types of tumours (adapted from [65]). IHC: immunohistochemistry; WB: western blot; N/A: not analyzed; N/S: not specified. # STAT3 responsive gene.

Tumour Type	Tumour Subtype	GRIM-19		STAT3	
		Methodology	Result	Methodology	Result
Thyroid carcinoma [1]	Hürthle	PCR/Sequencing (26 tumours)	4 mutations - 15.4%	RT-PCR for ICAM1# (in the 4 tumours with mutated GRIM-19)	Upregulated
	Non-Hürthle	PCR/Sequencing (20 tumours)	No mutations - 0%	N/A	N/A
Kidney (Renal Cell Carcinoma) [60]	Clear Cell	WB (11 tumours)	Absent in 4, very weakly expressed in 6 and moderately expressed in 1	N/A	N/A
		RT-PCR (5 tumours)	Downregulated; 1 mutation		
		IHC (20 tumours)	Absent in 19 cases and weakly expressed in 1	N/A	N/A
	Chromophobe	IHC (5 tumours)	Absent in 4 and weakly expressed in 1	N/A	N/A
	Papillary	IHC (4 tumours)	Absent	N/A	N/A
Colorectal Carcinoma [62]	N/S	RT-PCR/Sequencing (23 tumours) and WB (40 tumours)	Downregulated; no mutations	WB (40 tumours)	Upregulated
		IHC (40 tumours)	Weakly expressed	IHC (40 tumours)	Strongly expressed
Prostate Carcinoma [63]	N/S	IHC (38 tumours)	Weakly expressed	IHC (38 tumours)	Strongly expressed
Cervical Carcinoma [64]	Squamous	RT-PCR and WB (20 tumours)	Downregulated	RT-PCR and WB (20 tumours)	Upregulated
		IHC (20 tumours)	Weakly expressed		
Lung cancer [29]	NSCLC	IHC (49 tumours)	Weakly expressed	N/A	N/A

Thyroid tumours

Thyroid tumours are the most common type of endocrine neoplasia and are mostly derived from follicular cells [66]. It was predicted that this type of cancer accounts for 1% of all malignancies in developed countries and is estimated that 122 000 cases appear annually worldwide [67].

These tumours are firstly classified as benign or malignant, benign tumours are classified as follicular thyroid adenomas (FTA), and the malignant tumours or carcinomas are classified as well-differentiated carcinomas (mainly divided in: Follicular carcinoma, Papillary carcinoma and Follicular variant of papillary carcinoma, with or without Hürthle cells) and the less common, highly aggressive, poorly differentiated thyroid carcinomas, the anaplastic thyroid carcinoma (ATC) [66].

Papillary Thyroid Carcinoma (PTC) is one of the well-differentiated thyroid carcinoma and is cytological identified based on the presence of typical nuclear characteristics as large, pale staining, irregular "grooved" and "ground glass" nuclei as referred by Couto and co-workers [66]. In terms of molecular features, this carcinoma is identified by RET proto-oncogene rearrangements and $BRAF^{V600E}$ mutations as the most common features. $BRAF^{V600E}$ mutation has a frequency between 29 and 69% in the PTC cases. Other less common mutation $BRAF^{VK600-1E}$ was observed in some cases of tumours solid PTC and in some metastasis of conventional PTC [66].

Follicular Thyroid Carcinoma (FTC) has as principal molecular characteristics the prominence of aneuploidy and the high prevalence of RAS mutations and PAX8-PPARγ rearrangements [68, 69]. Beyond the molecular features it is also diagnosed by histological demonstration of capsular and/or vascular invasiveness [66].

The Follicular Variant of Papillary Thyroid Carcinoma (FVPTC) has the common features that are found in Follicular carcinoma (RAS mutations and PAX8-PPARγ rearrangements) but also $BRAF^{K601E}$mutations that is less common. The nuclear features of PTC histotype are also evident in this histotype [70].

Hürthle cell carcinomas are tumours presenting cells with a large amount of abnormal mitochondria (oncocytic) and will be mentioned in a specific topic.

Renal Cell Tumours

Renal cell tumours (RCT) are a group of malignancies that arise in epithelium of the renal tubules and represents, on average, over 90% of all malignancies of the kidney that occur in adults [71]. Cigarette smoking is a major cause of kidney cancer and accounts for at least 39% of all cases in males, although there are other risk factors like exposure to carcinogenic arsenic compounds, obesity, blood hypertension and others

[71]. In 2007, about 3.5% of all cancer diagnosis in the USA was renal cancer, with 51,190 new cases and 12.890 deaths attributed to the malignancy [72].

RCT represents distinct pathological entities that are distinguishable by histological subtype: clear cell RCC (75%), type 1 papillary RCC (5%), type 2 papillary RCC (10%), chromophobe RCC (5%) and oncocytoma (5%) [73, 74]. Specific genetic alterations are linked to the histological subtypes (Figure 7).

Clear cell RCC (CCRCC) is histologically characterized by the presence of cells with a clear cytoplasm that are arranged in sheets, acini or alveoli with a prominent thin-walled vasculature. The papillary RCC (PRCC) presents papillae with fibrovascular central part lined by a single layer of malignant epithelial cells and some tubules. The chromophobe renal carcinoma (CromRCC) is composed of malignant epithelial cells with a pale cytoplasm and prominent cellular membranes. Renal oncocytomas (ROnc) are benign tumours in which cells have a high number of mitochondria and so, have a eosinophilic cytoplasm [75].

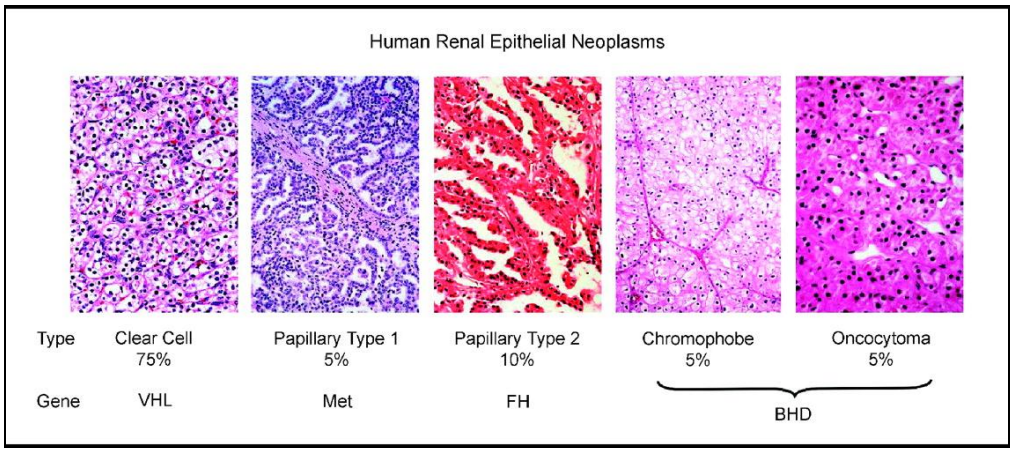

Figure 7 – Main types of inherited epithelial renal cancer that are associated with alterations in different genes [72]. VHL: Von Hippel-Lindau; FH: fumarate hydrolase; BHD: Birt-Hogg-Dubé.

Although the majority of renal malignancies are sporadic, about 4% are associated with hereditary cancer syndromes. In these inherited cancer syndromes associated with kidney tumours, an oncogene/tumour suppressor gene is involved and the respective germline mutations have been identified, which is important to perform a correct diagnosis of the patient with one of the syndromes and even to identify

asymptomatic gene carriers by germline mutation. Each of the inherited syndromes predisposes to distinct types of renal carcinoma [71].

Von Hippel-Lindau disease (VHL) —The VHL gene, located on chromosome 3p25-26 was identified in 1993 by Latif *et al*. through genetic linkage analysis [76]. This syndrome is caused by germline mutations or methylation (in a high percentage of tumours from patients with sporadic, non-inherited clear cell renal carcinoma) of the VHL tumour suppressor gene [71]. The kidney cancer in VHL is uniformly clear cell renal carcinoma [77], that is characterized by cells with clear or eosinophilic cytoplasm within a delicate vascular network [71].

Hereditary papillary renal carcinoma (HPRC) was detected by the first time as one type of hereditary kidney cancer in three families with many affected members developing type 1 papillary RCC [78]. In these families, where the syndrome was not linked to VHL gene, a new genetic linkage analysis was performed and Met proto-oncogene was identified which is located in the locus of the chromosome 7q31 [78]. Subsequent experiments identified missense mutations in the tyrosine kinase domain of Met in the germline of affected patients, suggesting that the mutation led to constitutive activation of the Met protein and the development of papillary RCC [79].

Birt-Hogg-Dubé syndrome (BHD) is an autosomal dominant inherited disorder characterised by benign skin tumours [71]. The renal cancer types associated with BHD patients may be chromophobe/oncocytic hybrid in 50% of the cases, being the most predominant, but can also be chromophobe renal carcinoma in 33% of the cases, oncocytoma in 7% and even clear cell renal carcinoma in 5% [77]. The genetic linkage analyses permitted to link BHD gene (that encodes the protein folliculin) to chromosome 17p11.2 [72, 79] and it seems to be a tumour suppressor once there were found frameshift mutations in the second copy of the gene that predicted truncation of the BHD protein [80].

Hereditary leiomyomatosis and renal cell cancer (HLRCC) is other kidney disease. Patients with this syndrome are at risk for aggressive form of type 2 papillary renal carcinoma as well as cutaneous and uterine leiomyomas [77], and differently from the other renal carcinoma syndromes since it is generally present as a solitary lesion that can be highly aggressive and even metastases, which give a bad prognosis to the patient [72]. HLRCC was linked, by linkage analysis, to the fumarate Hydratase (FH), an enzyme from the Krebs cycle, and that is located in chromosome 1q42.3-q43 [74].

Since mutations and loss of the second allele were found in patients affected with this syndrome, FH seems to act as a tumour suppressor gene [77].

Even knowing this association between these syndromes and some genes, little is known and more studies about kidney cancer are necessary to understand better the molecular basis of this malignancy.

Oncocytic or Oxyphilic Tumours

Oncocytic tumours, also called Oxyphilic tumours represent a distinctive set of lesions composed by cells with a high number of mitochondria, which correspond to distinctive granular, voluminous and eosinophilic cytoplasm (Figure 8) [1]. Hürthle cell tumours are specific oncocytic neoplasms of the thyroid gland. These unusual neoplasm cells have a large number of mitochondria (4000 to 5000) with morphological, functional and genetic abnormalities [81]. It is a subgroup of tumours that appear in parenchymatous organs like thyroid, parathyroids, kidneys, salivary glands adrenals and in other endocrine organs [81, 82].

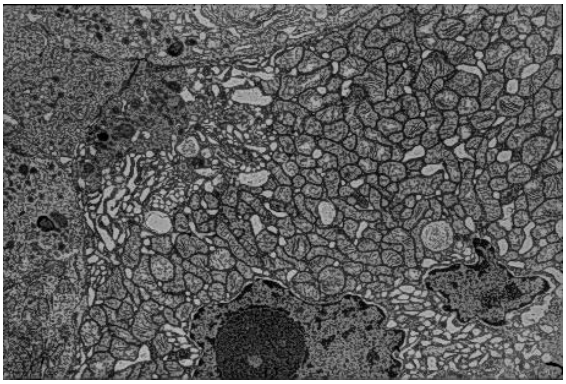

Figure 8 – Electronic microscopy image showing a cell with a high number of mitochondria, with an eosinophilic cytoplasm.

The lack of mitochondrial function is the presumable reason for the increased number of mitochondria by stimulation of its proliferation. This may be due to primary alterations of mitochondrial DNA (mtDNA) that encode mitochondrial enzymes [83]. A large deletion of mtDNA of about 4977bp (approximately one third of total mtDNA), also called “common deletion”, is the most characteristic alteration in oncocytic cells

[84]. Máximo *et al*. [83] also verified the existence of point mutations in the mtDNA genes that encodes enzymes required for complexes I and III to V of the MRC in Hürthle cells [83]. It was assumed that these mitochondria with altered mtDNA proliferate more than normal, leading to the increased number of mitochondria. It was also suggested that nDNA genes, that encode enzymes required for OXPHOS, can lead to the increase of mitochondrial number as a compensatory mechanism of deficient function [85, 86]. This can be explained because mitochondria is an important organelle required for energy metabolism and so, cellular requirement of ATP and OXPHOS dysfunction may lead to increase of mitochondrial number, in an attempt to compensate the weak production of energy [83].

There are evidences that all most all thyroid carcinomas have some oncocytic counterpart. Taking this in account, in the third edition of the World Health Organization (WHO) Book "Pathology and Genetics: Tumours of Endocrine Organs" the term Hürthle cell carcinoma was altered for oncocytic variant of follicular or papillary carcinomas [67].

AIMS

In recent years a large number of studies have attempted to evaluate GRIM-19 expression in several types of human tumours, as summarized before in table I. In all the studies, GRIM-19 was described as being downregulated in tumours when comparing with normal tissues from the same organ. However, none of the performed studies targeted oncocytic (or oxyphilic) tumours. Since GRIM-19 is a MRC complex I protein in which several subunits encoded by mtDNA were reported as being mutated in human oncocytic tumours and proposed to be one of the possible causes for the development of oncocytic tumours, we intended to clarify the role of GRIM-19 in this particular type of tumours. The study of Máximo *et al.* (2005) showed a possible and important role of GRIM-19 in the ethiopathogenesis of these Hürthle cell tumours (HCT) [1], but it needed to be confirmed.

1) Since our main aim was to understand the functional role of GRIM-19 in oxyphilic tumours, we analysed the expression of GRIM-19 in a series of thyroid tumours, including samples of Hürthle and non-Hürthle cell tumours from the major thyroid tumour histotypes (PTC, FVPTC, FTC, FTA) and ATC (the more aggressive histotype of thyroid tumours). GRIM-19 expression was evaluated by immunohistochemistry in paraffin-embedded tissues.

2) Oncocytic tumours are also frequent in kidney tumours. Alchanati *et al.* (2006) reported the importance of GRIM-19 in renal cell carcinomas, showing extremely low or even absence of GRIM-19 expression in some RCC [60]. However they did not include in their series the Renal Oncocytomas. Taking this into account, we also evaluated GRIM-19 expression, by immunohistochemistry, in a series of epithelial renal tumours: clear cell carcinomas, papillary carcinomas, chromophobe carcinomas and oncocytomas. With this evaluation we tried to better understand the importance of GRIM-19 in the etiopathogenesis of oncocytic tumours. Moreover we also intended to better clarify the GRIM-19 expression at the cellular level (mitochondria, cytoplasm and/or nucleus), a still controversial question.

3) Until now, several papers reported that STAT3 is overactivated or overexpressed when GRIM-19 was downregulated in tumours, as reviewed before in table I. However, GRIM-19 physiological interaction and regulation of STAT3 remains unclear. Since STAT3 apparently requires two principal phosphorylations (p-STAT3 Ser727 and p-STAT3 Tyr705) to become fully activated, and because Ser727 residue was identified as essential for GRIM-19—STAT3 interaction, we evaluated, by immunohistochemistry, the expression of the two phosphorylated forms of STAT3, trying to understand the possible role of GRIM-19 in the regulation of STAT3 activation and location. This evaluation was performed in the same series of renal and thyroid tumours used for GRIM-19 evaluation.

4) Some mutations in *GRIM-19* were found in Hürthle thyroid tumours. However, they were only observed in 4 of 26 cases [1]. GRIM-19 mutation can be one of the mechanisms by which GRIM-19 could be downregulated in tumours, but not the only mechanism taking into account the low frequency of such mutations. The study of Alchanati *et al.* (2006) indicates that epigenetic causes may contribute to GRIM-19 downregulation, at least in RCC, and perhaps in other type of cancers, since they observed that GRIM-19 mRNA was downregulated [60]. One of the possible epigenetic mechanisms involved is GRIM-19 promoter hypermethylation. With this purpose we intended to characterize the promoter region of this gene in order to access its methylation status. We used thyroid cancer cell lines available in our group to verify if any of them has low or even absent expression of GRIM-19 to use as primary model to study the promoter methylation, before the study in tumour samples.

This work is expected to contribute to a better understanding of the role of GRIM-19 in the etiopathogenesis of thyroid and kidney human tumours and, in particular, the involvement of GRIM-19 in ethiopathogenesis of oncocytic tumours. The status of STAT3 activation was also addressed in order to clarify how GRIM-19 is involved in STAT3 regulation.

MATERIAL AND METHODS

Material

The study was approved by the Ethical Committee of Hospital São João and the identity of all patients involved in this project was kept anonymous. All samples were obtained from the archives of Hospital São João - Porto and were selected by an expert pathologist of the same institution.

All samples are identified by a histological number indicating the institution where they came from (Hospital São João – H), followed by the year when the tissue was collected (the last two digits), the confidential number of the patient and the paraffin-embedded block, since it can exist more than one fragment from the same patient (B1, B2, B…). For example, the histological number H10/25330 B6 means that: the piece comes from Hospital São João, was collected in 2010, the confidential number of the patient is 25330 and it is the block 6 from this patient. The blocks were selected based in histotype of the tumour and by the presence of normal and tumoural tissue.

Haematoxylin and Eosin Staining (HE staining) was performed in all clinical samples of thyroid tumours and RCT (Renal cell tumours) with the objective of confirm the diagnosis of each case, and to select the normal adjacent and tumoural tissues for posterior DNA extraction for genetic analyses and to evaluate the expression of the different proteins under study.

In Figure 9 are represented the frequencies of each histotype of the thyroid tumours used in this project. We analysed 79 thyroid tumour lesions from 69 patients. The 79 lesions were classified as PTC (5 Hürthle and 12 non-Hürthle cell tumours), FTC (4 Hürthle and 3 non-Hürthle cell tumours), FVPTC (11 Hürthle and 20 non-Hürthle cell tumours), FTA (7 Hürthle and 7 non-Hürthle cell tumours) and 10 ATC.

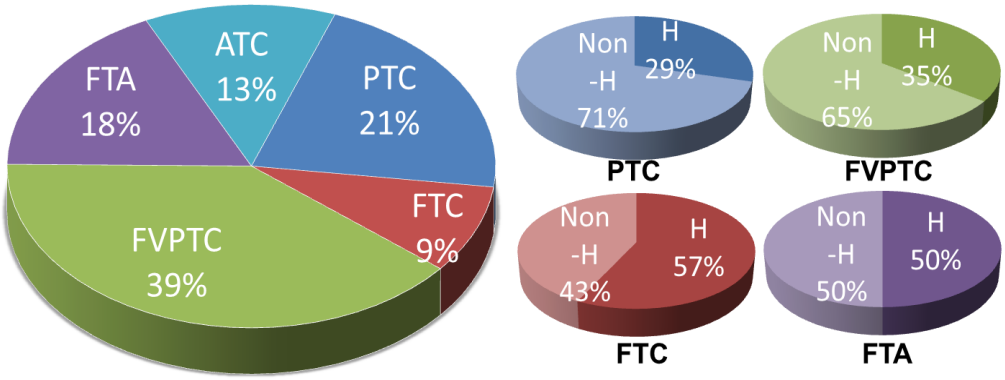

Figure 9 – Frequency of the histotypes of the thyroid tumours within this study (FTA – Follicular thyroid adenoma; PTC – Papillary thyroid carcinoma; FTC – Follicular thyroid carcinoma; FVPTC – Follicular variant of PTC; ATC - Anaplastic thyroid carcinoma), with Hürthle (H) and non-Hürthle (non-H) cell features.

In Figure 10 are represented the frequencies of each histotype of the RCT used in this project. Since the papillary renal cell carcinoma (PRCC) samples used in this project was in a small number, the types I and II were grouped as one only class, the PRCC.

We analysed 52 renal cell carcinomas from 44 patients. The 52 lesions were classified as CCRCC (n=20), CromRCC (n=3), PRCC (n=8), and ROnc (n=21). In this type of tumours there are no distinctions in oncocytic or non-oncocytic tumours inside each histotype, as is thyroid tumours. The oncocytic tumours are in a distinct histotype – Renal Oncocitoma and are considered benign lesions.

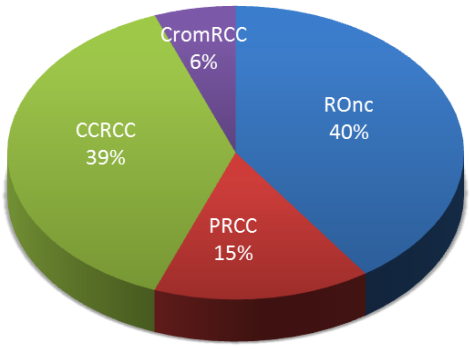

Figure 10 - Frequency of the histotypes of the kidney tumours within this study (CCRCC – Clear Cell Renal Cell Carcinoma; CromRCC – Chromophobe Rena Cell Carcinoma; PRCC – Papillary Renal Cell Carcinoma; ROnc – Renal Oncocitoma).

Paraffin-Embedded Tissue Microtomy

The paraffin blocks were placed into a refrigerated cold plate (CO-4, Kunz Instruments, Sweden) to harden the area to be cut. A sharp knife was installed in the microtome (Shandon Finesse 325, Thermo Scientific, UK) and the correct clearance angle and the desired thickness of the cut (2µm for HE and IHC or 10µm for DNA extraction) were set.

The paraffin block was then placed in the microtome with the correct orientation, being moved to the front until it reached the knife edge and a series of sections were cut. If required, the surface was fretted to adjust to the inclination of the sharp to obtain after a section of all tissue during the cuts. The material is gently moved to the surface of tap water with 100% v/v Ethanol to facilitate the flattening of the tissue section. The sections were placed in a warm water bath (~40ºC) to help the expansion of the tissue. Each section was then collected into a different glass slide and held vertically for further drying at least for a period of overnight or more at 37ºC.

Hematoxilin and Eosin (HE) staining

HE staining is a common method used in histology to observe a first overview of the structure of the tissue and specific areas like tumours in biopsy histological sections which, sometimes, can be histologically diagnosed by this simple technique. In other cases, it serves only as a first brief diagnosis that will be confirmed by other techniques.

Slides with 2 µm, from the paraffin-embedded tissue sections, were deparaffinised in Clear Rite (Richard-Allan Scientific, MI, USA) for 10 minutes for 2 times. Next, slides were rehydrated in 100, 100, 95 and 70% graded alcohols for 10, 5, 5, 5 minutes respectively and then in current water for 5 minutes.

Slides were stained with Gill 3 Haematoxylin (Richard-Allan Scientific, MI, USA), which stains the nucleus and basophilic structures with an intense blue, for five seconds, and washed for 3 minutes in current water. After this, the intense blue need to be attenuated and so, slides were placed in ammoniac water (fresh solution with current water and 1.5 mL of ammoniac) for 15 seconds with manual agitation and then washed again for 5 minutes in current water before the contrast stain. Acidophilic structures are

stained with Alcohol-based acidic eosin Y (Richard-Allan Scientific, MI, USA). With this purpose, slides were placed in 95% alcohol for 5 minutes and then stained with eosin alcoholic for 5 minutes.

To finish slides were dehydrated, clearing and coverslipped. Thus, slides were dehydrated in grades alcohols (95, 100 and 100% (v/v)) for 5, 10 and 10 minutes, respectively, and clearing with Clear Rite (Richard-Allan Scientific, MI, USA) for ten minutes two times. To end the procedure, slides were coverslipped with Mounting Medium (Richard-Allan Scientific, MI, USA). The slides were left to dry overnight and, if required, one more day to dry completely.

Immunohistochemestry assay

This approach was used to evaluate, for each clinical sample, the expression of the following proteins using the respective antibodies: SDHA [Complex II subunit 70kDa monoclonal antibody – Ref. #MS204 (MitoSciences Inc., Eugene, USA)], GRIM-19 [Complex I subunit GRIM-19 monoclonal antibody – Ref. #MS103 (MitoSciences Inc., Eugene, USA)], total STAT3 [Stat3 antibody – Ref. #9132 (Cell Signaling Technology Inc, Danvers, USA)], STAT3 phosphorilated in residues Serine 727 and Tyrosine 705 [Phospho-Stat3 (pSer727) (6E4) Monoclonal antibody – Ref. #9136 (Cell Signaling Technology Inc, Danvers, USA) and Phospho-Stat3 (pTyr705) (D3A7) Rabbit mAb – Ref. #9145 (Cell Signaling Technology Inc, Danvers, USA), respectively]. The procedure for these antibodies was performed with (Avidin-Biotin) Streptavidin-Peroxidase method.

Other two antibodies (MMP-2 – Rabbit Anti-Human MMP-2 Polyclonal Antibody Ab 19167 [Chemicon (Millipore), Billerica, USA] and VEGF – Mouse monoclonal [VG-1] Ab1316 [Abcam, Cambridge, UK]) were used in a few number of samples using EnVision^{TM} G|2 System/AP, Rabbit/Mouse (Permanent Red) kit (DAKO Corporation, CA, USA) that is based in alkaline phosphatase enzyme to obtain the staining.

Slides with 2 μm were deparaffinised in Clear Rite (Richard-Allan Scientific, MI, USA) for 10 minutes 2 times. After slides were rehydrated in 100, 100, 95 and 70% graded alcohols for 10, 5, 5, 5 minutes respectively and then in current water for 5 minutes.

The next step is antigen retrieval which is different to each antibody. Thus, slides were subjected to microwave treatment with the conditions described in the table II.

Table II – Antibodies used and respective conditions used in the procedures of IHC.

Primary antibody	Antigen retrieval	Antibody dilution	Incubation time	Incubation temperature
SDHA	1mM EDTA pH 9.00 solution at sub-boiling temperature for 10 minutes	1:1250	1 hour	Room temperature
GRIM-19	1mM EDTA pH 9.00 solution for 20 minutes at sub-boiling temperature	1:1250	1 hour	Room temperature
STAT3	10 mM sodium citrate buffer, pH 6.00 solution for 15 minutes at sub-boiling temperature	1:350	overnight	4ºC
p-STAT3 Tyr705	1mM EDTA pH 8.00 solution for 15 minutes at sub-boiling temperature	1:50	Overnight	4ºC
p-STAT3 Ser727	10 mM sodium citrate buffer, pH 6.00 solution for 15 minutes at sub-boiling temperature	1:100	Overnight	4ºC
VEGF	10 mM sodium citrate buffer, pH 6.00 solution for 10 minutes at sub-boiling temperature	1:700	1 hour	Room temperature
MMP-2	No antigen retrieval	1:60	30 minutes	Room temperature

Slides were cooled for 30 minutes and then washed with washing buffer [PBS1x/Tween20 (0.02%)] for 2 times (5 minutes) and tissues were delimited with a hidrofobic pen. After this step, different procedures were performed having in account with the antibody and respective procedure used.

(Avidin-Biotin) Streptavidin-Peroxidase method

This method is based in Peroxidase enzyme labelled to streptavidin as method of detection of the antigen. The DAB (3,3' Diaminobenzidine) substrate-chromogen system is high-sensitive forming a brown product when oxidation occurs by the peroxidase present in the local of the antigen in the tissue.

In order to reduce non-specific background staining it was performed a series of blocks. It was blocked endogenous peroxidase with 3% (v/v) hydrogen peroxide in methanol, endogenous avidin with Avidin Block (Thermo Scientific, Fremont, CA,

USA), biotin with Biotin block (Thermo Scientific, Fremont, CA, USA) each one for 10 minutes incubation and with 2 washes with Wash buffer of 5 minutes between each block. To incubate with the primary antibody, slides were washed again, incubated for 10 minutes with Ultra V Block (Thermo Scientific, Fremont, CA, USA) and then incubated with the primary antibody diluted in UltraAb Diluent (Thermo Scientific, Fremont, CA, USA) according to the condition described previously in table II.

Posteriorly, slides were washed for 3 times with wash buffer for 5 minutes each, overlaid with secondary antibody (Biotinylated Goat Anti-Polyvalent – Thermo Scientific, Fremont, CA, USA) for 10 minutes and with Streptavidin Peroxidase (Thermo Scientific, Fremont, CA, USA) for 10 minutes at room temperature, washed between them for 2 times, 5 minutes. Antigen detection was performed with DAB (DakoCytomation Liquid DAB + Substrate Chromogen System, DAKO Corporation, CA, USA) for 20 minutes. Slides were counterstained with Mayer's Hematoxilin (Bio-Optica Milano) during 10 seconds.

Finally, slides were dehydrated in grades alcohols (95, 100 and 100% (v/v)) for 5, 10 and 10 minutes, respectively, and clearing with Clear Rite (Richard-Allan Scientific, MI, USA) for ten minutes two times. To end the procedure, slides are coverslipped with Mounting Medium (Richard-Allan Scientific, MI, USA). They were left to dry overnight and, if required, one more day to dry completely.

EnVision™ G|2 System/AP, Rabbit/Mouse (Permanent Red) kit

This procedure is based in alkaline phosphatase-labelled amplification polymer to obtain the staining correspondent to the antigen of interest. It is based in a polymer amplification of the signal. A pink/red staining is obtained with this procedure since the reaction is visualized by Permanent Red Chormogen which is included in kit.

The procedure was performed accordingly to manufacturer's instructions [EnVisionTM G|2 System/AP, Rabbit/Mouse (Permanent Red) kit – DAKO Corporation, CA, USA]. The procedure was performed accordingly to manufacturer's instructions. The mounting of the slides were performed using aqueous mounting medium (Aquatex®, Merck, Darmstadt, Germany).

The immunohistochemistry results were evaluated by two observers (VM and MC) blinded to the clinical information of the cases. The results were evaluated considering the intensity of the staining for GRIM-19 and proportion of the cells/tissue

showing a positive staining for STAT3's antibodies. Cellular localization was also evaluated. Intensity was graded as 0 (no staining), 1 (a very weak staining), 2 (weak), 3 (moderate) and 4 (strong intensity). The percentage of cells/tissue positive stained was classified as 0 (≤ 5%), 1 (>5 and ≤25%), 2 (>25 and ≤50%), 3 (>50 and ≤75%) and 1 (>75). For p-STAT3's antibodies, a score were obtained by multiplying the intensity and percentage of positive staining. Immunoreactivity scores were classified as follows: negative (0), low (1), moderate (2, 3, 4, 6 and 8), or high (9, 12 and 16).

Table III – Immunohistochemical classification for GRIM-19, Phospho-Stat3 Tyr 705 and Phospho-Stat3 Ser 727.

GRIM-19	Intensity of staining	0	Absent
		1	Very low
		2	Low
		3	Moderate
		4	High
p-STAT3 Tyr705 and Ser727	Intensity of staining	0	Absent
		1	Very low
		2	Low
		3	Moderate
		4	High
	Percentage of stained cells	0	0 to ≤5%
		1	5% to ≤25%
		2	25 to ≤50%
		3	50 to ≤75%
		4	75 to 100%
	Combination of intensity and percentage of staining	0	0
		1	1
		2	2, 3, 4, 6, 8
		3	9, 12, 16

GRIM-19 promoter identification

For this purpose we used a web site (http://www.cpgislands.com/) which has a simple user interface to identify CpG islands, the ***The CpG Island Searcher*** which use an established a CpG-island-extraction algorithm developed by Takai, D and his group [87, 88].

We searched for the sequence of GRIM-19 (also called NDUFA13) in *ENSEMBLE* web site[89] and searched for the 5' upstream sequence at the beginning of the gene. Once this was obtained, the sequence were used in the referred web site[90] using the next parameters: %GC 55%; ObsCpG/ExpCpG 0.65; Length 500bp and Gap between adjacent islands 500bp. After submission, a possible and with high probability region of CpG islands correspondent to promoter sequence was obtained.

RNA extraction from cell lines

One mL of TRIzol Reagent (Life Technologies$_{TM}$, California, USA) was added directly to the cells previously collected to an eppendorf of 2mL and passed the cell lysate several times through the pipette. The remaining protocol was performed according to manufacturer's instrctions (TRIzol® Reagent, Life Technologies$_{TM}$, California, USA).

RNA was using NanoDrop® ND-1000 Spectrophotometer (NanoDrop Technologies, Inc., Delaware, USA) using RNase-free water as blank.

Reverse Transcriptase – Polymerase Chain Reaction (RT-PCR)

RT-PCR was performed in two steps. The first was used to perform the reverse transcription reaction, obtaining the cDNA from de mRNA. Posteriorly, conventional PCR was performed using cDNA obtained from the first step.

Reverse transcription reaction

The cDNA synthesis was performed with 1µg of RNA, using 100ρmol random hexamer primer (Fermentas), 220U RevertAidTM M-MuLV Reverse Transcriptase (Fermentas), 5x reaction buffer (Fermentas), 20U RiboLockTM RNase Inhibitor (Fermentas) and 1mM dNTPs mix (Bioron), to a final volume of 20µL. The thermal cycling conditions were 10 min at 25ºC, followed by 60 min at 37ºC and finally 5 min at 99ºC. The reactions were performed on a Bio-Rad MyCyclerTM Thermal Cycler (BIO RAD, CA, USA).

PCR (Polymerase Chain Reaction)

The primer sequences (forward and reverse) were designed based in GRIM-19 sequence available on ENSEMBL human sequence database. In table IV are described the primer sequences, the amplification size of the product and the optimal annealing temperature obtained after PCR optimization. A negative control was included in each PCR reaction, in order to detect possible PCR contamination.

Table IV - Primers sequences, its correspondent annealing temperature and product size.

	Primer	Primer sequences (5'-3')	Product size (bp)	Annealing Temperature (ºC)
Actin	Forward	CTTCCTTCCTGGGCATGGAGTC	155	58
	Reverse	CTTCTGCATCCTGTCGGCAATG		
GRIM-19	Forward	TACAGCATGCTGGCCATAGGGAT	175	58
	Reverse	AGGTTCTCCCGAAGCATCTGCAA		

After optimization, PCR amplifications were performed in 25 µL volume containing ~20µg of cDNA obtained from the RT reaction, 0.1µM of each of the forward and reverse primers (Invitrogen, UK), 1x PCR Buffer (5x Green GoTaq® Flexi Buffer, Promega, WI, USA), 1.5mM of Magnesium Chloride Solution (Promega, WI, USA) and 0.5U of GoTaq® DNA polymerase (Promega, WI, USA) and deionised water to fulfill the total reaction volume. The PCR reactions were performed in BIO RAD MyCycler™ thermal cycler (BIO RAD, CA, USA) with the following cycling conditions: a single predenaturation step at 94ºC for 5 minutes, followed by 35 cycles of denaturation at 94ºC for 30 seconds, annealing at a variable temperature for 30 seconds, elongation at 72ºC for 30 seconds, and a final elongation at 72ºC for 10 minutes. A negative control was included in each PCR reaction, in order to detect possible PCR contamination. A positive control was used to access the RT reaction: actin amplification was used with this purpose.

Electrophoresis in Agarose Gel

PCR products were separated by electrophoresis on a 2% w/v agarose gel and stained with Gel Star (Cambrex, Iowa, USA). Once polymerised, the gel was placed on an electrophoresis apparatus, previously filled with running buffer – 1x SGTB

(prepared from stock solution 10x) [Grisp, Porto, Portugal]. The addition of 5x ColorLess GoTaq® Flexi Buffer in the PCR mix allowed reactions to be loaded directly onto gels without loading dye, as this buffer contains a blue and yellow dye which migrates at the same rate as a 3-5kb DNA and faster than primers (<50bp), respectively. One kB Plus DNA Ladder (Invitrogen, UK), was used to have a control for the fragment length that are being analysed. Electrophoresis was then carried out at 80V for approximately 30-40 minutes.

The fluorescent intensity of the separated PCR products was visualised and photographed in the Quantity One – version 4.6.9 in the ChemiDoc^{TM} XRS Imaging system (BIO RAD, CA, USA).

DNA extraction from paraffin-embedded tissues

Using the hematoxilin-Eosin stained slides as guide, 10µm paraffin-embedded tissue section of the same block were macrodissected by light-microscopic macrodissection, separating the tumour area from the adjacent normal region and collected for an eppendorf of 1.5mL.

It was added 300µL of xilol to each eppendorf with paraffined material, shaked with vortex for a few seconds and then left for 5 minutes at least. Then, a centrifugation was performed with 16000g for 3 minutes at 4ºC and with further discard of the supernatant to separate the tissue from the paraffin. The procedure with xilol was repeated for more 2 times. After, 300µL of absolute ethanol (100% v/v) pro-analysis were added, eppendorfs were inverted about 50 times and then left for 5 minutes. It was performed a centrifugation with 16000g during 3 minutes at 4ºC and supernatant was discarded. This step was repeated one more time and then pellet was dried at 70ºC. 300µL of Cell Lysis solution – Ref. CL-250 (Citomed, Lisboa, Portugal) was added and overturned some times. Next was added 3µL of Proteinase K (20mg/mL), homogenised and incubated overnight at 55ºC with agitation with approximately 140 rpm.

In the next day, if material was not completely digested, was added more 1.5µL of Proteinase K and incubated for more 2 or 3 hours until all material was digested. All tubes were cooled at room temperature. It was added 100µL Protein Precipitation solution – Ref. PP125 (Citomed) and shaked vigorously for 20 seconds and was left in ice for 5 minutes, at least. A centrifugation was performed at 16000g, 0ºC for 3 minutes

and supernatant was transferred for a new tube (with 300µL of Isopropanol (Propan-2-ol) and 0.5µL of Glycogen) and inverted for 50 times. A new centrifugation was executed at 16000g and 4ºC for 3 minutes and supernatant was rejected with special careful to not remove the pellet – DNA. Next, DNA was washed with 300µL of Pro-analysis Alcohol and centrifuged for 16000g, 4ºC for 3 minutes, supernatant removed and this step repeated for two more times. To finish, the pellet of DNA was dried on air or at 50ºC and then eluted in 20µL of DNase and RNase free water.

Posteriorly, extracted DNA was quantified using NanoDrop® ND-1000 Spectrophotometer (NanoDrop Technologies, Inc., Delaware, USA) using DNase and RNase free water as blank. This full-spectrum (220-750nm) spectrophotometer measures 1µL samples with high accuracy and reproducibility.

DNA extraction from cell lines

This procedure was performed using Invisorb® Spin Tissue Mini Kit. The process was done accordingly to the manufacturer's instructions (Invisorb® Spin Tissue Mini Kit, Invitek, Berlin, Germany) for DNA isolation from 10-10^6 eukaryotic cells/cell pellets.

Extracted DNA was quantified using NanoDrop® ND-1000 Spectrophotometer (NanoDrop Technologies, Inc., Delaware, USA) using Elution Buffer D (Invisorb® Spin Tissue Mini Kit, Invitek, Berlin, Germany) as blank.

DNA methylation analysis

Bissulfite conversion and cleanup of converted DNA

This procedure was performed using EpiTect® Bisulfite kit. Methylation of DNA which usually occurs in cytosine residues, especially in CpG dinucleotides in small regions of DNA, the CpG islands that usually are clustered to regulatory region of the genes (like promoter). Methylation of these regions is usually associated with gene inactivation. With bisulfite conversion of the DNA, the unmethylated cytosines are converted into uracil, while methylated cytosines do not suffer any change. In this way, it is possible to determine different DNA sequences for methylated and unmethylated DNA which allows determining if DNA is methylated by a different sequence from the non-treated DNA (Figure 11).

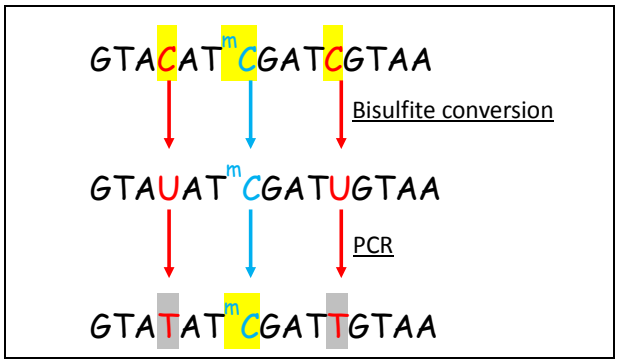

Figure 11 – Schematic representation of bisulfite reaction and detection of methylation.

The procedure was performed as manufacturer's instructions (EpiTect® Bisulfite kit, Qiagen, Hilden, Germany).

Extracted DNA was quantified using NanoDrop® ND-1000 Spectrophotometer (NanoDrop Technologies, Inc., Delaware, USA) using Buffer EB (EpiTect® Bisulfite kit, Qiagen, Hilden, Germany) as blank.

PCR amplification

The primer sequences (forward and reverse) were designed based in GRIM-19 promoter sequence obtained. The primers were constructed to anneal to a region without CGs to avoid the annealing in a region that can be altered by the bisulfite conversion, which could modify or even avoid the annealing of the primers to the DNA (Figure A1).

LRP1B promoter region was used as a control for bisulfite reaction. The conditions were performed with a primary PCR and a second *Nested PCR* accordingly to Prazeres *et al.* [91] conditions. The schematic representation of CGs is presented in Figure A2.

In table V are described the primer sequences, the amplification size of the product and the optimal annealing temperature obtained after PCR optimization. A negative control was included in each PCR reaction, in order to detect possible PCR contamination.

Table V - Primers sequences for methylated DNA, its correspondent annealing temperature and product size.

	Primer	Primer sequences (5'-3')	Product size (bp)	Annealing Temperature (ºC)
GRIM-19 Met	Forward	TGCTCAGGTCTGGGTAGCCAT	~436	61.8
	Reverse	TCCAAGGTGAAGGTGGCCACA		
Extern for LRP1B	Forward	GTAGGAGAAGGTTGATTGGTTGG	~300	58
	Reverse	TTCACACTCACTTATCTACAAACATC		
Intern (nested) for LRP1B	Forward	ATTTTTAGTGATATTTGTAAATGA	~230	52
	Reverse	AAAAAATATTCTCCTTACCT		

After the optimization, PCR amplifications were performed in 25 µL volume containing 100ng of bisulfite converted DNA, 0.05µM of each of the forward and reverse primers (Invitrogen, UK), 1x PCR Buffer (5x ColorLess GoTaq® Flexi Buffer, Promega, WI, USA), 2mM of Magnesium Chloride Solution (Promega, WI, USA) and 1.5U of GoTaq® DNA polymerase (Promega, WI, USA) and deionised water to fulfil the total reaction volume. The PCR reactions were performed in BIO RAD MyCycler^{TM} thermal cycler (BIO RAD, CA, USA) with the following cycling conditions: a single predenaturation step at 94ºC for 5 minutes, followed by 40 cycles of denaturation at 94ºC for 30 seconds, annealing at 61.8ºC (as described in table V) for 30 seconds and elongation at 72ºC for 45 seconds, and a final elongation at 72ºC for 10 minutes. A negative control was included in each reaction, in order to detect possible contamination.

The conditions for the gene LRP1B were the ones described by Prazeres *et al.* [91].

Electrophoresis in Agarose Gel

This procedure was performed as described previously. It allows checking if any bisulfite converted DNA was amplified in the polymerase chain reaction. If it was observable a band in the agarose gel, it was extracted, DNA purified and a sequencing reaction was performed.

DNA extraction from agarose gel

The EasySpin – DNA Gel extraction kit (EasySpin, Citomed, Lisboa, Portugal) was used to perform the DNA extraction. The procedure was performed as manufacturer's instructions (EasySpin, Citomed, Lisboa, Portugal).

Extracted DNA was quantified using NanoDrop® ND-1000 Spectrophotometer (NanoDrop Technologies, Inc., Delaware, USA) using Elution Buffer (EasySpin, Citomed, Lisboa, Portugal) as blank.

Sequencing Reaction

For sequencing reaction of the PCR products, a mix of 0.6 µL of BigDye® Terminator (Perkin-Elmer, California, USA), 3.5 µL of sequencing buffer (Perkin-Elmer, California, USA), 0.3 µL of reverse or forward primer (0.1µg/µL) (Invitrogen, UK), 3 µL of purified PCR product and deionised water were added to a final volume of 10 µL were placed in a PCR reaction tube. The sequencing reaction was performed in a BIO RAD MyCycler™ thermal cycler (BIO RAD, CA, USA) for the forward and reverse primers with the following cycling conditions: a single predenaturation step at 94ºC for 30 seconds, followed by 35 cycles of denaturation at 94ºC for 10 seconds, annealing at 59.8ºC for 10 seconds and elongation at 60ºC for 4 minutes, and a final elongation at 60ºC for 10 minutes.

In order to submit each sample to the ABI prism 3130 xl Automatic sequencer (Perkin-Elmer, Foster City, California, USA) the sequenced product had to be purified and precipitated.

A column of Sephadex (Sephadex™ G-50 Fine, GE Healthcare Bio-sciences AB, Uppsala, Sweden) was prepared adding 700µL of Sephadex (6.66g/100mL) and centrifuging at 3200 rpm, 4ºC for 2 minutes twice to remove the maximum of the liquid. The columns were transferred from the collecting tubes to a clean eppendorf, and the 10µL of sequencing reaction was added to the centre of the columns. A centrifugation was performed at 3200 rpm, 4ºC for 4 minutes. The final product was dried and DNA was ressuspended in 15µL of formamide to maintain the single stranded DNA. All the samples were then submitted to the ABI prism 3130 xl Automatic sequencer (Perkin-Elmer, Foster City, California, USA), for further automated sequencing analysis.

Statistical Analysis

All data was statistically analysed using StatView – version 5.0 – software (SAS Institute Inc., Cary, NC). The relationship between the results in terms of protein expression between different groups was evaluated using Student's t-test. Since the classifications given were nominal variables, it was necessary to convert them into continuous ones. A numeric value was therefore, given to each level of intensity according to table III. Analysis for two categoric variables was performed by Chi-square statistical test, or Fisher's test when the distribution show values less than 5 ($n<5$) for more accuracy of the statistical relations.

All statistical analysis referred following in results, are present in annex I more detailed.

RESULTS

Histological Analysis

There are several features that distinguish each histotype and subtypes of thyroid tumours. FTA are encapsulate tumours (not represented in the figure) showing follicular cell differentiation. FTC has the same characteristics mentioned for FTA, but presents capsule invasion (yellow arrows in Figure 12) and/or vascular invasiveness, being this the main distinguishable characteristic from FTA. PTC is composed by papillary architecture, large nucleus and pale staining, in addition to other characteristics that are not visible in these figures: irregular “grooved” and “ground glass” nuclei. FVPTC is a combination of FTC and PTC, since it has follicular architecture in at least 95% of the tumour and the nuclei present the same characteristics as the PTC. Finally, ATC are regarded as highly aggressive tumours characterized by loss of cell differentiation; usually these carcinomas are evaluated by analysis of the expression of thyroid markers. Figure 12 shows representative images of each histotype of thyroid tumours.

The different histotypes can have oncocytic and non-oncocytic features. The cells of oncocytic tumours show distinctive granular, voluminous and eosinophilic cytoplasm. As shown in Figure 12, the Hürthle (or oncocytic) cell tumours present the granular and large cytoplasm due to the high number of mitochondria present in cells.

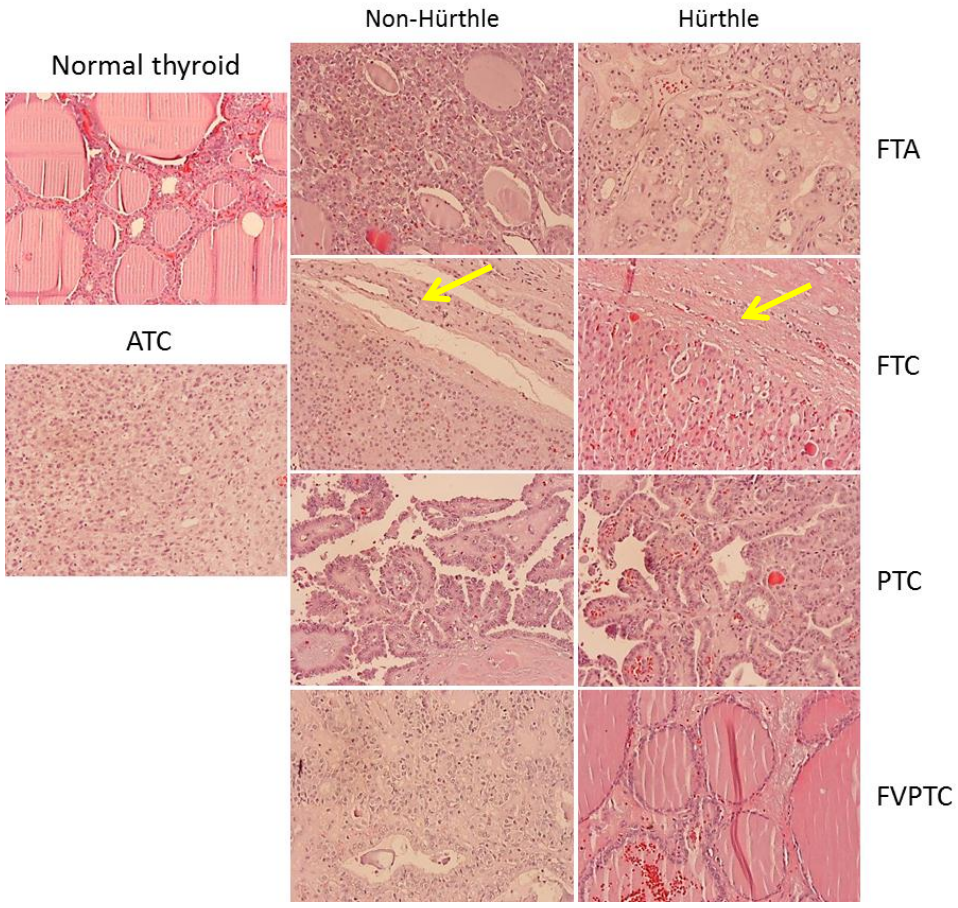

Figure 12 – Histological pictures from normal thyroid tissue and the major histotypes of thyroid tumours. Yellow arrows – capsule invasion in FTC histotype. All pictures were taken with 20x magnification.

As in thyroid, different RCT histotypes are distinguishable by the presence of specific histological characteristics of each one and from normal kidney tissue.

The normal kidney presents the glomerulus, Bowman's capsule and renal tubules, the constituents of the basic structural unit of the kidney – the nephron. The tumours do not show these structures, and even do not show an organized structure.

CCRCC present, as the major and more notorious characteristic, a clear cytoplasm, but also show large and polygonal cells. CromRCC show cells with prominent cell membranes and pale cytoplasm. PRCC are probably the more distinguishable histotype from the other ones, since the papillae structures are clearly the major characteristic. The distinction between papillary type I or II is sometimes difficult, but the papillary carcinoma type II has a more voluminous cytoplasm with a higher number of mitochondria, although not as high as in oncocytomas. ROnc presents

round cells that are very similar between them and an eosinophilic cytoplasm. The referred characteristics are shown in Figure 13.

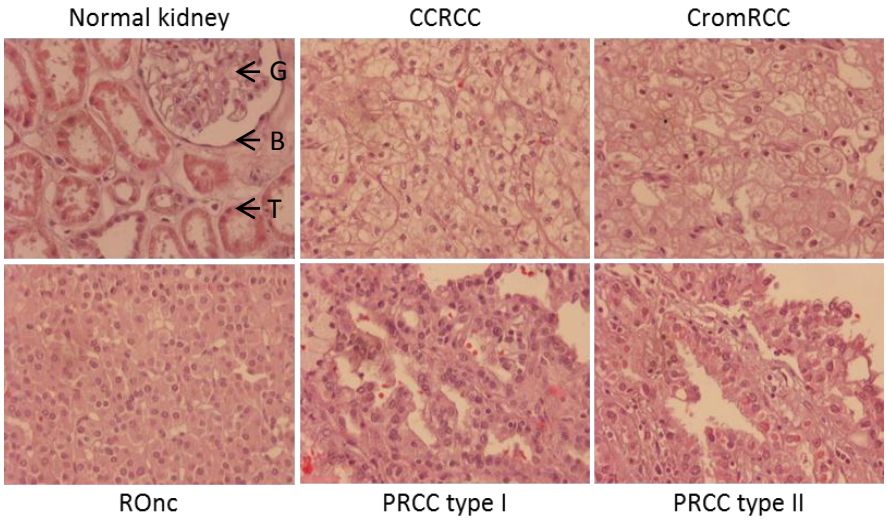

Figure 13 - Histological pictures from normal kidney tissue and the major histotypes of RCT. In the normal kidney tissue is possible to observe the glomerulus (G), the Bowman's capsule (B) and the tubules (T). All pictures were taken with 40x magnification.

GRIM-19 expression in tumours

Immunohistochemistry was performed to evaluate GRIM-19 expression in the thyroid and kidney tumours from our series, as well as in normal adjacent tissue, whenever present.

The expression, by immunohistochemistry, of Succinate dehydrogenase complex, subunit A (SDHA) was used as a positive control for the same cases evaluated for GRIM-19. SDHA stained all the mitochondria present within the cell, which allow checking the amount of mitochondria in the cells. It also allows distinguishing between oncocytic and non-oncocytic tumours. A second internal and positive control for each tumour sample was the expression of GRIM-19 in normal adjacent tissue.

GRIM-19 expression in thyroid tumours

Our data clearly showed that SDHA stains the cytoplasm of the cells (Figure 14 - pictures A). It is possible to compare the relative number of mitochondria in the several cases. Comparing the normal thyroid tissue with the non-Hürthle thyroid tumours, it appears not to be considerable differences in mitochondria number. However, when comparing normal thyroid tissue with the Hürthle cell thyroid tumours, there is an obvious difference in the relative number of mitochondria, showing, the Hürthle cell tumours, a higher amount of mitochondria - it is possible to observe an intense staining of the cytoplasm (Figure 14 – pictures A), characteristic of a mitochondria-rich cytoplasm.

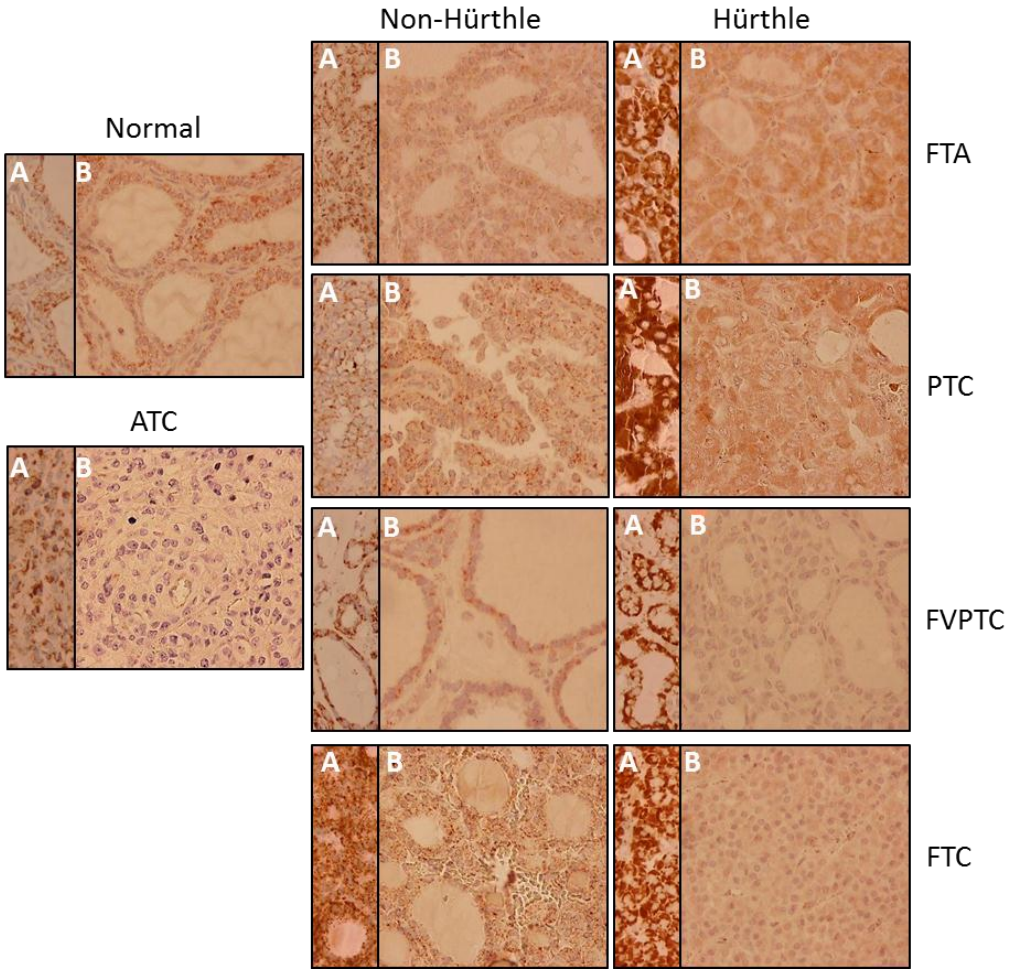

Figure 14 – SDHA (A – left) and GRIM-19 (B – right) expression in different histypes of thyroid tumours. All the pictures were taken with 40x magnification.

Concerning GRIM-19 expression, it is clearly observable that the GRIM-19 antibody stained the cytoplasm, but not the nucleus (Figure 15).

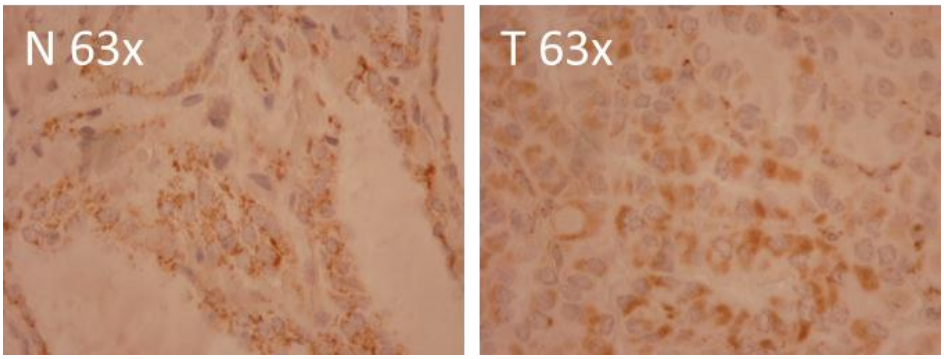

Figure 15 – Normal (N) and tumour (T) thyroid tissues showing GRIM-19 expression only in cytoplasm.

Comparing the GRIM-19 expression, between the different thyroid tumour histotypes and the normal adjacent tissue, it is possible to observe that FTCs (p=0.010) *and* ATCs (p=0.003) are the ones that show greater loss of GRIM-19 expression, as shown in Figure 16.

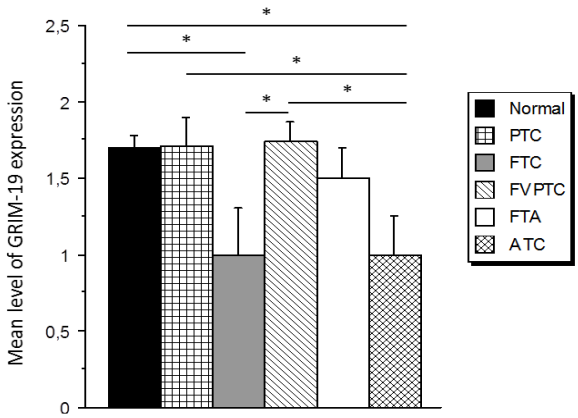

Figure 16 – GRIM-19 mean staining intensity in the different thyroid tumours and normal thyroid tissue (statistically significant difference: * - p< 0.05).

We attempted to investigate if there were differences between Hürthle *versus* non-Hürthle phenotypes of the different histotypes, concerning GRIM-19 expression. It was possible to observe that in all histotypes, HCT showed loss of GRIM-19 expression when comparing with the non-Hürthle cell tumours from the same histotype. A difference statistically significant was observed between Hürthle and non-Hürthle FVPTC (p=0.003) and between Hürthle and non-Hürthle FTC (p=0.046) (Figure 17 – A).

Grouping the tumours into Hürthle and non-Hürthle cell tumours, independently of their histotype, it was possible to note that the HCT had lower GRIM-19 expression than the normal thyroid tissues (p=0.0008) and the non-Hürthle cell tumours (p<0.0001) (Figure 17 – B). ATC were not used in these two observations since they do not have oncocytic features.

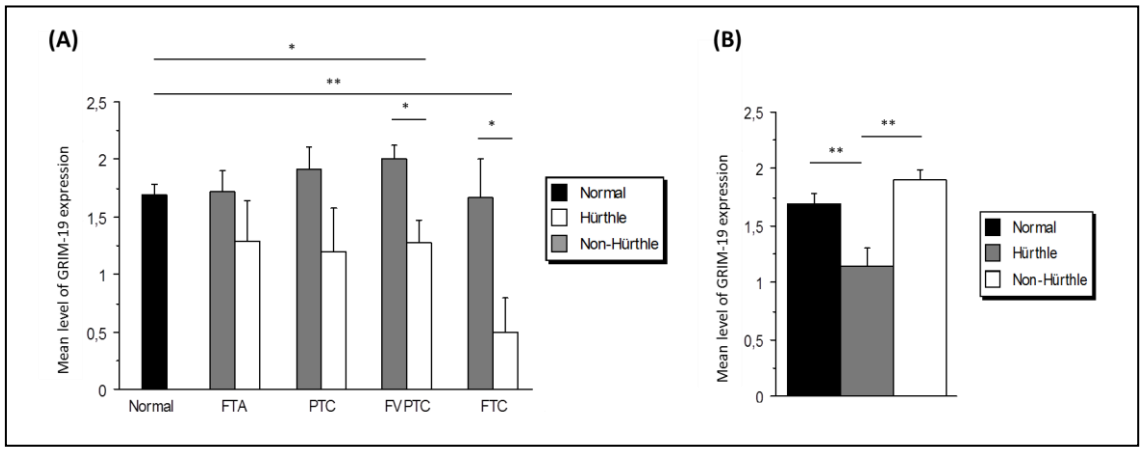

Figure 17 - GRIM-19 mean staining intensity in the different thyroid tumours grouped in Hürthle and non-Hürthle and normal thyroid tissue (A). GRIM-19 mean intensity in the normal tissue, Hürthle and non-Hürthle cell tumours (B) of the thyroid (statistically significant difference: * - p< 0.05; ** - p< 0.001).

Comparing with normal-matched thyroid tissue, we found that 18 out of 27 (67%) of the HCT lost GRIM-19 expression, being this loss complete in 4 out of 27 (15%) tumours. Concerning the non-Hürthle cell tumours, loss of GRIM-19 expression (when compared with normal-paired tissue) it was only observed in 2 out of 42 cases (5%).

GRIM-19 expression in kidney tumours

As observed in thyroid tumours, SDHA and GRIM-19 antibodies stained only the cytoplasm and not the nucleus of the cells. Since SDHA provides an idea about the number of mitochondria, it was possible to observe that ROnc presented a higher number of mitochondria. PRCC also present a higher amount of mitochondria, although less than ROnc. CromRCC and CCRCC present similar staining for SDHA as normal kidney tissue and less than ROnc and PRCC (Figure 18).

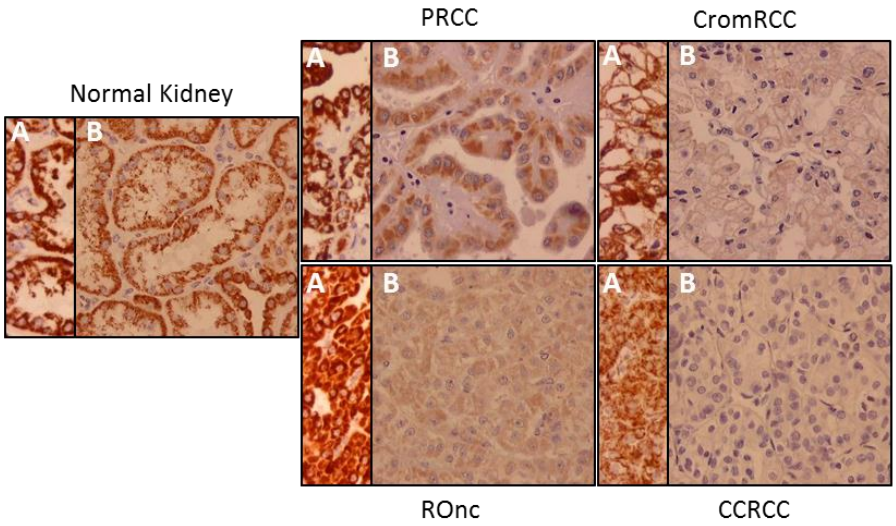

Figure 18 - Immunohistochemical analysis of SDHA (A) and GRIM-19 (B) expression in kidney tumours and normal tissue. All pictures were taken with 40x magnification.

GRIM-19 was evaluated in renal tissues based in the intensity of the staining. Overall loss of GRIM-19 expression in all RCT histotypes was observed (p<0.0001) (Figure 19 – A), being this loss higher in ROnc (p<0.0001), CromRCC (p<0.0001), and CCRCC, (p<0.0001) than in PRCC (p=0.002) when compared with the normal kidney tissue (Figure 19 - B). It is necessary to mention that we have only 3 samples of CromRCC.

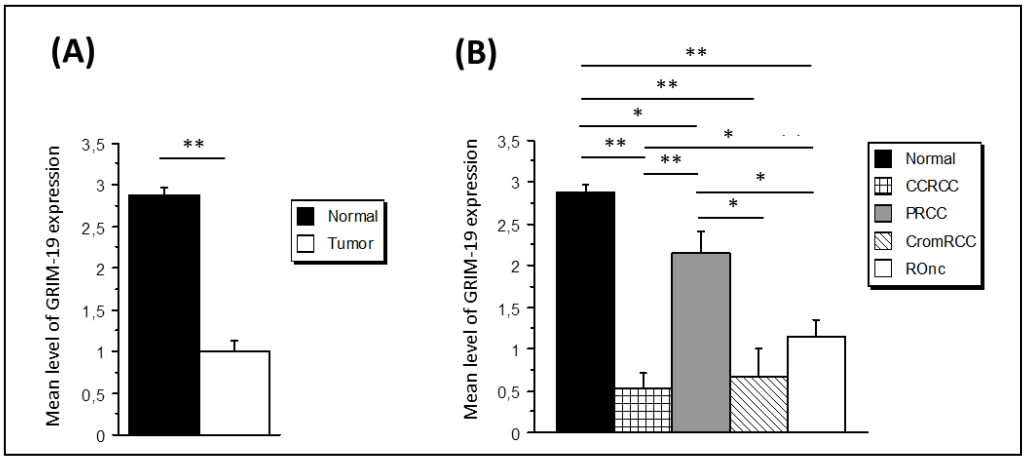

Figure 19 - GRIM-19 mean staining intensity in the normal kidney and kidney tumours grouped (left) and in the different kidney tumour histotypes (right). (statistically significant difference: * - p< 0.05; ** - p< 0.001).

Loss of expression (downregulation) of GRIM-19 was observed in 35/40 (88%) of RCT, being 11/11 CCRCC (100%), 2/2 CromRCC (100%), 19/20 ROnc (95%) and 3/7 PRCC (43%) comparing with the normal-matched kidney tissue (whenever present).

STAT3 expression in tumours

In this study, the controversial physical and functional interaction of GRIM-19 with the STAT3 transcription factor was addressed. With this purpose in mind, evaluation was done by immunohistochemistry, the expression of total STAT3 as well the expression of the both phosphorylated isoforms [Tyrosine 705 (p-STAT3 Tyr705) and Serine 727 (p-STAT3 Ser727)] assumed to be the required phosphorylations for STAT3 activation.

Total STAT3 was used as a control for phosphorylated forms of STAT3, and was evaluated in the same tissues as them. The second objective was to observe the presence of total (phosphorylated and unphosphorylated) STAT3 in nucleus, cytoplasm or in both compartments on different cases. Concerning total STAT3, it was observable that all the compartments showed brown staining, both in thyroid and kidney (Figure 20) and for this reason; it was only used as a positive control for p-STAT3 antibodies. A second positive control for phosphorylated STAT3 was the normal adjacent tissue.

The anaplastic histotype of thyroid tumours were not evaluated for STAT3 antibodies due to the low quantity of material, since they are rare histotypes.

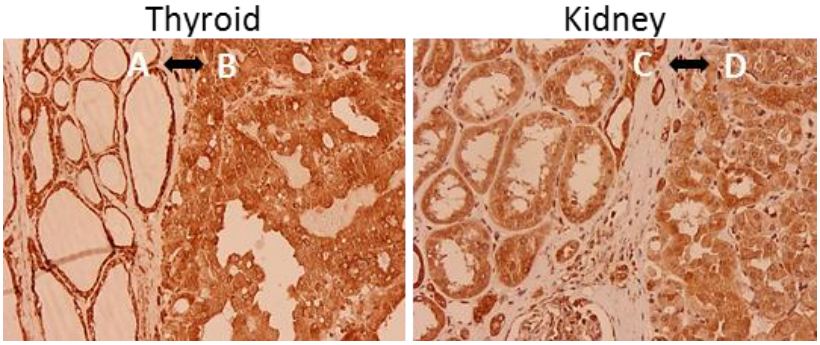

Figure 20 – Total STAT3 staining in thyroid and kidney normal tissue and tumours. Normal thyroid (A), Hürthle cell PTC (B), normal kidney (C) and ROnc (D). The pictures were taken with 20x magnification.

Phospho-STAT3 Tyr705 expression in tumours

Phospho-STAT3 Tyr705 was evaluated in thyroid and kidney tumours and normal adjacent tissues from each organ. It was described that when STAT3 is activated by phosphorylation at Tyr705, it translocates to the nucleus to exert its function as transcription factor. In this work, only nuclear staining of p-STAT3 Tyr705 antibody in thyroid and kidney tissues (both in normal and in tumour tissues) (Figures 23 and 24) were observed.

In thyroid tissues, it was possible to evaluate two parameters separately: the intensity of staining and the extension/percentage of cells stained in tumour and in normal tissues. With these scores it was possible to combine them into a single parameter (pTyr705 "combination"). However, in renal normal and tumour tissues, it was observable that the intensity of staining was similar between them, so, only the extension of the staining was taken into account for statistical analysis.

p-STAT3 Tyr705 expression in thyroid tumours

The evaluation of p-STAT3 Tyr705 permitted noting that thyroid tumours had less intensity and percentage of staining in comparison with normal thyroid tissues (Figure 21 - A). These differences were statistically significant in FVPTC (p=0.002) and in FTC (p=0.031) for intensity; and in PTC (p=0.021) and FVPTC (p=0.004) for extension of the p-STAT3 Tyr705 expression (Figure 21 – A). Combining these data, it was possible to observe PTC (p=0.015) and FVPTC (p=0.001) histotypes are significantly different from the normal tissue (Figure 21 – B).

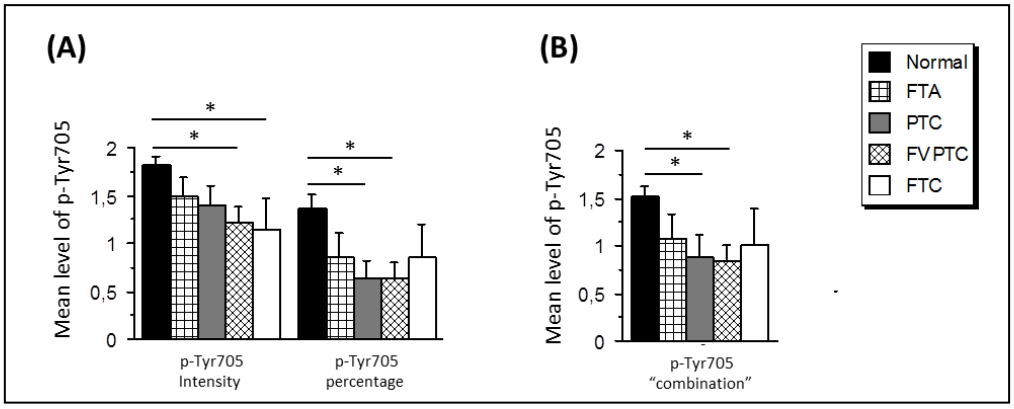

Figure 21 – Phospho-STAT3 Tyr705 mean levels in terms of Intensity and Percentage of stained cells (A) and the "combination" of them (B) for the normal and different thyroid tumour histotypes (statistically significant difference: * - $p< 0.05$).

Taking into account the normal and tumour thyroid tissues, it was possible to observe that usually tumour tissues have less p-STAT3 Tyr705 expression (p=0.0004) (Figure 22). This observation is evident in Figure 23-B, in which it can be seen that normal tissue (N) has higher Phospho-STAT3 Tyr705 expression than the tumour tissues (T).

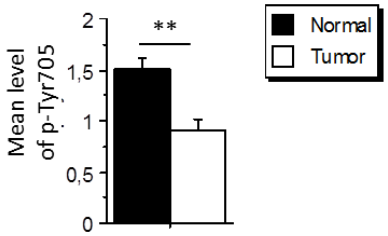

Figure 22 - Phospho-STAT3 Tyr705 mean staining in terms of "combination" for normal and tumours from thyroid gland (statistically significant difference: ** - $p< 0.001$).

No statistically significant differences were observed between Hürthle and non-Hürthle thyroid tumours, concerning Phospho-STAT3 Tyr705 expression.

One other remark was the high number of tumours presenting high p-STAT3 Tyr705 expression in the periphery of the tumour (15 in 69 analysed – 22%) and a progressive loss of its expression to the centre of the tumour (as exampled in Figure 23 – A).

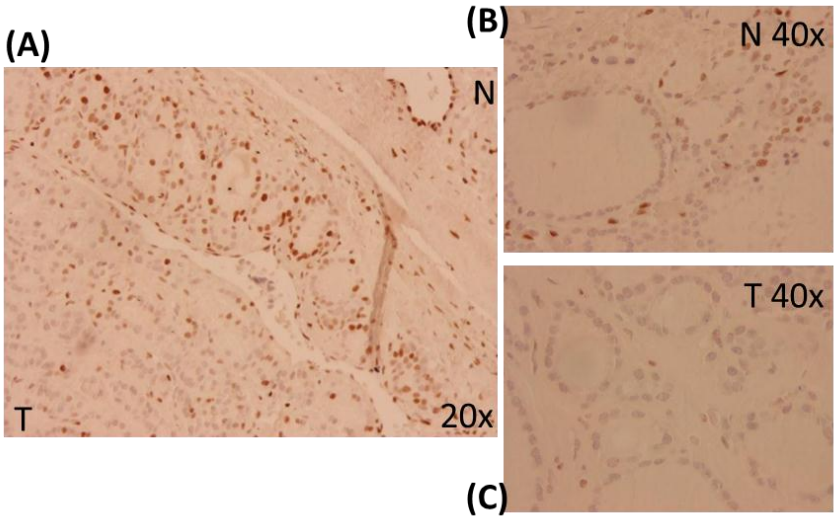

Figure 23 – Phospho-STAT3 Tyr705 expression in thyroid tumours. A – p-STAT3 Tyr705 is highly expressed in normal tissue (N) and in the periphery of the tumour and less in the centre of the tumour (T). P-STAT3 Tyr705 expression in normal thyroid tissue (B) and thyroid tumour (C). The magnification is referred in the pictures.

No association, statistically significant, was observed between GRIM-19 expression and phospho-STAT3 Tyr705 expression**.**

p-STAT3 Tyr705 expression in kidney tumours

As referred, the evaluation of p-STAT3 Tyr705 expression in kidney tissues was only evaluated in terms of the percentage of cells (only the nucleus stained – Figure 24).

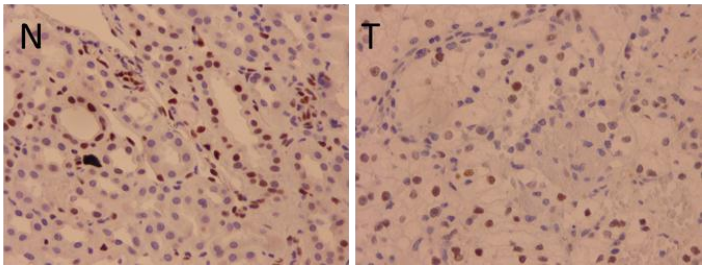

Figure 24 – Phospho-STAT3 Tyr705 nuclear staining in normal kidney (N) and a Kidney tumour - CCRCC (T). The pictures were taken with x40 magnification.

In contrast with thyroid tumours, there were no statistically significant differences between p-STAT3 Tyr705 expression in tumour and normal renal tissues (Figure 25 – A). CromRCC seems to have less percentage of tumour cells stained, but this difference is not statistically significant. No statistically significant difference was observed between tumour (grouped) and normal renal tissues (Figure 25 – B) either.

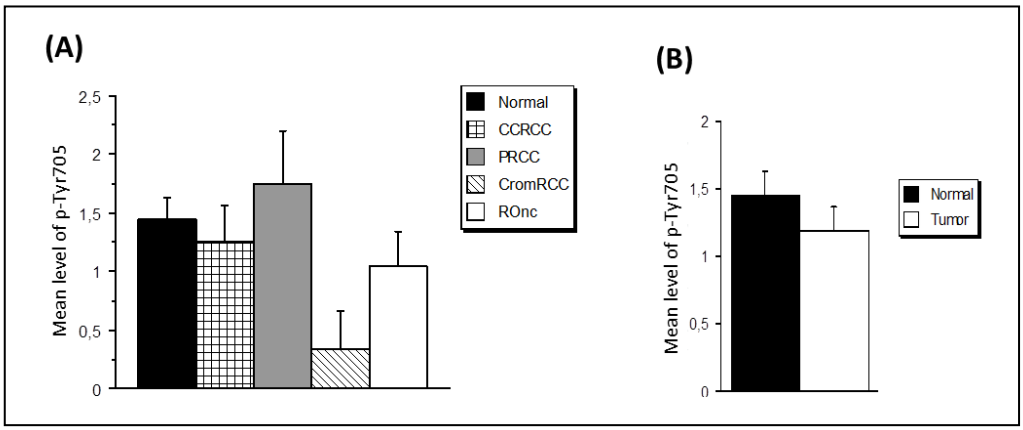

Figure 25 - Phospho-STAT3 Tyr705 mean percentage of staining for the normal and different kidney tumour histotypes (A) and kidney tumours grouped (B).

As in the thyroid, in kidney tumours, it was possible to observe more p-STAT3 Tyr705 in the periphery of the tumour than the centre, in a high number of cases: 22 out of 47 (47%).

The correlation analysis concerning the relation between GRIM-19 and p-STAT3 Tyr705 expression in kidney tissues did not present any statistically significant association.

Phospho-STAT3 Ser727 evaluation

As performed for p-STAT3 Tyr705, p-STAT3 Ser727 was evaluated in thyroid and kidney tumours and normal tissues from each organ, in order to address the status of STAT3 activation as well the location of the active isoforms. It is described that when STAT3 is phosphorylated in residues Ser727 and Tyr705, it has the maximum activity as a transcription factor. Other reports showed that, phosphorylation in Ser727 is sufficient to induce the activity of STAT3 independently of the other (p-STAT3

Tyr705) phosphorylation. Recent studies also reported that STAT3 phosphorylated in residue Ser727 is present in mitochondria and is essential for normal OXPHOS process.

As for p-STAT3 Tyr705, in thyroid tissues it was possible to evaluate the intensity and percentage of cells stained as well the "combination" of both parameters (named "combination" in figures). In normal and tumour tissues from the kidney, similarly to p-STAT3 Tyr705 form, it was observable that the intensity of staining was similar between them. Thus, only the extension of the staining was statistically evaluated.

p-STAT3 Ser727 expression in thyroid tumours

In thyroid tissues, this antibody usually stained the nucleus (Figure 26 – B and C). However, it was possible to observe that in 3 cases (4%) it appears to have a weak cytoplasmatic staining (both in tumour and in correspondent normal tissue), similar to those observed for GRIM-19 and SDHA, suggesting a putative mitochondrial staining.

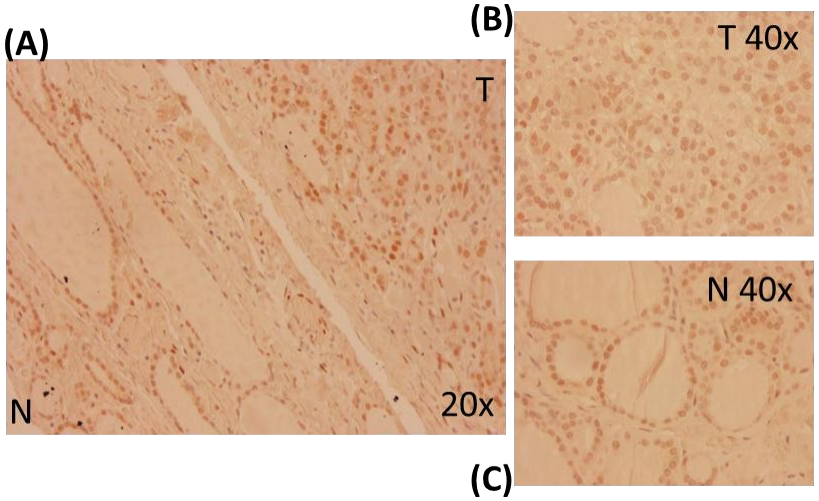

Figure 26 - Phospho-STAT3 Ser727 expression in thyroid tumours. A – p-STAT3 ser727 expression in normal tissue (N) is similar to the tumour (T) expression. Higher magnification (40x) of p-STAT3 Ser727 expression in normal thyroid tissue (B) and thyroid tumour tissue (C). The magnification is referred in the pictures.

Concerning Phospho-STAT3 Ser727 expression, it was not detected any relevant difference between normal tissue and the different histotypes for the evaluated

parameters (intensity and percentage of staining - Figure 27 – A; and for the combination of them – Figure 27 – B). It was also not observed any statistically significant difference between Phospho-STAT3 Ser727 expression in normal and in tumour thyroid tissues (Figure 28).

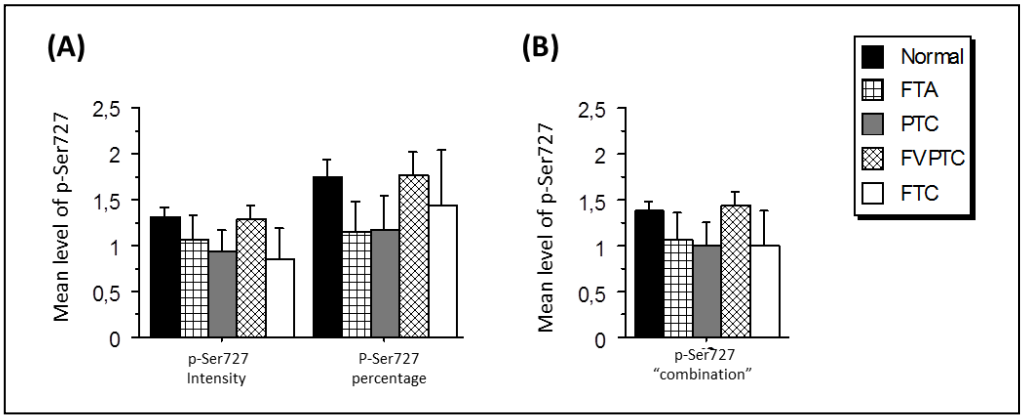

Figure 27 - Phospho-STAT3 Ser727 mean staining in terms of Intensity and Percentage of stained cells (A) and the "combination" of them (B) for the normal and different thyroid tumour histotypes.

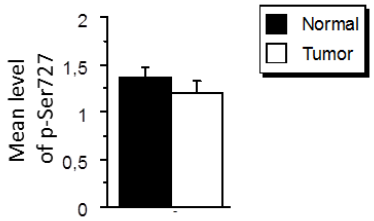

Figure 28 - Phospho-STAT3 Ser727 mean staining in terms of "combination" for normal and tumours from thyroid gland.

No statistically significant differences were attained, concerning the expression of phospho-STAT3 Ser727**,** in Hürthle and non-Hürthle cell tumours.

A statistical analysis was performed by correlation analysis to determine if there was any relation between GRIM-19 and p-STAT3 Ser727 expression in thyroid tissues. A statistically significant positive association was obtained between GRIM-19 and p-STAT3 Ser727 expression (combination) (p<0.0001).

p-STAT3 Ser727 expression in kidney tumours

The evaluation of p-STAT3 Ser727 expression in kidney tissues was evaluated in terms of the percentage of stained cells as well as in terms of the cellular compartment of staining.

This second evaluation was performed since it was observable that p-STAT3 Ser727 antibody stains the nucleus, the cytoplasm or the two compartments (Figure 29 A and B).

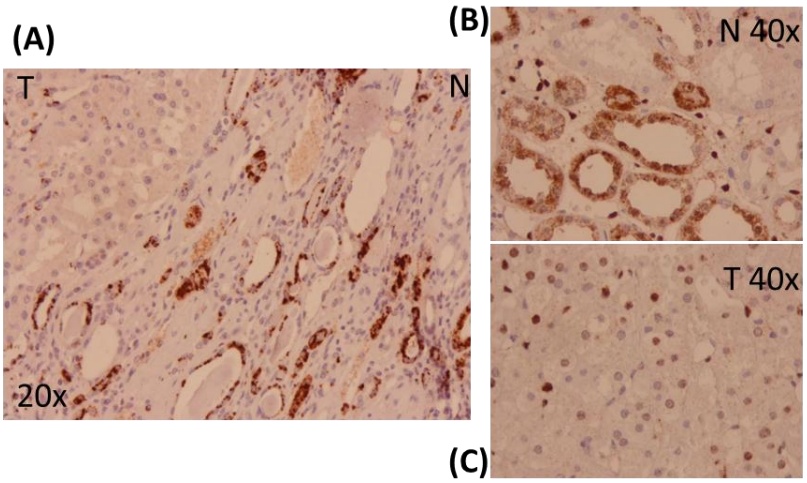

Figure 29 - Phospho-STAT3 Ser727 expression in kidney. A – p-STAT3 ser727 cytoplasmatic expression in normal tissue (N) and absence in tumour (T). Higher magnification to show p-STAT3 Ser727 nuclear and cytoplasmatic expression in normal thyroid tissue (B) and nuclear expression thyroid tumour (C). The magnification is referred to in the pictures.

Taking into account the p-STAT3 Ser727 expression, it appeared that ROnc histotype have lower expression of this STAT3 phosphorylated form, when comparing with the normal kidney tissue ($p<0.0001$). CCRCC also present a lower statistically significant expression level comparing with the normal kidney tissue ($p=0.033$) (Figure 30 – A).

When tumour histotypes were grouped into a single group, it was possible to observe that they had low levels of phospho-STAT3 Ser727 ($p=0.005$) (Figure 30 – B).

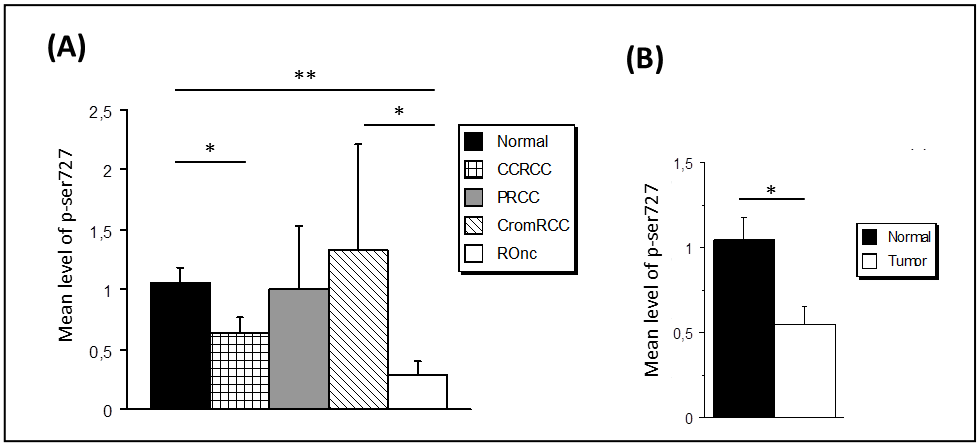

Figure 30 - Phospho-STAT3 Ser727 mean staining in terms of percentage of stained cells for the normal and different kidney tumour histotypes (A) and the kidney tumours grouped (B). (statistically significant difference: * - $p< 0.05$; ** - $p< 0.001$).

Although, in thyroid, it was possible to observe a small amount of cases that stained the cytoplasm, in kidney this it was observable in a great number of cases (26 out 52 – 50%). Comparing all the samples, it was possible to see a relation between nuclear staining and tumour tissues. The tumour tissues have more number of cases staining only the nucleus, in comparison to the normal kidney tissues that presents more cytoplasmatic or nuclear and cytoplasmatic staining (p=0.011) (Figure 31). This relation was obtained using the Chi-square test (χ^2).

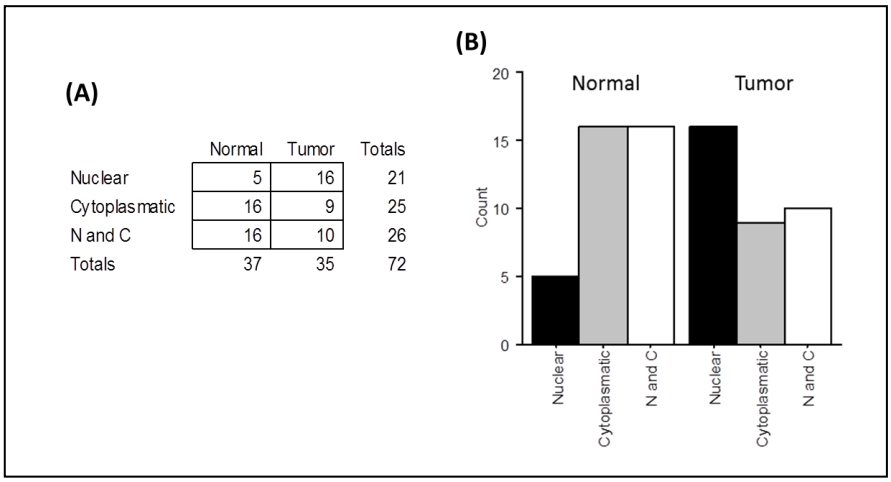

Figure 31 – Presence of p-STAT3 Ser727 in normal and kidney tumours into nucleus, cytoplasm or both places (N and C). Table (A) and graph (B) of number of cases with positive staining for the different cellular compartments.

It appeared that in tumours, phospho-STAT3 Ser727 was more evident in nucleus than in cytoplasm. However, in normal Kidney tissues it was more present in cytoplasm. Thus, we tried to check if there is also any relation between GRIM-19 expression and p-STAT3 Ser727. We compared the three locations of p-STAT3 Ser727 with presence [+ (1+, 2+ and 3+)] or almost absence [0 (0 and 0+)] of GRIM-19 in tissues.

Table VI – Distribution tables concerning GRIM-19 expression and p-STAT3 Ser727 localization (A); statistical Fisher's p-values for relation between GRIM-19 presence (+) or absence (-) and p-STAT3 Ser727 location in kidney tumours [nuclear, cytoplasmatic or N and C (nuclear and cytoplasmatic)] (B); (statistically significant difference: * - $p < 0.05$).

A

p-STAT3 Ser727 localization	GRIM-19 (-)	GRIM-19 (+)	Totals
Nuclear	6	10	16
Cytoplasmatic	8	1	9
Totals	14	11	25

	GRIM-19 (-)	GRIM-19 (+)	Totals
Nuclear	6	10	16
N and C	8	2	10
Totals	14	12	26

	GRIM-19 (-)	GRIM-19 (+)	Totals
Cytoplasmatic	8	1	9
N and C	8	2	10
Totals	16	3	19

B

GRIM-19 expression vs. Nuclear *and.* Cytoplasmatic phospho-STAT3 Ser727 staining	p=0.033 (*)
GRIM-19 expression vs. Nuclear *and* Nuclear and Cytoplasmatic phospho-STAT3 Ser727 staining	p=0.051
GRIM-19 expression vs. Cytoplasmatic *and* Nuclear and Cytoplasmatic phospho-STAT3 Ser727 staining	p>0.999

As observed in distribution tables, phospho-STAT3 Ser727 expression in kidney tumours was observed more frequently in the cytoplasm when the tumours did not express GRIM-19. Analysing this relation, we observed that, in general, when GRIM-19 was expressed, STAT3 phosphorylated at residue Ser727 was more present in the nucleus. On the other hand, when GRIM-19 was absent, p-STAT3 Ser727 was localized more in cytoplasm.

No statistically significant correlation was obtained concerning GRIM-19 and p-STAT3 Ser727 expression levels in kidney tissues.

MMP-2 and VEGF evaluation

STAT3 is a transcription factor responsible for the expression of some genes, namely VEGF and MMP-2, amongst others. Since we had these two antibodies available for evaluation of these two proteins in our laboratory, an immunohistochemical analysis was performed in few samples. We aimed to see if there was some association between VEGF and MMP-2 expression with GRIM-19, p-STAT3 Tyr705 and p-STAT3 Ser727 expression).

No association between GRIM-19 expression and phosphorylated p-STAT3 isoforms (p-STAT3 Tyr705 and p-STAT3 Ser727) was observable before. However, Zhang *et al.* [44] referred that GRIM-19 regulates STAT3 binding to transactivation domain (TAD) and blocks its activity, being serine 727 residue required for this process [44], but the authors did not explained how or what mechanisms were in base of STAT3 phosphorylation. Since it was apparently not related, we analysed these two (VEGF and MMP-2) STAT3 downstream genes trying to understand if GRIM-19 was really inhibiting STAT3 activity, independently of STAT3 phosphorylation.

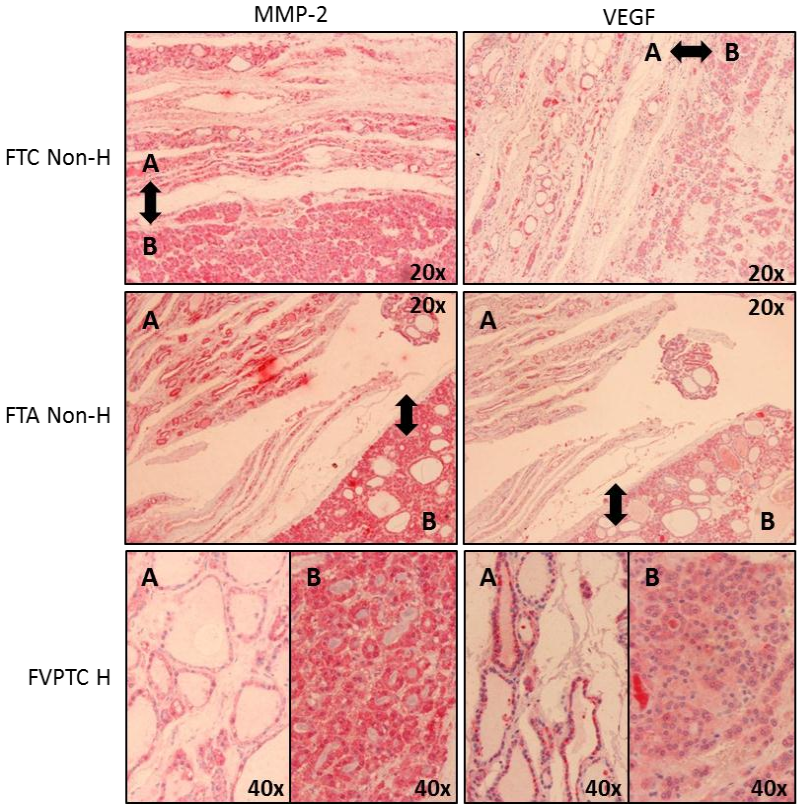

Figure 32 – MMP-2 and VEGF expression in different thyroid tumours and normal tissues [(A) Normal tissue, (B) tumour]. The magnification is described in the pictures.

MMP-2 and VEGF were evaluated in a small number of thyroid tumour samples. In non-Hürthle cell tumours no relevant differences between normal and tumour tissues (Figure 32) was observed. In Hürthle cell tumours there were not such homogeneous results. Higher expression of MMP-2 was observed and less expression of VEGF in tumours comparing with normal tissue as shown in Figure 32 (pictures with x40 magnification). Other cases showed the opposite results. Since few samples were analysed, a statistical analysis could not be performed. However, only by descriptive results, there was no obvious relation between GRIM-19 expression and phosphorylated forms of STAT3 and MMP-2 and VEGF expression.

Analysis of GRIM-19 promoter methylation

GRIM-19 (also named NDUFA13) promoter region is not known. In an attempt to reveal the putative GRIM-19 promoter region we collected, from *ENSEMBLE* [89], the gene sequence and also the 5' upstream sequence. The sequence obtained was inserted in ***The CpG Island Searcher*** [90], as mentioned before, and the putative region of the GRIM-19 gene promoter was obtained (Figure 33). This region has a length of 3439bp.

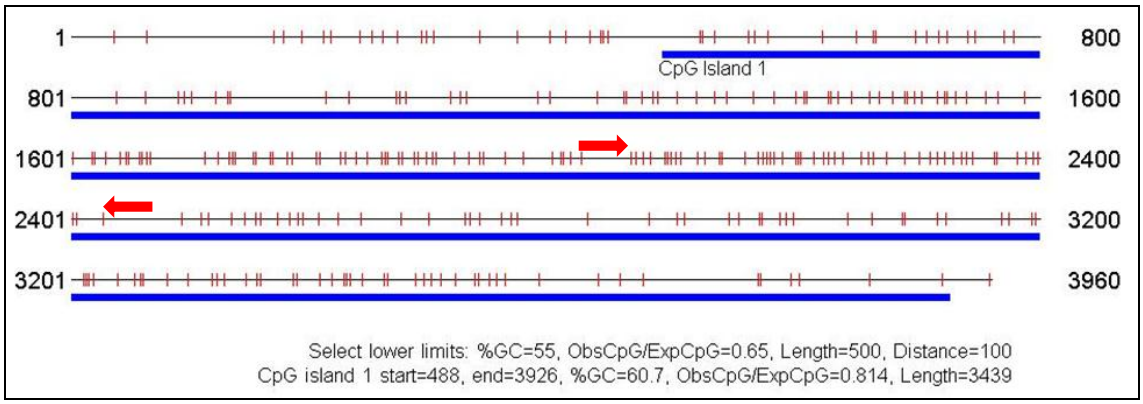

Figure 33 – Promoter region of GRIM-19. Obtained using *The CpG Island Searcher* [90]. Red arrows – "GRIM-19 Met" primers constructed to analyse methylation in a region with high number of CpGs.

Once obtained the promoter region of GRIM-19, the next step was to analyse the methylation of the CpG duplets. The final objective of this analysis was to perform the

analysis in DNA derived from paraffin-embedded tissues where GRIM-19 expression was evaluated. However, DNA extracted from paraffin-embedded tissues could have low quality and could be fragmented. Taking this into account, we first tried to analyse the methylation patterns in a cell line without GRIM-19 expression. It would facilitate the methylation pattern detection because DNA extracted from cell lines usually have better quality and can be amplified for a higher length.

With this purpose, a reverse transcription was performed – polymerase chain reaction (RT-PCR) to analyse GRIM-19 mRNA expression in several thyroid cell lines available in our laboratory. GRIM-19 mRNA expression was observed in all the cell lines analysed, as shown in Figure 34. Evaluation of actin mRNA expression was used as a control.

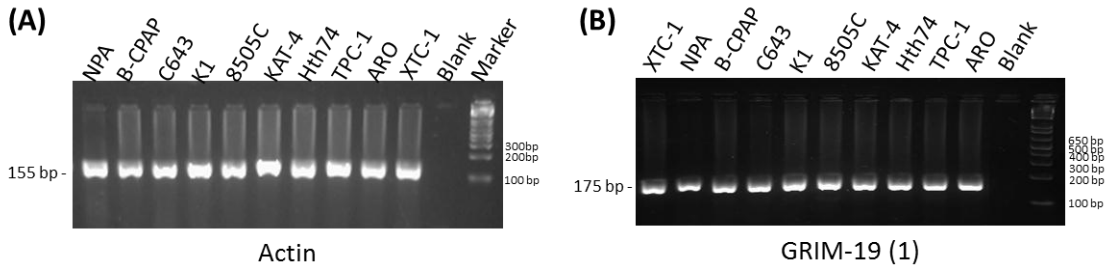

Figure 34 – RT-PCR products for actin (A) and GRIM-19 (B) in several thyroid cell lines.

Since a high number of samples of Clear Cell Renal Cell Carcinomas showed a completely loss of GRIM-19 expression (analysed by the immunohistochemistry analysis), we obtained two new cell lines derived from this type of tumours, 786-0 and Caki-2 cell lines. Total RNA was extracted and RT-PCR was performed in order to check for GRIM-19 expression. As shown in Figure 35 these two cell lines also expressed GRIM-19.

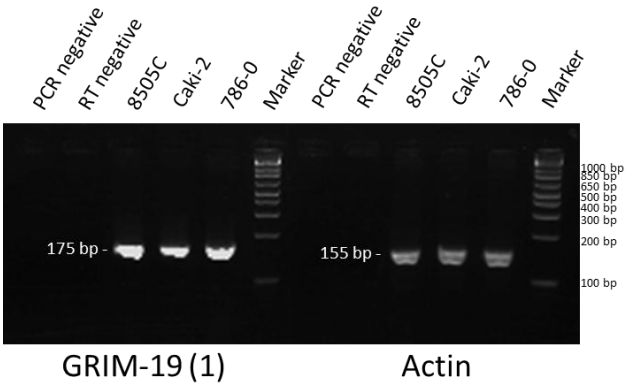

Figure 35 - RT-PCR products for GRIM-19 (left) and actin (right) for two renal cell lines (Caki-2 and 786-0) and a control thyroid cell line (8505-C).

None of the cell lines studied had a complete loss of GRIM-19 mRNA expression. Since that was the case, GRIM-19 mRNA and protein levels should be evaluated to observe if any of them had lower levels of GRIM-19 expression.

Even though we decided to start the methylation study in some of the aforementioned cell lines with the expectation to find a cell line with a distinct methylation pattern, the latter would enable us to relate that methylation status with the expression of GRIM-19 mRNA and protein levels.

A pair of primers was constructed to a specific region with a high number of CpGs in the promoter region of GRIM-19. The primers were constructed avoiding the regions with CpG, in the edges of the CpGs regions (red arrows in Figure 33).

The optimizations were performed for this pair of primers in DNA extracted from a thyroid cell line (TPC-1) and from DNA extracted from two paraffin-embedded samples (in which low levels of GRIM-19 protein were observed) to ensure that the primers function properly in both DNA extracted from the different sources.

With optimized conditions, DNA was converted using bisulphite reaction from DNA extracted from: three thyroid cell lines (NPA, XTC-1 and TPC 1); two renal tumour cell lines (786-0 and Caki-2): and from paraffin-embedded samples (in which low levels of GRIM-19 protein were observed), in order to know if there was any distinct pattern of methylation in CpGs, comparing with non-converted DNA.

As shown in Figure 36, the converted DNA from the paraffin-embedded tissue does not present any amplification for the converted DNA (Figure 36 – B). One possible explanation could be the chemical reaction performed by bisulphite conversion which could eventually lead to a loss of the DNA under purification. Another possible

explanation is the poor quality of the DNA. DNA extracted from paraffin-embedded tissues was converted several times and the same result (no amplification) was obtained.

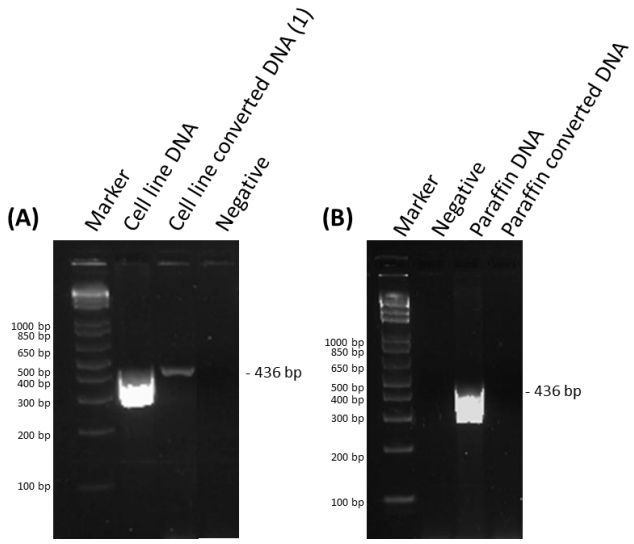

Figure 36 – GRIM-19 promoter region amplification in bisulphite converted and non-converted DNA for a cell line – NPA (A) and paraffin-embedded tissue - H10/25330 B4 tumour (B).

Converted and non-converted DNA (from the aforementioned cell lines) was amplified, purified and sequenced. We observed that all CpG duplets in the region analysed were methylated (Figure 37).

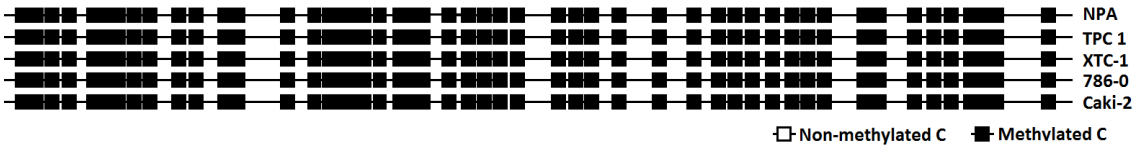

Figure 37 – Schematic representation of methylation results of GRIM-19 promoter studied region in cell lines.

To confirm this result, the evaluation of another gene studied was performed in our laboratory (LRP1B). The same bisulphite converted DNA was used to analyse methylation of GRIM-19 promoter region. We selected two cell lines: TPC 1 and XTC-1. TPC-1 was shown as not being methylated, and so, it will be as a negative control for our studied region of GRIM-19 promoter [91].

As shown in Figure 38, TPC 1 cell line is not methylated and XTC-1 has a specific pattern of methylation similar to that one reported before by our group.

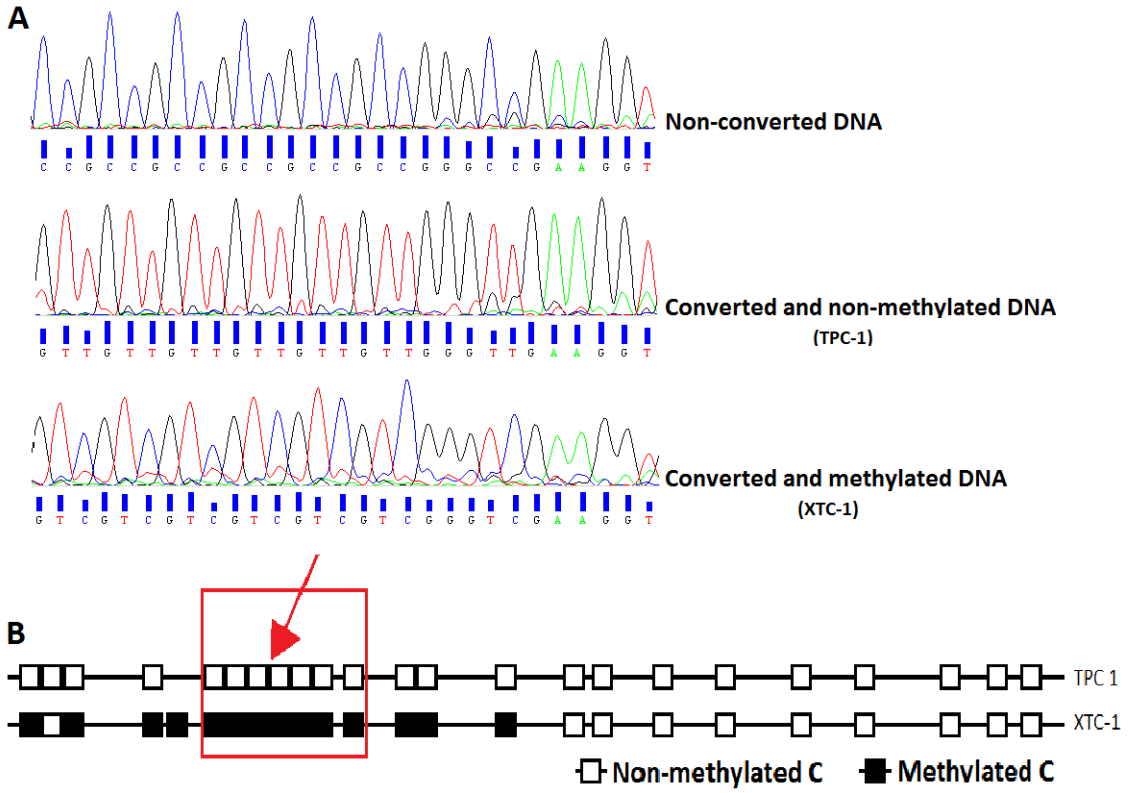

Figure 38 – Small region representative of the obtained chromatograms after bisulphite conversion (A); Schematic representation of LRP1B methylation studied region in TPC 1 and XTC-1 cell lines based in chromatograms (B).

With this data, it was confirmed that the fragment of GRIM-19 CpG island analysed is completely methylated.

DISCUSSION

IFNs and RA have been shown to suppress tumour growth and are used in the treatment of several types of cancer [92]. GRIM-19 was identified by Angell *et al.* [9] as being one gene associated with the IFN/RA-induced cell death [9]. Since its discovery, several works have been supporting its tumour suppressor feature with a dual function: as part of MRC, being a complex I subunit and as participating in IFN/RA induced mortality [25, 28]

Several studies were performed in diverse types of human tumours concerning GRIM-19 mutations and expression, but none of them accessed its expression neither in thyroid tumours nor in mitochondrion-rich or oncocytic tumours. Most of the studies in which the authors evaluated GRIM-19 expression, in different types of tumours, showed that generally GRIM-19 has lower expression in tumour tissues (summarized in Table I). Taking this into account, we performed a study in which we aimed to assess GRIM-19 expression levels in human thyroid tumours, with an emphasis in Hürthle cell tumours (thyroid tumour composed of cells with large and granular eosinophylic cytoplasm due to the huge number of mitochondria). In 1998, Canzian *et al.* [13] mapped, by linkage analysis in a French family, a gene responsible for familial thyroid tumours with cell oxyphilia (*TCO*) to chromosome 19p13.2 [13]. *GRIM-19* was mapped also in this region 19p13.2 [7] suggesting its putative involvement in ethiopathogenesis of HCT. Máximo *et al.* [1] searched for *GRIM-19* mutations in a series of 52 thyroid tumours and found three somatic missense mutations and one germline mutation in 4 out of 26 of sporadic Hürthle cell carcinomas (15%). No mutations were observed in non-Hürthle thyroid tumours. The authors also studied six cases of familial Hürthle cell tumour, from the aforementioned French family, but they did not observe any mutation supporting the identification of *GRIM-19* as the TCO gene. However, the identification of such mutations suggests a putative involvement of *GRIM-19* in the ethiopathogenesis of oxyphilic thyroid tumours, through its dual function in apoptosis and in mitochondrial biogenesis [1].

In this study we evaluated the expression of GRIM-19 in a series of 79 thyroid tumours [17 PTC (5 Hürthle and 12 non-Hürthle cell tumours), 7 FTC (4 Hürthle and 3 non-Hürthle cell tumours), 31 FVPTC (11 Hürthle and 20 non-Hürthle cell tumours), 14 FTA (7 Hürthle and 7 non-Hürthle cell tumours) and 10 ATC], and we found that the only tumour histotype that has a clearly loss in GRIM-19 expression, comparing with the normal thyroid tissues (p=0.010), is the Anaplastic thyroid tumour, the most

aggressive type of thyroid tumours. However, when we separate the diverse histotypes by their oncocytic phenotype (Hürthle or non-Hürthle cell tumours) we observe that the HCTs (from all the histotypes) have less GRIM-19 expression than the non-Hürthle cell tumours (p=0.0008). Comparing with normal paired-tissue 18 in 27 (66%) Hürthle cell tumours and only 2 in 42 (5%) non-Hürthle thyroid tumours have loss of expression of GRIM-19. Concerning the different histotypes individually, the Hürthle cell tumours from FVPTC and FTC show lower GRIM-19 expression than the non-Hürthle cell tumours (p=0.003 and p=0.046, respectively). The results from FTC must be observed with reservations, once we studied few samples. ATC histotype was not included in this analysis because they do not present this Hürthle phenotype.

Our data shows that, in thyroid tumours, GRIM-19 expression seems not to be related with thyroid tumourigenesis in general. It seems to be downregulated specifically in HCT, which suggests the involvement of GRIM-19 in HCT ethiopathogenesis.

Our data confirms that GRIM-19 loss of function, by mutations [described by Máximo *et al.* [1] – 4 out of 26 (15%)]or by loss of expression [18 out of 27 (66%)], is frequent in Hürthle cell tumours and may have a role in the etiopathogenesis of these type of thyroid tumours, supporting the hypothesis advanced by Máximo *et al.* [1] that GRIM-19 inactivation may be involved in ethiopathogenesis of Hürthle thyroid tumours.

While Máximo *et al.* [1] observed mutations in *GRIM-19*, in this work downregulation of the protein was found in Hürthle cell thyroid tumours. The mutations found may be one explanation for GRIM-19 inactivation in HCT. However, the frequency of such mutations cannot be the only reason, since the frequency of such mutations were low [4 out of 26 (15%)] comparing with the frequency of GRIM-19 downregulation in this work (18 out of 27 Hürthle cell tumours – 66%). Besides GRIM-19 mutations, other mechanisms may be involved in GRIM-19 inactivation, namely epigenetic events such as promoter hypermethylation or histone deacetilation.

Why is GRIM-19 specifically downregulated in HCT of thyroid? At this stage, it is impossible to give the clear answer taking into account the little data available concerning this issue. However, we put forward the hypothesis that it may be related with the role of mitochondrial complex I in the ethiopathogenesis of HCT. Several studies, by our group [83] and others [93, 94], show that mutations and downregulation of complex I subunits can be one of the causes of oncocytic phenotype development.

However, the majority of these works focused their study in mtDNA complex I encoded subunits. Here, we demonstrate, for the first time, the downregulation of a complex I subunit encoded by nDNA, in HCT. Our hypothesis points to a role of loss of expression of GRIM-19 in mitochondrial complex I dysfunction and in the ethiopathogenesis of HCT.

In addition, our data shows that GRIM-19 loss of expression is also associated with ATC, suggesting also a role of GRIM-19 inactivation in the etiopathogenesis of ATC. Although, due to small number of samples this data needs to be confirmed in a larger series of ATCs.

GRIM-19 loss of expression in thyroid seems to be involved in the ethiopathogenesis of Hürthle cell phenotype. Since this was an interesting result, it would be interesting to study other types of oncocytic (mitochondrion-rich tumours) to confirm our hypothesis. Tumours of the Kidney also have mitochondrion-rich tumours – the Renal Oncocytoma. A study concerning GRIM-19 expression in renal cell carcinomas (RCC) was performed previously by Anchanati *et al.*[60], however, in this study the main focus was in the clear cell phenotype [60] and ROnc were not included in the series. Taking this into account, we also analysed the expression of GRIM-19 in a series of kidney tumours with an emphasis in renal mitochondrion-rich tumours (ROnc).

Our results show that RCT lose GRIM-19 expression when comparing with normal kidney tissue. CCRCC is the histotype with higher loss of GRIM-19 (mean value=0.400; $p<0.0001$) [also CromRCC but we will not focus on this due to the few numbers of samples (mean value=0.667; $p<0.0001$)] followed by ROnc (mean value=1.143; $p<0.001$) comparing with normal kidney tissue (mean value=2.875). The PRCC histotype also had loss of GRIM-19 compared with normal renal tissue (mean value=2.125; $p=0.0016$), although less than the other histotypes. Only comparing the tumours that had the normal paired-tissue, it was observed that 35 in 40 samples (88%) had downregulation of GRIM-19 expression, being 11/11 (100%) CCRCC, 2/2 (100%) CromRCC, 19/20 (95%) ROnc and 3/7 (45%) PRCC.

In comparison with thyroid results, we expected to observe higher loss of GRIM-19 in mitochondria-rich tumours comparing with the other ones, as Hürthle cell tumours of the thyroid. However, it was not observed. In kidney tumours it was observed that CCRCC, the most aggressive one, has the lowest expression and the highest number of negative cases for GRIM-19 and the PRCC are the ones that, despite their loss comparing with the normal tissues, had the highest expression of GRIM-19

when compared with the other histotypes. The renal oncocytomas, the benign tumours, had an intermediate expression of GRIM-19. This data, does not support the hypothesis that, GRIM-19 inactivation is specifically associated with the mitochondrion-rich tumours from the kidney.

Alchanati *et al.* [60] results showed that 93% of RCC had completely loss of GRIM-19 expression and that higher loss was associated with clear-cell histotype [60]. Our results also confirmed that CCRCC is the histotype with higher loss and downregulation of GRIM-19. However, we only observed GRIM-19 downregulation (and not complete loss of expression) in 86% (35 out 40) of the renal cell tumour cases. Only 37% (19 out 52) of the RCT cases studied showed complete loss of GRIM-19 expression (14 CCRCC, 1 CromRCC and 4 ROnc). If we focus our attention only in CCRCC histotype, we observe that 70% (14 out 20) had complete loss of GRIM-19, being the histotype with a higher percentage of cases with complete loss of GRIM-19.

Summarizing, the most aggressive phenotypes are the ones with higher loss of GRIM-19, but in contrast the benign ones (ROnc) are not the ones with higher expression of GRIM-19, which make the association between aggressiveness and GRIM-19 expression difficult. It is important to note that the abnormal number of mitochondria in ROnc can make it difficult to classify GRIM-19 expression, due to the huge amount of mitochondria (which can lead to an overvaluation of immunohistochemical evaluation). Future experiments, such as western blot in samples extracted from frozen tumours, could be performed to clarify this issue.

Despite this pertinent question, the loss of GRIM-19 seems to be higher in the most aggressive histotype. Doing a parallelism with thyroid, it raises the question if Hürthle cell tumours can be more aggressive than non-Hürthle. This is still a question that raises controversy. In 1950s oncocytic tumours from thyroid were classified as malignant according to American Cancer Society. Several studies performed afterwards showed that this is not true in all the cases and that the criteria of vascular and capsular invasion should be applied in evaluation of malignance of these types of tumours. Today it is accepted that Hürthle cell tumours are subtypes of thyroid tumours, the benign and the malignant ones [81], being as malignant as the respective non.-Hürthle cell counterpart. Despite this classification there are some authors that argue that Hürthle cell tumours are frequently more malignant than the non-Hürthle cell tumours. A higher percentage of Hürthle cell tumours than non-Hürthle cell tumours in FTC with signs of malignancy are observed, the discussible worse prognosis of Hürthle FTC and

the higher mortality rate that seems to occur in patients with these types of tumours (may be due to the decreased efficiency in iodine intake and hormone synthesis of Hürthle cell tumours) are some reasons for their hypothesis (see [81, 85] for a review). However, future studies will be important to understand the role of loss of GRIM-19 expression in malignant tumours of the kidney as well as in ATC from the thyroid.

Several subunits from MRC complex I have been shown downregulated or mutated in oncoytic tumours [83, 93-95], which is assumed to induce a compensatory mechanism, for increasing the number of mitochondria. This mechanism may explain the role of GRIM-19 inactivation in oncocytic tumours of the thyroid. However, in Renal Oncocytomas, GRIM-19 inactivation seems not to lead to this increase in the number of mitochondria, and so, other mechanism may be involved in the role of GRIM-19 inactivation in the etiopathogenesis of these tumours. Complex I was described, several times, as being a key component of the apoptotic process. GRIM-19 as a MRC complex I subunit and as part of the apoptotic process (involved in IFN/RA-induced cell death) can also regulate cell growth and therefore contribute to a greater or lesser degree of aggressiveness of tumours [94].

It is interesting to note that seven genes associated with kidney cancer (*VHL – von Hippel-Lindau –*, proto-oncogene *MET – hepatocyte growth factor receptor –*, *TSC1 and TSC2 – tuberous sclerosis genes –*, *FLCN – Folliculin –*, *FH – fumarate hydratase* – and *SDH – succinate dehydrogensase*) are somehow involved in cellular metabolism, some of them with direct action into mitochondria. This leads Linehan *et al.* [96] to affirm that "kidney cancer is a disease of deregulated cellular metabolism" (see more details in [96]). This is an interesting association that seems to be related with our results. GRIM-19 is a component of complex I of OXPHOS, being an essential component to the normal energy production [25, 28]. Our results show that GRIM-19, at least in kidney tumours, may be one more mitochondrial gene that is the basis of genesis of these types of tumours.

Concluding, GRIM-19 behaviour in thyroid and in kidney seems to be a quite different. It suggests that GRIM-19 activity and role may be tissue-type specific.

GRIM-19 localization is also an unsolved problem because it was described initially as nuclear [9] and after as exclusively mitochondrial (cytoplasm), rejecting the first description of the location [28]. Very recently, it was been shown that GRIM-19, effectively, can be in one of them or in both places. Here, in all the samples, GRIM-19

expression it was only observed in the cytoplasm with a punctuated staining similar to that observed for SDHA, suggesting a mitochondrial location [29, 30].

What mechanisms can contribute to GRIM-19 downregulation in several types of tumours, and in particular in Hürthle cell thyroid tumours and kidney tumours analysed in this study?

Until now there has been no obvious answer. The mutations observed by Máximo *et al.* [1] could be one of the reasons for downregulation/inactivation in the same cases, however, other mechanism should be involved [1]. Alchanati *et al.* [60] reported that in the cases when GRIM-19 was depressed, mRNA also was decreased [60]. Taking this in account, it seems that GRIM-19 may be downregulated by epigenetic mechanism at transcription level. It suggests that hypermethylation of the promoter, histone deacetylation or loss of the connection between the promoter and some transcription factors could be in the basis of this dowregulation.

Hypermethylation in promoter region frequently leads to gene inactivation and silencing. This epigenetic event was associated several times with cancer development and can lead to aberrant silencing of normal tumour suppressor function (see [97, 98] for reviews). GRIM-19 is a tumour suppressor that seems to be downregulated in several types of cancer, being this epigenetic mechanism a possible explanation for its inactivation. We searched for the putative GRIM-19 promoter region with the objective to verify this hypothesis.

Our data showed that all CpG duplets in the fragment of CpG island analysed were methylated, although this result needs to be validated.

To improve this strategy we used a positive and a negative control for the bisulphite reaction. For that, a gene that has been studied in our group (LRP1B) was used, using a cell line where we know that this specific gene is partially methylated (XTC-1) and another one, where it had been proved as being not methylated (TPC 1) [91]. With these controls we can be sure that the conversion occurs and it is complete. One of the limitations for the bisulphite conversion is the false positives due to an incomplete conversion which can be overpassed using the mentioned controls. Another limitation for the reaction is the DNA quality of DNA that could be interfering with the bisulphite conversion. The fragment length is another limitation, at least for paraffin-embedded tissues, that can justify the non-amplification of this DNA.

Using the referred controls it was possible to conclude that our results were not false positives, and in fact the region that we were studying is completely methylated.

Taking this into account, we can propose that the studied region should not be most important in the regulation of GRIM-19 gene transcription. Thus, others regions of the promoter must be checked to prove (or not) if hypermethylation is the epigenetic mechanism underlying the reduced levels of GRIM-19 observed in tumours.

Taking into account our results concerning GRIM-19 mRNA expression, we need to check the levels of expression by another technique like Real time PCR, and proceed to methylation analysis only in cell lines with mRNA underexpression.

Another hypothesis that we have to mention is the fact that the mechanism of GRIM-19 downregulation in cancer (namely in our samples) could be related to protein regulation and not to mRNA. We should check protein levels in our cell lines.

Until now, in literature, cell lines without GRIM-19 expression have never been described. Since we could not find a cell line without GRIM-19 expression, efforts must be concentrated in cell lines with low GRIM-19. Western blot analysis to evaluate protein expression and real-time polymerase chain reaction (qRT-PCR) to evaluate mRNA expression should be performed to find such cell lines and then evaluate the methylation pattern.

Despite the setbacks, we have good prospects that our hypothesis really occurs. Breast cancer therapy of 16 patients treated with a demethylating agent (hydralazine) and a histone deacetylase inhibitor (magnesium valporate) was able to up- or downregulate at least 3-fold, 1091 and 89 genes, respectively. GRIM-19 (or NDUFA-13) was one of the genes that were upregulated, about 8-fold, after the treatment [99].

Other possible epigenetic causes for gene silencing can be the impairment of transcription factors assessment to the promoter region to regulate gene expression. If the hypothesis of the methylation of GRIM-19 promoter is not validated as the cause of GRIM-19 regulation, this other epigenetic mechanism should be investigated since there are several transcription factors that bind to GRIM-19 promoter region (Figure 39).

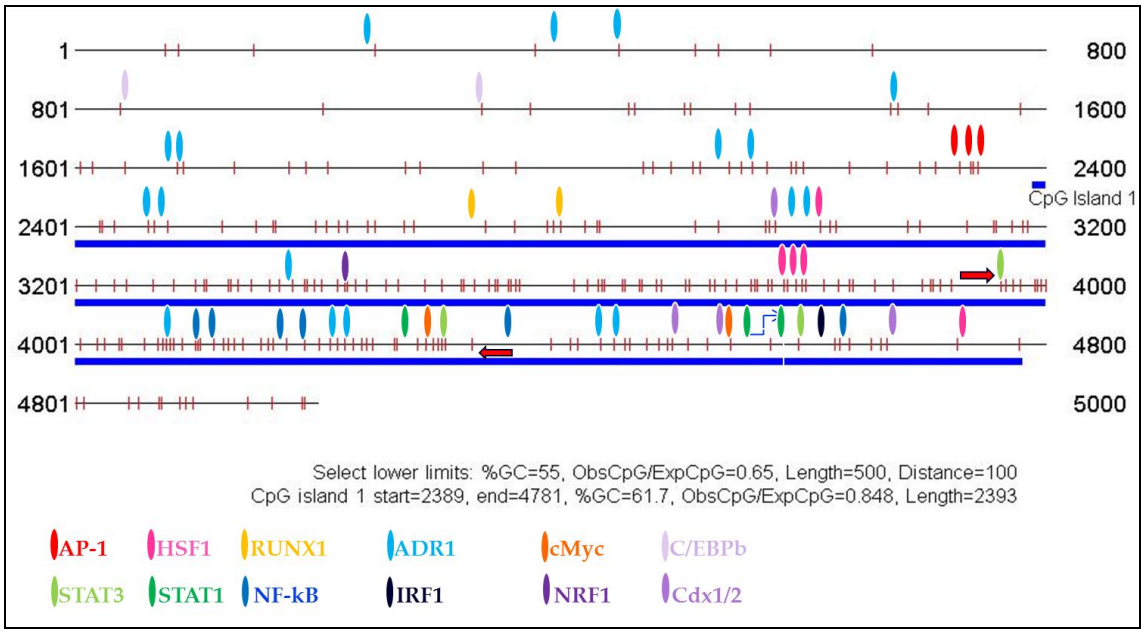

Figure 39 – GRIM-19 promoter region and the several growth factors that potentially binds to this control of transcription region.

Several GRIM-19 interacting proteins have been discovered in the previous years. One of them, whose role has been highly investigated in cells and more specifically in cancer, is STAT3 (signal and transducer of transcription 3). Two papers appeared in the same year identifying this interaction and the GRIM-19 inhibitory role in STAT3 activation, but they disagreed in the way how this inhibition was taken out [44, 57]. One of them reported that GRIM-19 binds to the coiled-coil, DNA binding and linker domains of STAT3 and this interaction inhibits STAT3 translocations to the nucleus [57]. The other publication stated that GRIM-19 regulates STAT3 binding to the transactivation domain (TAD) and blocks its activity (and not its nuclear translocation, neither its capability to bind to DNA), being Ser727 required [44].

STAT3 is commonly referred as being activated when its tyrosine residue (Tyr705) is phosphorylated by growth factor receptors [41]. Not so consensual is the phosphorylation at serine residue (Ser727). Some authors defend that this second phosphorylation is required for fully activation of STAT3, others defend that this residue is required for STAT3 activation, but in an independent manner of the Tyr705 residue [49, 55]. There are also some studies pointing to repressive activity of phosphorylation at residue Ser727 to STAT3 functionality [41].

Taking into account the not so well explained way in which GRIM-19 represses STAT3 activity as a transcription factor and the two possible phosphorylations that

occur to the activation of STAT3; we performed an evaluation of phospho-STAT3 Tyr705 and Ser727 in the tumour series from thyroid and kidney, in which GRIM-19 expression was studied, to verify if there was any relationship between GRIM-19 expression and the expression of the two phospho-isoforms of STAT3.

In thyroid tumours, STAT3 seems to be less activated, according to our data, since p-STAT3 Tyr705 is downregutated in tumour tissues, comparing with the adjacent normal thyroid tissues. Nevertheless, for p-STAT3 Ser727 we did not observe any differences between the different thyroid tumour histotypes. This surprising data may suggest that unlike what is described, in thyroid tumourigenesis STAT3 can function as a tumour suppressor gene and not as an oncogene. This phenomenon was also described in brain tumours [100].

In renal tumours, STAT3 activation seems to have a different behaviour. P-STAT3 Tyr705 seems to have a similar expression comparing with normal tissues, but p-STAT3 Ser727 has less expression. When we performed a correlation analysis to check if there are any relation between the two p-STAT3 forms and between them and GRIM-19 we also observe divergent results between the two tissues. In the thyroid, we see a positive correlation between GRIM-19 and p-STAT3 Ser727 ($p<0.0001$) and between p-STAT3 Tyr705 and p-STAT3 Ser727 ($p=0.003$), but not between GRIM-19 and p-STAT3 Tyr705 ($p=0.937$). However, when we check for correlations in renal tumours it is not possible to observe any significant correlation between GRIM-19 and p-STAT3 Ser727 or Tyr705, but there is a visible tendency (not significant) for a positive relation between STAT3 Tyr705 and p-STAT3 Ser727 ($p=0.087$).

In our study, we can see a positive correlation ($p=0.003$) between both phosphorylation forms of STST3, which suggests that both are present at the same time and thus, should be required for STAT3 activation. In kidney cancer there seems to be a tendency for the same result $p=0.087$. To eliminate the doubts the series analysed should be enlarged to confirm if this value becomes significant. This enlargement should take in account the few cases of CromRCC and PRCC to eliminate also some doubts in terms of GRIM-19 expression. If the *p*-value becomes significant, the same conclusion that was taken for thyroid can be advanced.

Regarding the relationship between the GRIM-19 and the STAT3 phosphorylations, only a positive correlation between GRIM-19 and p-STAT3 Ser727 in thyroid tumours was observed. It is interesting, since GRIM-19 was shown to negatively regulate (repress) STAT3 activation. However, here we observe that, when

GRIM-19 is less expressed, p-STAT3 Ser727 is also less expressed). Taking into account all the results obtained, it seems that GRIM-19 does not regulate STAT3 activity through its phosphorylations. Thus, having the availability of VEGF and MMP-2 antibodies, we searched for their expression in a few number of samples to discern if these two downstream STAT3 genes are upregulated when GRIM-19 was downregulated (since GRIM-19 represses STAT3). With the few samples analysed it was not possible to check the possible relation due to the diversity of results obtained. A higher number of tumours should be analysed to detect this relation. It is also known that these two genes, MMP-2 [101-103] and VEGF [104, 105], are regulated by several other pathways. Consequently, the expression evaluation of other STAT3 regulated genes that were described as being regulated by GRIM-19, such as *c-myc, fas* or *pdk* [58] should be performed .

STAT3 is commonly accepted and numerous times referred as being an oncogene [41, 106]. However, in the last few years some evidence appears to show that STAT3 may not always have an oncogene function. Depending on the cellular context, genetic background of the tumours and some mutations occurring in other important genes, STAT3 can also play a role similar to a tumour suppressor gene [100, 107-109]. De la Iglésia *et al.* (2008) showed that STAT3 can play the two distinctive functions: oncogene and tumour suppressor depending on the genetic background of the tumour. *Phosphatase and tensin homolog* gene (*PTEN*) mutations and a mutant isoform of *Epidermal growth factor receptor* gene (EGFR) - EGFRvIII are one of the common genetic abnormalities in high-grade gliomas and glioblastomas, respectively. The authors disrupted *PTEN* gene and verified that STAT3 phosphorylation in residue Tyr705 was indirectly inhibited. With this result, the investigators went to check STAT3 action. They knockout STAT3 in astrocytes and verified (1) an increase of astrocytes number, (2) none or little effect on cell death, (3) a higher invading potential of astrocytes. In this study they found that EGFRvIII and STAT3 interact more efficiently in nucleus than cytoplasm. STAT3 knockout also led a high decrease in astrocytes expressing EGFRvIII, and blocked its ability to induce malignant transformation in astrocytes. With these results, the authors suggested that STAT3 can play two different and opposing roles depending on the "genetic environment" [100]. In our study, despite the difference regarding the two p-STAT3 isoforms, we clearly see a dowregulation of p-STAT3 in tumours comparing with normal tissues. This

downregulation raised questions regarding the role of STAT3 as an oncogene mentioned in literature, since we were expecting STAT3 overregulation in tumours.
So, our data seems to suggest that STAT3 can function as a tumour suppressor rather than as an oncogene in thyroid and kidney tumourigenesis.

Despite not being observed in the thyroid, in kidney p-STAT3 Ser727 appeared in the nucleus, in the cytoplasm or in both locations in the same sample. Some recent studies showed that STAT3 can be located in mitochondria and phosphorylation at residue Ser727 seems to be critical for this location, regardless of its function in the nucleus [56]. Our data corroborated these observations, showing that p-STAT3 Ser727 can also be located in the cytoplasm, probably in mitochondria, as referred [56]. *In vitro* results from our group also showed that p-STAT3 Ser727 is present in the cytoplasm co-localized with GRIM-19 in mitochondria, confirming the mitochondrial location of p-STAT3 Ser727 (Figure 40 – unpublished data).

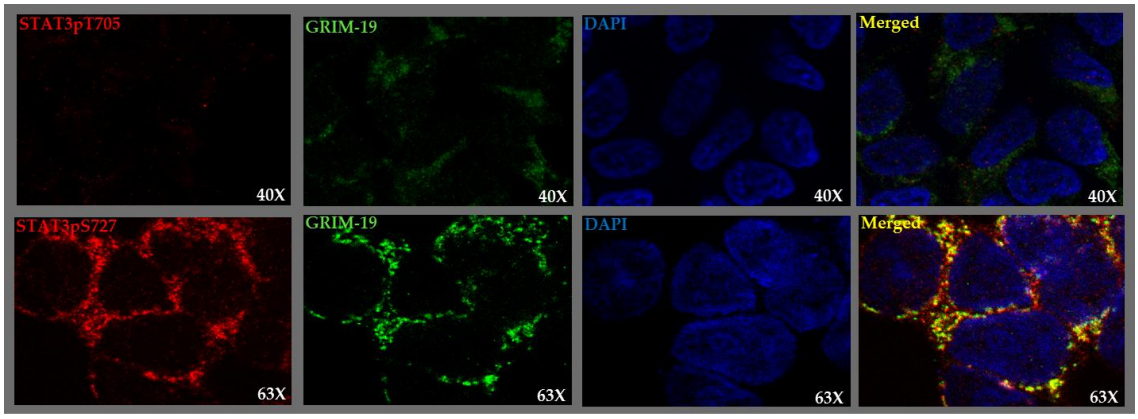

Figure 40 – GRIM-19 and p-STAT3 Ser727, but not pSTAT3 Tyr705 co-localizes in mitochondria as observed by merged pictures from GRIM-19 and p-STAT3 Ser727 immunocytochemistry stain for each one (unpublished data).

It was observable, in kidney tissues, that p-STAT3 Ser727 expression is more frequent in the nucleus of the cell of tumour tissue than in the nucleus of the cell of normal tissue. Based on this, we tried to find out if this is correlated with GRIM-19 expression. It was observed that there is a statistically significant association between GRIM-19 loss of expression and cytoplasmatic location of p-STAT3 ser727 (p=0.033). According to our data distribution Table (Anex I), it seems that when GRIM-19 is almost or completely absent, p-STAT3 ser727 localizes more in the cytoplasm. It is a surprising relation, since we expected that, as GRIM-19 suppresses STAT3 function,

when GRIM-19 was absent STAT3 should be more in the nucleus since its activation is inhibited by GRIM-19. It was also expected that when there is more GRIM-19 expression, there should be more STAT3 in mitochondria (cytoplasm). However, our results are contradictory with this hypothesis. Taking into account the role of GRIM-19 into mitochondria and the recent described role of STAT3 in mitochondria, this result may also be interesting. The impairment of mitochondrial complex I appears to be related with the etiopathogenesis of several cancers, in particularly with Hürthle thyroid tumours, and probably other oncocytic tumours [94]. In these types of tumours there seems to exist a compensatory mechanism to overcome deficiencies in OXPHOS process due to the inefficient functioning of complex I, by augmentation of mitochondrial number. This surprising result can be another compensatory mechanism. Since GRIM-19 is downregulated in tumours, STAT3, as required for OXPHOS, it can be confined to mitochondria as a compensation for GRIM-19 lack and complex I impairment. This is our supposition, but further investigations should be performed to clarify this hypothesis.

Our data is slightly different from those initially expected, but they are nevertheless interesting. To have an evident and clear confirmation of this data, *in vitro* assays should be performed. Our data shows that GRIM-19 is frequently downregulated in HCT from the thyroid and in renal cell tumours in general. This suggests that GRIM-19 loss confers some growth advantage to tumour cells. The *in vitro* studies should be performed to confirm the possible advantages conferred to the cells with GRIM-19 loss. GRIM-19 role in localization and regulation of phosphorylated STAT3 in Tyr705 and Ser727 residues should also be addressed by *in vitro* studies to understand better our results obtained in human samples.

CONCLUSIONS AND FUTURE DEVELOPMENTS

Conclusions

GRIM-19 is a novel tumour suppressor gene that has been associated with cancer as being downregulated and as participating in several processes that, directly or indirectly, leads to cancer formation and progression.

This present study was performed in a series of thyroid and kidney tumours, allowing us to get to some major conclusions:

- GRIM-19 may have an important role in ethiopathogensis in Hürthle cell thyroid tumours of the thyroid, but not in non-Hürthle cell tumours, since there is a downregulation of GRIM-19 protein expression only in Hürthle cell tumours.

- GRIM-19 may also have a role in ATC ethiopathogesis.

- In RCT, GRIM-19 was found to be downregulated in the majority of the tumours, suggesting a role of GRIM-19 in kidney tumourigenesis in general.

- In RCT GRIM-19 loss of expression is associated with the most aggressive phenotype and not with oncocytic features, in contrast with thyroid tumours.

- The role and activity of GRIM-19 in human cancers may be tissue-specific.

- GRIM-19 was noticed as the first MRC complex I protein, encoded by the nuclear DNA, downregulated in HCT, supporting the assumption that mitochondrial complex I dysfunction is involved in the pathogenesis of oncocytic tumours of the thyroid.

- Inhibition of STAT3 through GRIM-19 was proved not to be performed by regulation of its phosphorylation, since there are no correlations between GRIM-19 expression and the expression of STAT3 phosphorylated forms.

- Phosphorylation of the two residues of STAT3 (Ser727 and Tyr705) is likely not to be associated, and independent of STAT3 activation.

- GRIM-19 and STAT3 phosphorylated at residue Ser727 may be two compensatory proteins for the maintenance of complex I correct functioning.

- In kidney tumours p-STAT3 Ser727 appears to be more expressed in the nucleus than in cytoplasm.

- Although most of the literature considers STAT3 as an oncogene, in this study STAT3 was found to be downregulated in tumours and, therefore, may have the opposite role.

- We identified for the first time the putative region of the GRIM-19 gene promoter.

Despite several studies performed in recent years concerning the physiological role and importance of GRIM-19, little is known about this protein. For example, throughout this work several questions/hypothesis about GRIM-19 function were raised.

GRIM-19 has been associated with various mechanisms that, directly or indirectly, are associated with apoptosis, proliferation and cell cycle control; all of them related with cancer. Thus, GRIM-19 seems to have an important role in human tumourigenesis. Additional work should be performed to better understand the mechanisms of action of the GRIM-19, as this protein can be a powerful target for novel cancer therapies; this is particularly relevant considering that GRIM-19 expression can be modified by IFNs and RA treatment.

Future developments

While we were performing the work presented in this thesis, several questions were raised concerning validations and complementary work that would be important to carry out to clarify some issues. Below mentioned is summarized some of the aforementioned tasks that were pointed out during the thesis and some other relevant tasks related with the theme.

- At least in ROnc, the question if evaluation of GRIM-19 from the immunohistochemical procedure was not overvalued due to higher number of mitochondria was raised. In HCT a decrease comparing with normal and non-Hürthle cell tumours was observed. In the kidney we were expecting something similar, but it was not observed. This could be due to an overvaluation of the staining in ROnc due to the higher number of mitochondria. In fact, ROnc could have less expression than all the other RCT histotypes as observed in Hürthle cell tumours in thyroid. To clarify this question Western blot analysis in frozen tissues was suggested. With this procedure it will be possible to have a quantification of SDHA expression that will serve as a control of the number of mitochondria. It will allow evaluation, in a more qualitative and objective form, the expression of GRIM-19.

- Total STAT3 expression could not be evaluated by immunohistochemistry, since the antibody stains with no significant difference between cytoplasm and/or nucleus and intensity in each of these two cellular compartments in the several tumour samples tested. Some papers correlate directly GRIM-19 expression with STAT3 expression and activity. WB, for the aforementioned reasons raised in the first topic, an experiment in frozen tissues to discern if loss of GRIM-19 in tumours is related with more or less STAT3 expression should be performed. Phospho-STAT3s Tyr705 and Ser727 could also be analysed to confirm the results obtained in this study by immunohistochemistry.

- Despite the putative independent role of phospho-STAT3 Ser727 and Tyr705 in STAT3 activation, at least in kidney, must be clarified. By IHC technique it was possible to observe some relation, but it did not show if the two phosphorylated residues can be present in the same molecule or can be present in different molecules, activating them alone. To confirm this doubt, a Proximity Ligation Assay (PLA) technique could be performed to discern the role of the two phosphorylations that can occur in STAT3 molecule.

- It would be useful to define patterns of methylation of the GRIM-19 promoter in a cell line with complete, or almost complete, loss of mRNA expression. Thus, a search might be performed to find such a cell line. Once analysed, the pattern of methylation, would be able to construct primers to analyse the methylation status in the paraffin-embedded tissues. Until now, so far, no cell line without GRIM-19 expression has been found, our attention must be focused in the two oral squamous cell carcinoma cell lines that were described as expressing low levels of GRIM-19 - HSC2 and HSC3

- The fragment of GRIM-19 CpG island analysed is completely methylated in the studied cell lines. Thus, other region of the putative GRIM-19 promoter should be studied for methylation analysis.

- Other GRIM-19 expression regulatory mechanisms could also be addressed. Most of the data from the literature points to mRNA regulation mechanisms, although other regulatory mechanism at the protein level, could also contribute to GRIM-19 loss of expression.

- Despite the relations observed in this work between GRIM-19 and STAT3 expression, it might be confirmed also by *in vitro* studies. With this purpose, thyroid cancer cell lines and kidney cancer cell lines could be used. In these experiments, GRIM-19 can be downregulated or complete repressed, namely by shRNA, and the effects confirmed. Thus, we will simulate the downregulation of

GRIM-19, found by the immunohistochemical procedure, in thyroid and kidney tumours.

- Other *in vitro* studies should be performed to understand GRIM-19 function. Downregulation of GRIM-19 can be performed in order to analyse the expression of a set of genes related with proliferation, cell death pathways, cell cycle (where GRIM-19 seems to interfere) by gene expression profiling or microarray analysis.

- *In vivo* studies can also be performed in order to better understand the GRIM-19 importance, in normal cell physiology and also in tumour initiation, progression and development. It was been shown that GRIM-19 knockout leads to early embryonic lethality. Thus, a conditional gene knockout technique that will allow to obtain specific downregulation of GRIM-19 in a single organ in the body rather than in the whole body could be performed .

Here, only a small number of experiments that could be performed to unveiling the role of GRIM-19 both in cell physiology and tumour development were described. There is also a large field concerning GRIM-19 function that is still to be understood. Its tumour suppressor activity and its role in OXPHOS, make GRIM-19 a good candidate as a therapeutic target in cancer and putatively in metabolic disorders. However, there are still many issues to understand in order accomplish this major aim.

REFERENCES

1. Maximo V, Botelho T, Capela J, Soares P, Lima J, Taveira A, Amaro T, Barbosa AP, Preto A, Harach HR *et al*: **Somatic and germline mutation in GRIM-19, a dual function gene involved in mitochondrial metabolism and cell death, is linked to mitochondrion-rich (Hurthle cell) tumours of the thyroid**. *Br J Cancer* 2005, **92**(10):1892-1898.
2. Brenner D, Mak TW: **Mitochondrial cell death effectors**. *Curr Opin Cell Biol* 2009, **21**(6):871-877.
3. Youle RJ, Strasser A: **The BCL-2 protein family: opposing activities that mediate cell death**. *Nat Rev Mol Cell Biol* 2008, **9**(1):47-59.
4. Kalvakolanu DV, Nallar SC, Kalakonda S: **Cytokine-induced tumor suppressors: a GRIM story**. *Cytokine* 2010, **52**(1-2):128-142.
5. Hofmann ER, Boyanapalli M, Lindner DJ, Weihua X, Hassel BA, Jagus R, Gutierrez PL, Kalvakolanu DV: **Thioredoxin reductase mediates cell death effects of the combination of beta interferon and retinoic acid**. *Mol Cell Biol* 1998, **18**(11):6493-6504.
6. Darnell JE, Jr., Kerr IM, Stark GR: **Jak-STAT pathways and transcriptional activation in response to IFNs and other extracellular signaling proteins**. *Science* 1994, **264**(5164):1415-1421.
7. Chidambaram NV, Angell JE, Ling W, Hofmann ER, Kalvakolanu DV: **Chromosomal localization of human GRIM-19, a novel IFN-beta and retinoic acid-activated regulator of cell death**. *J Interferon Cytokine Res* 2000, **20**(7):661-665.
8. Freemantle SJ, Spinella MJ, Dmitrovsky E: **Retinoids in cancer therapy and chemoprevention: promise meets resistance**. *Oncogene* 2003, **22**(47):7305-7315.
9. Angell JE, Lindner DJ, Shapiro PS, Hofmann ER, Kalvakolanu DV: **Identification of GRIM-19, a novel cell death-regulatory gene induced by the interferon-beta and retinoic acid combination, using a genetic approach**. *J Biol Chem* 2000, **275**(43):33416-33426.
10. Piedrafita FJ, Pfahl M: **Nuclear retinoid receptors and mechanisms of action**. In: *Handbook Exp Pharmacol.* vol. 139; 1999: 153-184.
11. Kalvakolanu DV: **The GRIMs: a new interface between cell death regulation and interferon/retinoid induced growth suppression**. *Cytokine Growth Factor Rev* 2004, **15**(2-3):169-194.
12. Gao AC, Lou W, Ichikawa T, Denmeade SR, Barrett JC, Isaacs JT: **Suppression of the tumorigenicity of prostatic cancer cells by gene(s) located on human chromosome 19p13.1-13.2**. *Prostate* 1999, **38**(1):46-54.
13. Canzian F, Amati P, Harach HR, Kraimps JL, Lesueur F, Barbier J, Levillain P, Romeo G, Bonneau D: **A gene predisposing to familial thyroid tumors with cell oxyphilia maps to chromosome 19p13.2**. *Am J Hum Genet* 1998, **63**(6):1743-1748.
14. Ernster L, Schatz G: **Mitochondria: a historical review**. *J Cell Biol* 1981, **91**(3 Pt 2):227s-255s.
15. Carew JS, Huang P: **Mitochondrial defects in cancer**. *Mol Cancer* 2002, **1**:9.
16. Maximo V, Lima J, Soares P, Sobrinho-Simoes M: **Mitochondria and cancer**. *Virchows Arch* 2009, **454**(5):481-495.
17. McBride HM, Neuspiel M, Wasiak S: **Mitochondria: more than just a powerhouse**. *Curr Biol* 2006, **16**(14):R551-560.
18. Alberts B, Johnson A, Lewis J, Raff M, Roberts K, Walter P: **Molecular Biology of the Cell, 4(th) edition.**, 4th edn. New York: Garlan Science; 2002.
19. **Cell Biology and Microscopy Stucture and Function of Cells & viruses - Mitochondria** [http://micro.magnet.fsu.edu/cells/mitochondria/mitochondria.html]
20. Solano A, Playan A, Lopez-Perez MJ, Montoya J: **[Genetic diseases of the mitochondrial DNA in humans]**. *Salud Publica Mex* 2001, **43**(2):151-161.

21. Orth M, Schapira AH: **Mitochondria and degenerative disorders**. *Am J Med Genet* 2001, **106**(1):27-36.
22. Wallace DC: **Mitochondrial DNA mutations in disease and aging**. *Environ Mol Mutagen* 2010, **51**(5):440-450.
23. Penta JS, Johnson FM, Wachsman JT, Copeland WC: **Mitochondrial DNA in human malignancy**. *Mutat Res* 2001, **488**(2):119-133.
24. Eng C, Kiuru M, Fernandez MJ, Aaltonen LA: **A role for mitochondrial enzymes in inherited neoplasia and beyond**. *Nat Rev Cancer* 2003, **3**(3):193-202.
25. Fearnley IM, Carroll J, Shannon RJ, Runswick MJ, Walker JE, Hirst J: **GRIM-19, a cell death regulatory gene product, is a subunit of bovine mitochondrial NADH:ubiquinone oxidoreductase (complex I)**. *J Biol Chem* 2001, **276**(42):38345-38348.
26. Hu J, Angell JE, Zhang J, Ma X, Seo T, Raha A, Hayashi J, Choe J, Kalvakolanu DV: **Characterization of monoclonal antibodies against GRIM-19, a novel IFN-beta and retinoic acid-activated regulator of cell death**. *J Interferon Cytokine Res* 2002, **22**(10):1017-1026.
27. Murray J, Zhang B, Taylor SW, Oglesbee D, Fahy E, Marusich MF, Ghosh SS, Capaldi RA: **The subunit composition of the human NADH dehydrogenase obtained by rapid one-step immunopurification**. *J Biol Chem* 2003, **278**(16):13619-13622.
28. Huang G, Lu H, Hao A, Ng DC, Ponniah S, Guo K, Lufei C, Zeng Q, Cao X: **GRIM-19, a cell death regulatory protein, is essential for assembly and function of mitochondrial complex I**. *Mol Cell Biol* 2004, **24**(19):8447-8456.
29. Zhou AM, Zhao JJ, Ye J, Xiao WH, Kalvakolanu DV, Liu RY: **[Expression and clinical significance of GRIM-19 in non-small cell lung cancer]**. *Ai Zheng* 2009, **28**(4):431-435.
30. Nallar SC, Kalakonda S, Sun P, Ohmori Y, Hiroi M, Mori K, Lindner DJ, Kalvakolanu DV: **Identification of a structural motif in the tumor-suppressive protein GRIM-19 required for its antitumor activity**. *Am J Pathol* 2010, **177**(2):896-907.
31. Zhang X, Huang Q, Yang Z, Li Y, Li CY: **GW112, a novel antiapoptotic protein that promotes tumor growth**. *Cancer Res* 2004, **64**(7):2474-2481.
32. Huang Y, Yang M, Yang H, Zeng Z: **Upregulation of the GRIM-19 gene suppresses invasion and metastasis of human gastric cancer SGC-7901 cell line**. *Exp Cell Res* 2010, **316**(13):2061-2070.
33. Seo T, Lee D, Shim YS, Angell JE, Chidambaram NV, Kalvakolanu DV, Choe J: **Viral interferon regulatory factor 1 of Kaposi's sarcoma-associated herpesvirus interacts with a cell death regulator, GRIM19, and inhibits interferon/retinoic acid-induced cell death**. *J Virol* 2002, **76**(17):8797-8807.
34. Ma X, Kalakonda S, Srinivasula SM, Reddy SP, Platanias LC, Kalvakolanu DV: **GRIM-19 associates with the serine protease HtrA2 for promoting cell death**. *Oncogene* 2007, **26**(33):4842-4849.
35. Sun P, Nallar SC, Raha A, Kalakonda S, Velalar CN, Reddy SP, Kalvakolanu DV: **GRIM-19 and p16(INK4a) synergistically regulate cell cycle progression and E2F1-responsive gene expression**. *J Biol Chem* 2010, **285**(36):27545-27552.
36. Barnich N, Hisamatsu T, Aguirre JE, Xavier R, Reinecker HC, Podolsky DK: **GRIM-19 interacts with nucleotide oligomerization domain 2 and serves as downstream effector of anti-bacterial function in intestinal epithelial cells**. *J Biol Chem* 2005, **280**(19):19021-19026.
37. Chin KL, Aerbajinai W, Zhu J, Drew L, Chen L, Liu W, Rodgers GP: **The regulation of OLFM4 expression in myeloid precursor cells relies on NF-kappaB transcription factor**. *Br J Haematol* 2008, **143**(3):421-432.
38. Martins LM, Iaccarino I, Tenev T, Gschmeissner S, Totty NF, Lemoine NR, Savopoulos J, Gray CW, Creasy CL, Dingwall C *et al*: **The serine protease Omi/HtrA2 regulates**

apoptosis by binding XIAP through a reaper-like motif. *J Biol Chem* 2002, **277**(1):439-444.

39. Kobayashi K, Inohara N, Hernandez LD, Galan JE, Nunez G, Janeway CA, Medzhitov R, Flavell RA: **RICK/Rip2/CARDIAK mediates signalling for receptors of the innate and adaptive immune systems**. *Nature* 2002, **416**(6877):194-199.
40. Maximo V, Lima J, Soares P, Silva A, Bento I, Sobrinho-Simoes M: **GRIM-19 in Health and Disease**. *Adv Anat Pathol* 2008, **15**(1):46-53.
41. Bowman T, Garcia R, Turkson J, Jove R: **STATs in oncogenesis**. *Oncogene* 2000, **19**(21):2474-2488.
42. Takeda K, Noguchi K, Shi W, Tanaka T, Matsumoto M, Yoshida N, Kishimoto T, Akira S: **Targeted disruption of the mouse Stat3 gene leads to early embryonic lethality**. *Proc Natl Acad Sci U S A* 1997, **94**(8):3801-3804.
43. Akira S: **Roles of STAT3 defined by tissue-specific gene targeting**. *Oncogene* 2000, **19**(21):2607-2611.
44. Zhang J, Yang J, Roy SK, Tininini S, Hu J, Bromberg JF, Poli V, Stark GR, Kalvakolanu DV: **The cell death regulator GRIM-19 is an inhibitor of signal transducer and activator of transcription 3**. *Proc Natl Acad Sci U S A* 2003, **100**(16):9342-9347.
45. Gouilleux-Gruart V, Gouilleux F, Desaint C, Claisse JF, Capiod JC, Delobel J, Weber-Nordt R, Dusanter-Fourt I, Dreyfus F, Groner B *et al*: **STAT-related transcription factors are constitutively activated in peripheral blood cells from acute leukemia patients**. *Blood* 1996, **87**(5):1692-1697.
46. Bromberg JF: **Activation of STAT proteins and growth control**. *Bioessays* 2001, **23**(2):161-169.
47. Fletcher S, Drewry JA, Shahani VM, Page BD, Gunning PT: **Molecular disruption of oncogenic signal transducer and activator of transcription 3 (STAT3) protein**. *Biochem Cell Biol* 2009, **87**(6):825-833.
48. Yang SF, Yuan SS, Yeh YT, Wu MT, Su JH, Hung SC, Chai CY: **The role of p-STAT3 (ser727) revealed by its association with Ki-67 in cervical intraepithelial neoplasia**. *Gynecol Oncol* 2005, **98**(3):446-452.
49. Wen Z, Zhong Z, Darnell JE, Jr.: **Maximal activation of transcription by Stat1 and Stat3 requires both tyrosine and serine phosphorylation**. *Cell* 1995, **82**(2):241-250.
50. Ram PA, Park SH, Choi HK, Waxman DJ: **Growth hormone activation of Stat 1, Stat 3, and Stat 5 in rat liver. Differential kinetics of hormone desensitization and growth hormone stimulation of both tyrosine phosphorylation and serine/threonine phosphorylation**. *J Biol Chem* 1996, **271**(10):5929-5940.
51. Bromberg JF, Horvath CM, Besser D, Lathem WW, Darnell JE, Jr.: **Stat3 activation is required for cellular transformation by v-src**. *Mol Cell Biol* 1998, **18**(5):2553-2558.
52. Turkson J, Bowman T, Adnane J, Zhang Y, Djeu JY, Sekharam M, Frank DA, Holzman LB, Wu J, Sebti S *et al*: **Requirement for Ras/Rac1-mediated p38 and c-Jun N-terminal kinase signaling in Stat3 transcriptional activity induced by the Src oncoprotein**. *Mol Cell Biol* 1999, **19**(11):7519-7528.
53. Zhang Y, Liu G, Dong Z: **MSK1 and JNKs mediate phosphorylation of STAT3 in UVA-irradiated mouse epidermal JB6 cells**. *J Biol Chem* 2001, **276**(45):42534-42542.
54. Lim CP, Cao X: **Serine phosphorylation and negative regulation of Stat3 by JNK**. *J Biol Chem* 1999, **274**(43):31055-31061.
55. Kim JH, Yoon MS, Chen J: **Signal transducer and activator of transcription 3 (STAT3) mediates amino acid inhibition of insulin signaling through serine 727 phosphorylation**. *J Biol Chem* 2009, **284**(51):35425-35432.
56. Wegrzyn J, Potla R, Chwae YJ, Sepuri NB, Zhang Q, Koeck T, Derecka M, Szczepanek K, Szelag M, Gornicka A *et al*: **Function of mitochondrial Stat3 in cellular respiration**. *Science* 2009, **323**(5915):793-797.

57. Lufei C, Ma J, Huang G, Zhang T, Novotny-Diermayr V, Ong CT, Cao X: **GRIM-19, a death-regulatory gene product, suppresses Stat3 activity via functional interaction**. *EMBO J* 2003, **22**(6):1325-1335.
58. Kalakonda S, Nallar SC, Lindner DJ, Hu J, Reddy SP, Kalvakolanu DV: **Tumor-suppressive activity of the cell death activator GRIM-19 on a constitutively active signal transducer and activator of transcription 3**. *Cancer Res* 2007, **67**(13):6212-6220.
59. Gough DJ, Corlett A, Schlessinger K, Wegrzyn J, Larner AC, Levy DE: **Mitochondrial STAT3 supports Ras-dependent oncogenic transformation**. *Science* 2009, **324**(5935):1713-1716.
60. Alchanati I, Nallar SC, Sun P, Gao L, Hu J, Stein A, Yakirevich E, Konforty D, Alroy I, Zhao X *et al*: **A proteomic analysis reveals the loss of expression of the cell death regulatory gene GRIM-19 in human renal cell carcinomas**. *Oncogene* 2006, **25**(54):7138-7147.
61. He X, Cao X: **Identification of alternatively spliced GRIM-19 mRNA in kidney cancer tissues**. *J Hum Genet* 2010, **55**(8):507-511.
62. Gong LB, Luo XL, Liu SY, Tao DD, Gong JP, Hu JB: **[Correlations of GRIM-19 and its target gene product STAT3 to malignancy of human colorectal carcinoma]**. *Ai Zheng* 2007, **26**(7):683-687.
63. Zhang L, Gao L, Li Y, Lin G, Shao Y, Ji K, Yu H, Hu J, Kalvakolanu DV, Kopecko DJ *et al*: **Effects of plasmid-based Stat3-specific short hairpin RNA and GRIM-19 on PC-3M tumor cell growth**. *Clin Cancer Res* 2008, **14**(2):559-568.
64. Zhou Y, Li M, Wei Y, Feng D, Peng C, Weng H, Ma Y, Bao L, Nallar S, Kalakonda S *et al*: **Down-regulation of GRIM-19 expression is associated with hyperactivation of STAT3-induced gene expression and tumor growth in human cervical cancers**. *J Interferon Cytokine Res* 2009, **29**(10):695-703.
65. Moreira S, Correia M, Soares P, Maximo V: **GRIM-19 function in cancer development**. *Mitochondrion* 2011.
66. Couto JP, Prazeres H, Castro P, Lima J, Maximo V, Soares P, Sobrinho-Simoes M: **How molecular pathology is changing and will change the therapeutics of patients with follicular cell-derived thyroid cancer**. *J Clin Pathol* 2009, **62**(5):414-421.
67. DeLellis R, Lloyd R, Heitz P, Eng C: **World Health Organization Classification of Tumours. Pathology and Genetics of Tumours of Endocrine Organs.** Lyon: IARC Press; 2004.
68. Sobrinho-Simoes M, Preto A, Rocha AS, Castro P, Maximo V, Fonseca E, Soares P: **Molecular pathology of well-differentiated thyroid carcinomas**. *Virchows Arch* 2005, **447**(5):787-793.
69. Castro P, Roque L, Magalhaes J, Sobrinho-Simoes M: **A subset of the follicular variant of papillary thyroid carcinoma harbors the PAX8-PPARgamma translocation**. *Int J Surg Pathol* 2005, **13**(3):235-238.
70. Castro P, Rebocho AP, Soares RJ, Magalhaes J, Roque L, Trovisco V, Vieira de Castro I, Cardoso-de-Oliveira M, Fonseca E, Soares P *et al*: **PAX8-PPARgamma rearrangement is frequently detected in the follicular variant of papillary thyroid carcinoma**. *J Clin Endocrinol Metab* 2006, **91**(1):213-220.
71. Eble J, Sauter G, Epstein J, Sesterhenn I: **World Health Organization Classification of Tumours. Pathology and Genetics of Tumours of the Urinary System and Male Genital Organs**, vol. 7. Lyon: IARC Press; 2004.
72. Pfaffenroth EC, Linehan WM: **Genetic basis for kidney cancer: opportunity for disease-specific approaches to therapy**. *Expert Opin Biol Ther* 2008, **8**(6):779-790.
73. Richard S, Lidereau R, Giraud S: **The growing family of hereditary renal cell carcinoma**. *Nephrol Dial Transplant* 2004, **19**(12):2954-2958.

74. Vira MA, Novakovic KR, Pinto PA, Linehan WM: **Genetic basis of kidney cancer: a model for developing molecular-targeted therapies**. *BJU Int* 2007, **99**(5 Pt B):1223-1229.
75. Ficarra V, Martignoni G, Galfano A, Novara G, Gobbo S, Brunelli M, Pea M, Zattoni F, Artibani W: **Prognostic role of the histologic subtypes of renal cell carcinoma after slide revision**. *Eur Urol* 2006, **50**(4):786-793; discussion 793-784.
76. Latif F, Tory K, Gnarra J, Yao M, Duh FM, Orcutt ML, Stackhouse T, Kuzmin I, Modi W, Geil L *et al*: **Identification of the von Hippel-Lindau disease tumor suppressor gene**. *Science* 1993, **260**(5112):1317-1320.
77. Linehan WM, Vasselli J, Srinivasan R, Walther MM, Merino M, Choyke P, Vocke C, Schmidt L, Isaacs JS, Glenn G *et al*: **Genetic basis of cancer of the kidney: disease-specific approaches to therapy**. *Clin Cancer Res* 2004, **10**(18 Pt 2):6282S-6289S.
78. Zbar B, Klausner R, Linehan WM: **Studying cancer families to identify kidney cancer genes**. *Annu Rev Med* 2003, **54**:217-233.
79. Schmidt L, Junker K, Nakaigawa N, Kinjerski T, Weirich G, Miller M, Lubensky I, Neumann HP, Brauch H, Decker J *et al*: **Novel mutations of the MET proto-oncogene in papillary renal carcinomas**. *Oncogene* 1999, **18**(14):2343-2350.
80. Vocke CD, Yang Y, Pavlovich CP, Schmidt LS, Nickerson ML, Torres-Cabala CA, Merino MJ, Walther MM, Zbar B, Linehan WM: **High frequency of somatic frameshift BHD gene mutations in Birt-Hogg-Dube-associated renal tumors**. *J Natl Cancer Inst* 2005, **97**(12):931-935.
81. Sobrinho-Simoes M, Maximo V, Castro IV, Fonseca E, Soares P, Garcia-Rostan G, Oliveira MC: **Hurthle (oncocytic) cell tumors of thyroid: etiopathogenesis, diagnosis and clinical significance**. *Int J Surg Pathol* 2005, **13**(1):29-35.
82. Sobrinho-Simões M, Magalhães J, Fonseca E, Amendoeira I: **Diagnostic pitfalls of thyroid pathology**. *Current Diagnostic Pathology* 2005, **11**(1):52-59.
83. Maximo V, Soares P, Lima J, Cameselle-Teijeiro J, Sobrinho-Simoes M: **Mitochondrial DNA somatic mutations (point mutations and large deletions) and mitochondrial DNA variants in human thyroid pathology: a study with emphasis on Hurthle cell tumors**. *Am J Pathol* 2002, **160**(5):1857-1865.
84. Muller-Hocker J, Jacob U, Seibel P: **Hashimoto thyroiditis is associated with defects of cytochrome-c oxidase in oxyphil Askanazy cells and with the common deletion (4,977) of mitochondrial DNA**. *Ultrastruct Pathol* 1998, **22**(1):91-100.
85. Maximo V, Sobrinho-Simoes M: **Hurthle cell tumours of the thyroid. A review with emphasis on mitochondrial abnormalities with clinical relevance**. *Virchows Arch* 2000, **437**(2):107-115.
86. Attardi G, Yoneda M, Chomyn A: **Complementation and segregation behavior of disease-causing mitochondrial DNA mutations in cellular model systems**. *Biochim Biophys Acta* 1995, **1271**(1):241-248.
87. Takai D, Jones PA: **Comprehensive analysis of CpG islands in human chromosomes 21 and 22**. *Proc Natl Acad Sci U S A* 2002, **99**(6):3740-3745.
88. Takai D, Jones PA: **The CpG island searcher: a new WWW resource**. *In Silico Biol* 2003, **3**(3):235-240.
89. **e!ENSEMBL** [http://www.ensembl.org/index.html]
90. **CpG Island Searcher** [http://www.cpgislands.com/]
91. Prazeres H, Torres J, Rodrigues F, Pinto M, Pastoriza MC, Gomes D, Cameselle-Teijeiro J, Vidal A, Martins TC, Sobrinho-Simoes M *et al*: **Chromosomal, epigenetic and microRNA-mediated inactivation of LRP1B, a modulator of the extracellular environment of thyroid cancer cells**. *Oncogene* 2011, **30**(11):1302-1317.
92. Pelicano L, Chelbi-Alix MK: **[Interferon and retinoic acid in the treatment of human cancer: mechanisms of action]**. *Bull Cancer* 1998, **85**(4):313-318.

93. Gasparre G, Porcelli AM, Bonora E, Pennisi LF, Toller M, Iommarini L, Ghelli A, Moretti M, Betts CM, Martinelli GN *et al*: **Disruptive mitochondrial DNA mutations in complex I subunits are markers of oncocytic phenotype in thyroid tumors**. *Proc Natl Acad Sci U S A* 2007, **104**(21):9001-9006.
94. Zimmermann FA, Mayr JA, Neureiter D, Feichtinger R, Alinger B, Jones ND, Eder W, Sperl W, Kofler B: **Lack of complex I is associated with oncocytic thyroid tumours**. *Br J Cancer* 2009, **100**(9):1434-1437.
95. Zimmermann FA, Mayr JA, Feichtinger R, Neureiter D, Lechner R, Koegler C, Ratschek M, Rusmir H, Sargsyan K, Sperl W *et al*: **Respiratory chain complex I is a mitochondrial tumor suppressor of oncocytic tumors**. *Front Biosci (Elite Ed)* 2011, **3**:315-325.
96. Linehan WM, Srinivasan R, Schmidt LS: **The genetic basis of kidney cancer: a metabolic disease**. *Nat Rev Urol* 2010, **7**(5):277-285.
97. Baylin SB: **DNA methylation and gene silencing in cancer**. *Nat Clin Pract Oncol* 2005, **2 Suppl 1**:S4-11.
98. Jones PA, Baylin SB: **The fundamental role of epigenetic events in cancer**. *Nat Rev Genet* 2002, **3**(6):415-428.
99. Arce C, Perez-Plasencia C, Gonzalez-Fierro A, de la Cruz-Hernandez E, Revilla-Vazquez A, Chavez-Blanco A, Trejo-Becerril C, Perez-Cardenas E, Taja-Chayeb L, Bargallo E *et al*: **A proof-of-principle study of epigenetic therapy added to neoadjuvant doxorubicin cyclophosphamide for locally advanced breast cancer**. *PLoS One* 2006, **1**:e98.
100. de la Iglesia N, Konopka G, Puram SV, Chan JA, Bachoo RM, You MJ, Levy DE, Depinho RA, Bonni A: **Identification of a PTEN-regulated STAT3 brain tumor suppressor pathway**. *Genes Dev* 2008, **22**(4):449-462.
101. Overall CM, Wrana JL, Sodek J: **Transcriptional and post-transcriptional regulation of 72-kDa gelatinase/type IV collagenase by transforming growth factor-beta 1 in human fibroblasts. Comparisons with collagenase and tissue inhibitor of matrix metalloproteinase gene expression**. *J Biol Chem* 1991, **266**(21):14064-14071.
102. Lee JG, Dahi S, Mahimkar R, Tulloch NL, Alfonso-Jaume MA, Lovett DH, Sarkar R: **Intronic regulation of matrix metalloproteinase-2 revealed by in vivo transcriptional analysis in ischemia**. *Proc Natl Acad Sci U S A* 2005, **102**(45):16345-16350.
103. Jansen PL, Rosch R, Jansen M, Binnebosel M, Junge K, Alfonso-Jaume A, Klinge U, Lovett DH, Mertens PR: **Regulation of MMP-2 gene transcription in dermal wounds**. *J Invest Dermatol* 2007, **127**(7):1762-1767.
104. Mueller MD, Vigne JL, Minchenko A, Lebovic DI, Leitman DC, Taylor RN: **Regulation of vascular endothelial growth factor (VEGF) gene transcription by estrogen receptors alpha and beta**. *Proc Natl Acad Sci U S A* 2000, **97**(20):10972-10977.
105. He C, Chen X: **Transcription regulation of the vegf gene by the BMP/Smad pathway in the angioblast of zebrafish embryos**. *Biochem Biophys Res Commun* 2005, **329**(1):324-330.
106. Levy DE, Inghirami G: **STAT3: a multifaceted oncogene**. *Proc Natl Acad Sci U S A* 2006, **103**(27):10151-10152.
107. Rivat C, De Wever O, Bruyneel E, Mareel M, Gespach C, Attoub S: **Disruption of STAT3 signaling leads to tumor cell invasion through alterations of homotypic cell-cell adhesion complexes**. *Oncogene* 2004, **23**(19):3317-3327.
108. Musteanu M, Blaas L, Mair M, Schlederer M, Bilban M, Tauber S, Esterbauer H, Mueller M, Casanova E, Kenner L *et al*: **Stat3 is a negative regulator of intestinal tumor progression in Apc(Min) mice**. *Gastroenterology* 2010, **138**(3):1003-1011 e1001-1005.
109. Ecker A, Simma O, Hoelbl A, Kenner L, Beug H, Moriggl R, Sexl V: **The dark and the bright side of Stat3: proto-oncogene and tumor-suppressor**. *Front Biosci* 2009, **14**:2944-2958.

ANNEXES

Anex I – Statistical analysis

1. ***Unpaired T-test for analysis of <u>GRIM-19 distribution</u> between different <u>thyroid</u> tumour histotypes:***

	(n)	Mean	Standard error
Normal	60	1.700	0.083
PTC	17	1.706	0.187
FTC	7	1.000	0.309
FVPTC	31	1.742	0.122
FTA	14	1.500	0.203
ATC	10	1.000	0.258

	p-value (unpaired t-test)
Normal – PTC	0.9748
Normal – FTC	0.0103
Normal – FVPTC	0.7739
Normal – FTA	0.3163
Normal – ATC	0.0032
PTC – FTC	0.0575
PTC – FVPTC	0.8679
PTC – FTA	0.4626
PTC – ATC	0.0337
FTC – FVPTC	0.0166
FTC – FTA	0.1811
FTC – ATC	-
FVPTC – FTA	0.2932
FVPTC – ATC	0.0069
FTA – ATC	0.1374

2. ***Unpaired T-test for analysis of <u>GRIM-19 distribution</u> between different <u>thyroid</u> tumour accordingly to histotype and Hürthle/non-Hürthle:***

	(n)	Mean	Standard error
Normal	60	1.700	0.083
FTA non-H	7	1.714	0.184
FTA H	7	1.286	0.360
PTC non-H	12	1.917	0.193
PTC H	5	1.200	0.374
FVPTC non-H	20	2.000	0.126
FVPTC H	11	1.273	0.195
FTC non-H	3	1.667	0.333
FTC H	4	0.500	0.281

	p-value (unpaired t-test)
Normal – FTA non-H	**0.9551**
Normal – FTA H	**0.1318**
Normal – PTC non-H	**0.2950**
Normal – PTC H	**0.1083**
Normal – FVPTC non-H	**0.0674**
Normal – FVPTC H	**0.0476**
Normal – FTC non-H	**0.9305**
Normal – FTC H	**0.0006**
FTA non-H – FTA H	**0.3097**
PTC non-H – PTC H	**0.0801**
FVPTC non-H – FVPTC H	**0.0028**
FTC non-H – FTC H	**0.0457**

3. ***Unpaired T-test for analysis of GRIM-19 distribution between Hürthle/non-Hürthle thyroid tumours:***

	(n)	Mean	Standard error
Normal	60	1.700	0.083
Hurthle	27	1.148	0.148
Non-Hurthle	42	1.905	0.089

	p-value (unpaired t-test)
Normal – Hürthle	**0.0008**
Normal – non-Hürthle	**0.1028**
Hürthle – non-Hürthle	**<0.0001**

4. ***Unpaired T-test for analysis of GRIM-19 distribution between normal and tumours from kidney tissue:***

	(n)	Mean	Standard error
Normal	40	2.875	0.089
Tumour	52	0.981	0.133

	p-value (unpaired t-test)
Normal – Tumour	**<0.0001**

5. ***Unpaired T-test for analysis of GRIM-19 distribution between different kidney tumour histotypes:***

	(n)	Mean	Standard error
Normal	40	2.875	0.089
CCRCC	20	0.400	0.152
PRCC	8	2.125	0.227
CromRCC	3	0.667	0.333
ROnc	21	1.143	0.199

	p-value (unpaired t-test)
Normal – CCRCC	<0.0001
Normal – PRCC	0.0016
Normal – CromRCC	<0.0001
Normal – Ronc	<0.0001
CCRCC – PRCC	<0.0001
CCRCC – CromRCC	0.5281
CCRCC – Ronc	0.0054
PRCC – CromRCC	0.0075
PRCC – Ronc	0.0097
CromRCC - ROnc	0.3928

6. ***Unpaired T-test for analysis of <u>p-STAT3 Tyr705 distribution</u> between different <u>thyroid tumour</u> histotypes:***

	Intensity			Percentage			Combination		
	(n)	Mean	Standard error	(n)	Mean	Standard error	(n)	Mean	Standard error
Normal	60	1.817	0.097	60	1.367	0.154	60	1.517	0.120
FTA	14	1.500	0.203	14	0.857	0.254	14	1.071	0.267
PTC	17	1.412	0.193	17	0.647	0.170	17	0.882	0.225
FVPTC	31	1.226	0.165	31	0.645	0.158	31	0.839	0.168
FTC	7	1.143	0.340	7	0.857	0.340	7	1.000	0.378

	p-value (unpaired t-test)		
	Intensity	Percentage	Combination
Normal – FTA	0.1591	0.1407	0.1157
Normal – PTC	0.0556	0.0205	0.0152
Normal – FVPTC	0.0014	0.0038	0.0014
Normal – FTC	0.0306	0.2791	0.1718
FTA – PTC	0.7560	0.4845	0.5892
FTA – FVPTC	0.3359	0.4683	0.4528
FTA – FTC	0.3507	-	0.8788
PTC – FVPTC	0.4868	0.9939	0.8774
PTC – FTC	0.4756	0.5450	0.7848
FVPTC - FTC	0.8301	0.5690	0.6860

7. ***Unpaired T-test for analysis of <u>p-STAT3 Tyr705 distribution</u> between normal and tumours from <u>thyroid tissue</u>:***

	(n)	Mean	Standard error
Normal	60	1.517	0.120
Tumour	69	0.913	0.113

	p-value (unpaired t-test)
Normal – Tumour	**0.0004**

8. ***Unpaired T-test for analysis of <u>p-STAT3 Tyr705 distribution</u> between different <u>thyroid tumour</u> accordingly to histotype and Hürthle/non-Hürthle:***

	(n)	Mean	Standard error
FTA non-H	7	1.429	0.369
FTA H	7	0.714	0.360
PTC non-H	12	0.917	0.260
PTC H	5	0.800	0.490
FVPTC non-H	20	0.950	0.211
FVPTC H	11	0.636	0.279
FTC non-H	3	1.000	0.577
FTC H	4	1.000	0.577

	p-value (unpaired t-test)
FTA non-H – FTA H	**0.1907**
PTC non-H – PTC H	**0.8218**
FVPTC non-H – FVPTC H	**0.3802**
FTC non-H – FTC H	**0.120**

9. ***Unpaired T-test for analysis of <u>p-STAT3 Tyr705 distribution</u> between different <u>kidney tumour</u> histotypes:***

	(n)	Mean	Standard error
Normal	40	1.450	0.179
CCRCC	20	1.250	0.307
PRCC	8	1.750	0.453
CromRCC	3	0.333	0.333
ROnc	21	1.048	0.297

	p-value (unpaired t-test)
Normal – CCRCC	0.5502
Normal – PRCC	0.5059
Normal – CromRCC	0.1006
Normal – Ronc	0.2233
CCRCC – PRCC	0.3834
CCRCC – CromRCC	0.2736
CCRCC – Ronc	0.6378
PRCC – CromRCC	0.1054
PRCC – Ronc	0.2177
CromRCC - ROnc	0.3857

10. Unpaired T-test for analysis of p-STAT3 Tyr705 distribution between normal and tumours from kidney tissue:

	(n)	Mean	Standard error
Normal	40	1.450	0.179
Tumour	52	1.192	0.184

	p-value (unpaired t-test)
Normal – Tumour	**0.3285**

11. Unpaired T-test for analysis of p-STAT3 Ser727 distribution between different thyroid tumour histotypes:

	Intensity			Percentage			Combination		
	(n)	Mean	Standard error	(n)	Mean	Standard error	(n)	Mean	Standard error
Normal	60	1.317	0.102	60	1.750	0.179	60	1.367	0.109
FTA	14	1.071	0.267	14	1.143	0.345	14	1.071	0.286
PTC	17	0.941	0.218	17	1.176	0.356	17	1.000	0.243
FVPTC	30*	1.300	0.137	30*	1.767	0.261	30*	1.433	0.157
FTC	7	0.810	0.340	7	1.429	0.612	7	1.000	0.378

* - Due a technical problem, the evaluation of one tumour (FVPTC) could not be evaluated for p-STAT# Ser727.

	p-value (unpaired t-test)		
	Intensity	Percentage	Combination
Normal – FTA	0.3243	0.1395	0.2667
Normal – PTC	0.0981	0.1411	0.1331
Normal – FVPTC	0.9239	0.9577	0.7260
Normal – FTC	0.1564	0.5697	0.2890
FTA – PTC	0.7052	0.9471	0.8494
FTA – FVPTC	0.4021	0.1727	0.2358
FTA – FTC	0.6378	0.6651	0.8847
PTC – FVPTC	0.1495	0.1849	0.1242
PTC – FTC	0.8371	0.7137	-
FVPTC - FTC	0.1835	0.5859	0.2509

12. ***Unpaired T-test for analysis of p-STAT3 Ser727 distribution (combination) between normal and tumours from thyroid tissue:***

	(n)	Mean	Standard error
Normal	60	1.367	0.109
Tumour	68*	1.206	0.116

	p-value (unpaired t-test)
Normal – Tumour	**0.3174**

13. ***Unpaired T-test for analysis of p-STAT3 Ser727 distribution between different thyroid tumour accordingly to histotype and Hürthle/non-Hürthle:***

	(n)	Mean	Standard error
FTA non-H	7	1.571	0.369
FTA H	7	0.571	0.369
PTC non-H	12	0.833	0.241
PTC H	5	1.400	0.600
FVPTC non-H	19*	1.526	0.177
FVPTC H	11	1.273	0.304
FTC non-H	3	1.333	0.667
FTC H	4	0.750	0.479

	p-value (unpaired t-test)
FTA non-H – FTA H	**0.0793**
PTC non-H – PTC H	**0.3018**
FVPTC non-H – FVPTC H	**0.4452**
FTC non-H – FTC H	**0.4960**

* - Due a technical problem, the evaluation of one tumour (FVPTC) could not be evaluated for p-STAT3 Ser727.

14. ***Unpaired T-test for analysis of p-STAT3 Ser727 distribution between different kidney tumour histotypes:***

	(n)	Mean	Standard error
Normal	40	1.050	0.129
CCRCC	20	0.600	0.134
PRCC	8	0.875	0.479
CromRCC	3	1.333	0.882
ROnc	21	0.286	0.122

	p-value (unpaired t-test)
Normal – CCRCC	0.0327
Normal – PRCC	0.6250
Normal – CromRCC	0.5865
Normal – Ronc	0.0003
CCRCC – PRCC	0.4566
CCRCC – CromRCC	0.1239
CCRCC – Ronc	0.0904
PRCC – CromRCC	0.6393
PRCC – Ronc	0.1038
CromRCC - ROnc	0.0250

15. ***Unpaired T-test for analysis of p-STAT3 Ser727 distribution between normal and tumours from kidney tissue:***

	(n)	Mean	Standard error
Normal	40	1.050	0.129
Tumour	52	0.558	0.115

	p-value (unpaired t-test)
Normal – Tumour	**0.0054**

16. ***Correlation analysis between GRIM-19, p-STAT3 Tyr705 and p-STAT3 Ser727 in thyroid:***

	Correlation	p-value
GRIM-19 – p-STAT3 Tyr705 (combination)	0.143	0.1067
GRIM-19 – p-STAT3 Ser727 (combination)	0.362	<0.0001
p-STAT3 Tyr705 - p-STAT3 Ser727 (combinations)	0.256	0.0034

17. ***Correlation analysis between GRIM-19, p-STAT3 Tyr705 and p-STAT3 Ser727 in kidney:***

	Correlation	p-value
GRIM-19 – p-STAT3 Tyr705	0.096	0.3656
GRIM-19 – p-STAT3 Ser727	0.061	0.5639
p-STAT3 Tyr705 - p-STAT3 Ser727	0.180	0.0866

18. ***Chi-square analysis to relate normal or tumour from kidney and p-STAT3 Ser727 location:***

Observed Frequencies

	Normal	Tumor	Totals
Nuclear	5	16	21
Cytoplasmatic	16	9	25
N and C	16	10	26
Totals	37	35	72

DF	2
Chi-square	9.058
Chi-square p-value	0.0108

19. Fisher's analysis to relate GRIM-19 presence or absence and p-STAT3 Ser727 location in kidney:

	(-)	(+)	Totals
Nuclear	6	10	16
Cytoplasmatic	8	1	9
Totals	14	11	25

	(-)	(+)	Totals
Nuclear	6	10	16
N and C	8	2	10
Totals	14	12	26

	(-)	(+)	Totals
Cytoplasmatic	8	1	9
N and C	8	2	10
Totals	16	3	19

	DF	Fisher's Exact P-value
GRIM-19 expression vs. Nuclear *and.* Cytoplasmatic phospho-STAT3 Ser727 staining	1	0.0330 (*)
GRIM-19 expression vs. Nuclear *and* Nuclear and Cytoplasmatic phospho-STAT3 Ser727 staining	1	0.0511
GRIM-19 expression vs. Cytoplasmatic *and* Nuclear and Cytoplasmatic phospho-STAT3 Ser727 staining	1	>0.9999

20. Count number of thyroid tumours who loss GRIM-19 expression and the ones who had completely absence, relating with Hürthle phenotype.

	Loss	No loss	Totals
Hürthle	18	9	27
Non-Hürthle	2	40	42
Totals	20	49	69

	(-)	(0+)	(1+)	(2+)	Totals
Loss	4	15	1	0	20
No loss	2	5	37	5	49
Totals	6	20	38	5	69

21. Count number of kidney tumours who loss GRIM-19 expression

	Normal	CCRCC	PRCC	CromRCC	ROnc	Totals
No loss	0	0	4	0	.1	4
Loss	0	11	3	2	19	35
Totals	0	11	7	2	20	40

Anex II – Figures

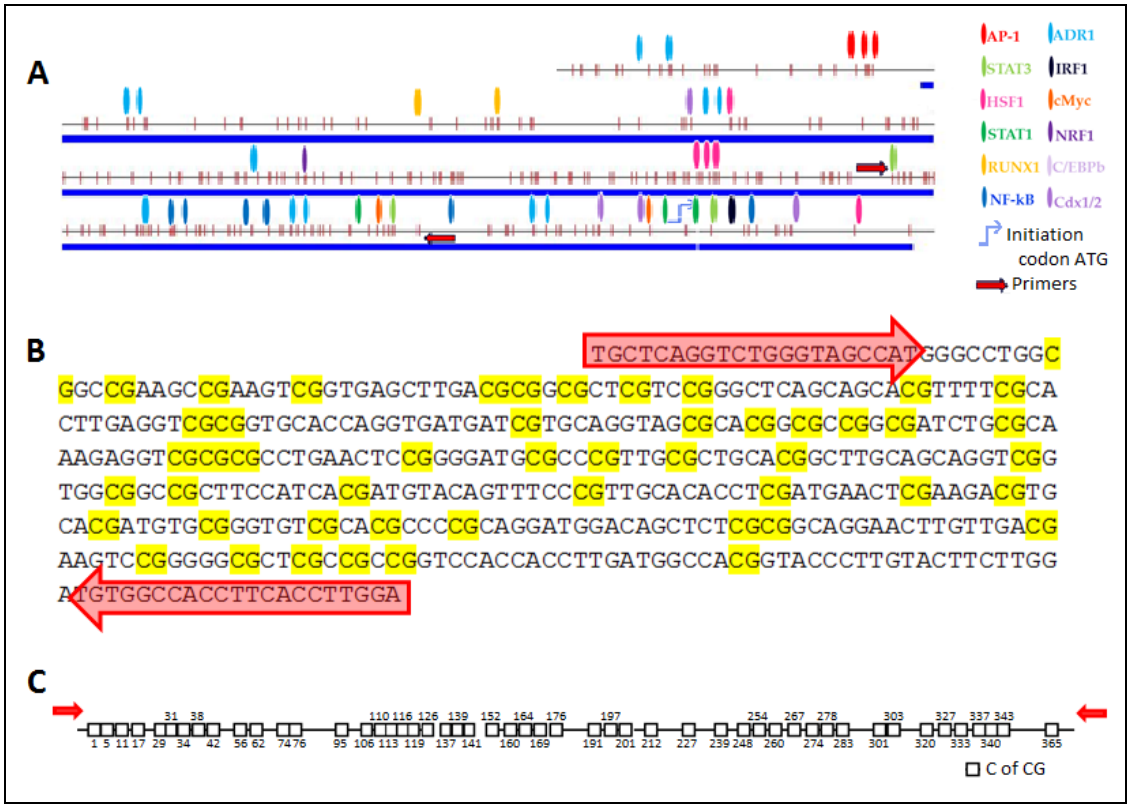

Figure A 1 – CpG islang of *GRIM-19* gene. (A) Putative promoter region of GRIM-19 showing several transcription factors that bioinformatically were determined as possible regulators; and the two primers constructed to the study; (B) The sequence studied with CG disclosed; (C) Scheme of CG dinucleotides in studied region.

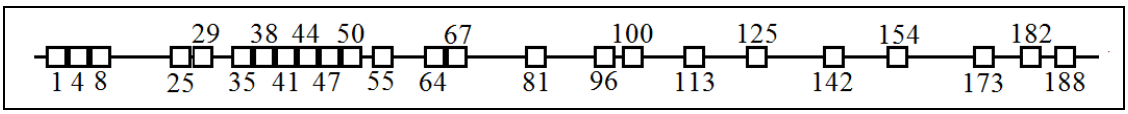

Figure A 2 - Scheme of CG dinucleotides in LRP1B studied region.

ARTICLE IN PRESS

MITOCH-00643; No of Pages 7

Mitochondrion xxx (2011) xxx–xxx

Contents lists available at ScienceDirect

Mitochondrion

journal homepage: www.elsevier.com/locate/mito

Review

GRIM-19 function in cancer development

Severina Moreira [a], Marcelo Correia [a], Paula Soares [a,b], Valdemar Máximo [a,b,*]

[a] Institute of Molecular Pathology and Immunology of the University of Porto (IPATIMUP), Rua Dr. Roberto Frias, s/n, 4200-465 Porto, Portugal
[b] Department of Pathology, Medical Faculty, University of Porto, Porto, Portugal

ARTICLE INFO

Article history:
Received 11 November 2010
Received in revised form 5 April 2011
Accepted 25 May 2011
Available online xxxx

Keywords:
Mitochondrial protein
GRIM-19
STAT3
Tumorigenesis

ABSTRACT

Cancer development involves multiple genetic changes, which can occur in tumor suppressor genes and lead to loss of function in a recessive manner. Recent findings have identified a novel tumor suppressor gene named GRIM-19. Similar to what has been observed for other known tumor suppressor proteins such as p53, GRIM-19 gene mutations and loss of protein expression have been observed in several tumor types. In this review, we perform a detailed description on the current understanding of GRIM-19 function in carcinogenesis.

Contents

1. Introduction

Gene associated with retinoid-IFN-induced mortality (GRIM)-19 was identified by a research group interested in unveiling the molecular basis of cell death associated with exposure to interferon (IFN)-β and retinoic acid (RA) (Angell et al., 2000). IFNs and RA have both been shown to suppress tumor growth and are used in the treatment of several cancers (Altucci and Gronemeyer, 2001; Gresser and Belardelli, 2002; Ikeda et al., 2002). By employing an anti-sense knock-out approach, the group was able to identify several genes associated with IFN-β and RA-induced mortality, including GRIM-19 (Angell et al., 2000). In breast carcinoma cell lines, both GRIM-19 mRNA and protein expression increased in the presence of IFN-β/RA. Further experiments

Abbreviations: GRIM-19, Gene associated with retinoid-IFN-induced mortality; IFN, interferon; RA, retinoic acid; MRC, mitochondrial respiratory chain; OXPHOS, oxidative phosphorylation; TCO, tumors with cell oxyphilia; RCC, renal cell carcinoma; STAT3, signal transducer and activator of transcription 3; sh, short hairpin; Bcl, B-cell lymphoma protein, mcl-1, myeloid cell leukemia sequence 1; TAD, transactivation domain; S, serine; T, tyrosine; V, valine; Q, glutamic acid; D, aspartate; M, methionine; P, proline; K, lysine; N, asparagine; OLFM4, Olfactomedin 4; NF-κB, nuclear factor-κB; MMP, matrix metalloproteinase; u-PA, urokinase-type plasminogen activator; VEGF, vascular endothelial growth factor; CDK, cyclin-dependent kinase; INK, Inhibitor of CDK kinase; RB, retinoblastoma; SDH, succinate dehydrogenase; PGL, paragangliomas; HHV-8, human Herpesvirus-8; HPV, human Papillomavirus; HHV-6B, human Herpesvirus-6B; CMV, Cytomegalovirus; VV, Vaccinia virus; HIV-1, human Immunodeficiency virus-1; NOD2, Nucleotide-binding Oligomerization Domain containing 2.

* Corresponding author at: IPATIMUP, Rua Dr. Roberto Frias, S/N, 4200-465 Porto, Portugal. Tel.: +351 22 55 70 700; fax: +351 22 55 70 799.
E-mail address: vmaximo@ipatimup.pt (V. Máximo).

1567-7249/$ – see front matter © 2011 Elsevier B.V. and Mitochondria Research Society. All rights reserved.
doi:10.1016/j.mito.2011.05.011

Please cite this article as: Moreira, S., et al., GRIM-19 function in cancer development, Mitochondrion (2011), doi:10.1016/j.mito.2011.05.011

to characterize GRIM-19 protein showed that its overexpression induced apoptotic cell death in response to IFN-β/RA treatment, while GRIM-19 knock-down seemed to confer cell resistance to these factors. In this context, GRIM-19 inhibition confers some growth advantage. By immunofluorescence, GRIM-19 was shown to localize predominantly in the nucleus of transfected HeLa cells, although some punctate cytoplasmic staining could also be observed. In addition, a study by Chidambaram et al. (2000) described the localization of GRIM-19 to chromosome 19p13.2, a region crucial for prostate tumor suppression and with loss of heterozygosity in sporadic and familial forms of thyroid cancer (Prazeres et al., 2008; Stankov et al., 2004). Altogether, these results led the authors to propose that GRIM-19 could be a novel tumor suppressor.

Studies performed by different groups demonstrated that GRIM-19 is also a component of complex I of the mitochondrial respiratory chain (MRC), which is responsible for ATP production (Fearnley et al., 2001; Hu et al., 2002; Murray et al., 2003). Indeed, GRIM-19 is essential for early embryonic development in mice as demonstrated by genetic ablation experiments. Homologous deletion of the GRIM-19 gene resulted in embryonic lethality by day 9.5, partially due to oxidative phosphorylation (OXPHOS) failure (Huang et al., 2004). In addition, GRIM-19 knock-out blastocysts not only showed retarded growth *in vitro* but also exhibited abnormal mitochondrial structure, morphology and distribution. Careful analysis of GRIM-19 localization in several cell types indicated that this protein is mainly present in the mitochondria and that its elimination results in complex I disassembly and disruption of electron transfer (Huang et al., 2004). It is possible that this somewhat contradictory evidence regarding GRIM-19 localization within the cell may actually reflect different roles of this protein in cell biology (Maximo et al., 2008). It is now clear that GRIM-19 is a dual function gene that is involved in mitochondrial metabolism and IFN-β/RA-induced cell death. The involvement of mitochondria in cell death pathways may be the link between these functions (Maximo et al., 2008).

Although it is beyond the scope of the present review, it is important to stress that GRIM-19 appears also to participate in viral infection and innate immune response as its activity is modulated by several viruses and bacteria [for a thorough review see (Kalvakolanu et al., 2010)]. Briefly: the viral IFN regulatory factor 1 (vIRF1) from human Herpesvirus-8 (HHV-8) binds to GRIM-19 and blocks its ability to induce apoptosis (Seo et al., 2002); the human Papillomavirus (HPV) E6 protein of the high-risk strains, but not the low-risk strains, binds to GRIM-19 (Seo et al., 2002); the human Herpesvirus-6B (HHV-6B) U95 interacts with GRIM-19 (Yeo et al., 2008); the non-coding 2.7-kb viral RNA (β2.7) from Cytomegalovirus (CMV) interacts with GRIM-19 and regulates mitochondria induced cell death (Reeves et al., 2007); other viruses, such as Vaccinia virus (VV) and human Immunodeficiency virus-1 (HIV-1), appear to target GRIM-19 *via* different mechanisms (Guerra et al., 2003; Tripathy et al., 2010). These data suggest that GRIM-19 is a general target of viral proteins.

Furthermore, intra-cellular bacteria, such as *Salmonella typhimurium* and *Porphyromonas gingivalis*, appear also to regulate GRIM-19 expression (Barnich et al., 2005; Zhou and Amar, 2006). GRIM-19 has been shown to interact also with Nucleotide-binding Oligomerization Domain containing 2 (NOD2), suggesting that GRIM-19 may be a key component in NOD2-mediated innate mucosal response and serve to regulate cell responses to microbes (Barnich et al., 2005).

2. GRIM-19 gene mutations and loss of expression in tumors

The initial discovery of GRIM-19 as a growth suppressor in a genetic screen hinted that it could be a target for genetic inactivation events. This hint was supported by the finding of mutations in the coding region of the GRIM-19 gene in Hürthle cell thyroid carcinomas by our group (Maximo et al., 2005). Hürthle cell tumors' main feature is that they are formed by cells packed with abnormal mitochondria. Somatic missense mutations in the GRIM-19 gene were found in 3 out of 20 sporadic Hürthle cell carcinomas. In addition, 1 germline mutation in a Hürthle cell papillary carcinoma was identified in a thyroid with multiple Hürthle cell nodules. However, no mutations were detected in the 20 non-Hürthle cell tumors nor in the 96 blood samples analyzed (Table 1), strongly suggesting the involvement of GRIM-19 alterations in the etiopathogenesis of mitochondrion-rich thyroid tumors. Indeed, a previous report suggested that mutations in genes involved in mitochondrial function and consequently in cellular energy production could be responsible for the increase in mitochondrial number observed in Hürthle cell tumors (Katoh et al., 1998). This was proposed after the observation that a defect in the cells' energetic capacity can lead to a secondary increase in the number of mitochondria through a feedback mechanism (Attardi et al., 1995). Since GRIM-19 is an essential component of the MRC, it is possible that mutations in or deregulation of GRIM-19 protein is the reason for accumulation of mitochondria in these tumor cells, as a compensatory mechanism (Maximo et al., 2005). As the gene predisposing patients to thyroid tumors with cell oxyphilia (TCO) has been mapped to chromosome 19p13.2 (Canzian et al., 1998), the exact same location as that of the GRIM-19 gene, we hypothesized that GRIM-19 could be the TCO gene whose identity was unknown. However, the results obtained did not corroborate our hypothesis. Still, the mutations we have reported in the GRIM-19 gene remain the only nuclear gene mutations specific to Hürthle cell tumors identified to date.

In a study by Alchanati et al. (2006), the authors reported that GRIM-19 protein expression was lost or severely repressed in a number of primary renal cell carcinomas (RCC). Western blot analysis revealed that of the 11 clear cell RCCs analyzed, GRIM-19 protein expression was completely lost in 4, very weak in 6 and moderately decreased in 1 when compared with paired-normal tissue (Table 1). This finding was further supported by immunohistochemical experiments, which showed that GRIM-19 expression was completely absent in 27 of the 29 paraffin embedded RCC samples analyzed (20 of the clear cell type, 5 of the chromophobe type and 4 of the papillary type). The other 2 tumors exhibited weak positive staining (1 of the chromophobe type and the other of the clear cell type) when compared to the normal kidney tissue. Curiously, these results suggest that at least in RCCs, GRIM-19 alterations do not correlate with mitochondrion-enriched tumor cells. Studies performed by our group corroborate these observations (Fig. 1, unpublished results). GRIM-19 protein downregulation was linked with severe to complete loss of mRNA expression in tumors. Although very preliminary, the mRNA expression data together with the observation that GRIM-19 gene harbors no mutations in all cases analyzed but one (which had a conservative substitution) led the authors to suggest that GRIM-19 downregulation occurs at the transcriptional level (Alchanati et al., 2006). Analysis of GRIM-19 ablation in a RCC cell line revealed that cells electroporated with antisense GRIM-19 mRNA exhibited increased growth rates both *in vitro* and *in vivo*; this effect was at least in part, mediated by signal transducer and activator of transcription 3 (STAT3), as expression of STAT3-dependent genes was significantly increased (Alchanati et al., 2006).

More recently, various studies described loss or decrease in GRIM-19 protein expression in colorectal, prostate and cervical carcinomas. Gong et al. (2007) described that in 23 colorectal specimens analyzed, mRNA expression of GRIM-19 was clearly lower than in normal tissues. These observations were further corroborated by western blot and immunohistochemistry experiments, which also revealed an upregulation of STAT3 specifically in the carcinoma tissues (Table 1). Constitutive activation or overexpression of STAT3 has been detected in a variety of human tumors (Bromberg et al., 1999; Buettner et al., 2002, see later for further details). Zhang et al. (2008) demonstrated that GRIM-19 expression is also reduced in primary prostate cancer. By immunostaining, they found that GRIM-19 expression levels in primary prostate tumors were significantly lower than in normal prostate tissues. Interestingly, low GRIM-19 expression correlated

Please cite this article as: Moreira, S., et al., GRIM-19 function in cancer development, Mitochondrion (2011), doi:10.1016/j.mito.2011.05.011

Table 1
Summary of GRIM-19 alterations and correlation with STAT3 levels in various types of tumors.

Tumor type	Tumor subtype	GRIM-19		STAT3	
		Methodology	Result	Methodology	Result
Thyroid (Maximo et al., 2005)	Hürthle	PCR/sequencing (26 tumors)	4 mutations — 15.4%	RT-PCR for ICAM1* (in the 4 tumors with mutated GRIM-19)	Upregulated
	Non-Hürthle	PCR/sequencing (20 tumors)	No mutations — 0%	N/A	N/A
Kidney (renal cell carcinoma) (Alchanati et al., 2006)	Clear cell	WB (11 tumors)	Absent in 4, very weakly expressed in 6 and moderately expressed in 1	N/A	N/A
		RT-PCR (5 tumors)	Downregulated; 1 mutation		
		IHC (20 tumors)	Absent in 19 cases and weakly expressed in 1	N/A	N/A
	Chromophobe	IHC (5 tumors)	Absent in 4 and weakly expressed in 1	N/A	N/A
	Papillary	IHC (4 tumors)	Absent	N/A	N/A
Colorectal carcinoma (Gong et al., 2007)	N/S	RT-PCR/sequencing (23 tumors) and WB (40 tumors)	Downregulated; no mutations	WB (40 tumors)	Upregulated
		IHC (40 tumors)	Weakly expressed	IHC (40 tumors)	Strongly expressed
Prostate carcinoma (Zhang et al., 2008)	N/S	IHC (38 tumors)	Weakly expressed	IHC (38 tumors)	Strongly expressed
Cervical carcinoma (Zhou et al., 2009)	Squamous	RT-PCR and WB (20 tumors)	Downregulated	RT-PCR and WB (20 tumors)	Upregulated
		IHC (20 tumors)	Weakly expressed		

Note: comparisons were always made between tumor and normal tissue samples. IHC: immunohistochemistry; WB: western blot; N/A: not analyzed; N/S: not specified.
* STAT3 responsive gene.

with increased expression levels of STAT3, similar to the findings in colorectal carcinomas (Table 1). Because STAT3 and GRIM-19 have opposite effects on cell growth, the authors decided to investigate their functional roles both *in vitro* and *in vivo*. STAT3 inhibition by short hairpin (sh) RNA together with GRIM-19 overexpression in highly malignant PC-3M cells resulted in significant cell growth inhibition, which correlated with a decline in the expression levels of several STAT3-induced genes (Zhang et al., 2008). Using mouse xenograft models, the authors were able to verify that dual expression of shSTAT3 and GRIM-19 led to the development of tumors remarkably smaller than those on control animals. TUNEL assays, to determine the percentage apoptotic cells, showed that these small tumors had undergone massive apoptosis. In addition, it was also shown that dual expression of shSTAT3 and GRIM-19 was sufficient to block tumor metastasis into muscle or lymph nodes (Zhang et al., 2008). Analogous findings were described for primary cervical carcinomas, where GRIM-19 expression is also reduced and correlates with high basal levels of STAT3 and STAT3-target genes (Table 1) (Zhou et al., 2009). Through surrogate model experiments, it was demonstrated that restoring GRIM-19 levels produced robust tumor suppression, which was linked with suppressed expression of invasion and angiogenic factors. Overall, these studies undoubtedly demonstrate a major role for GRIM-19 in tumor suppression as GRIM-19 loss or decreased expression may correlate with growth advantage

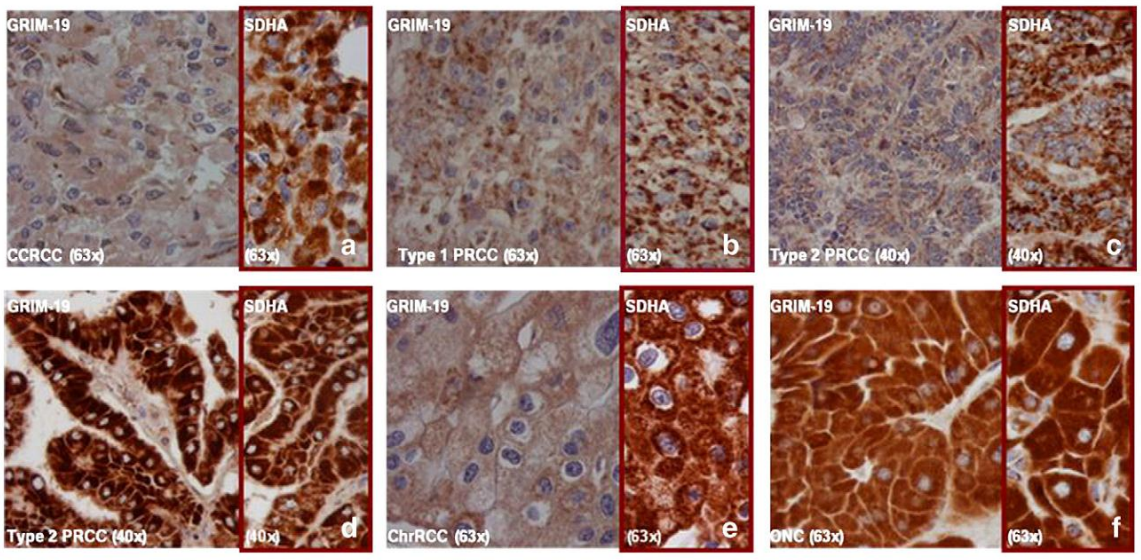

Fig. 1. GRIM-19 (a–f) and SDHA (a–f, inset) immunohistochemical analysis in RCC tumors. (a) Expression in a clear-cell RCC (CCRCC); (b, c and d) expression in type 1 and type 2 papillary RCCs (PRCC); (e) expression in a chromophobe RCC (ChrRCC) and (f) in a renal oncocytoma (Onc). It is clear a decrease in the expression levels of GRIM-19 protein when compared to SDHA. Magnification indicated in the figure.

Please cite this article as: Moreira, S., et al., GRIM-19 function in cancer development, Mitochondrion (2011), doi:10.1016/j.mito.2011.05.011

for cancer cells. Determining the extent to which this contributes to tumorigenesis requires further studies.

3. GRIM-19 interacting proteins and their roles in tumorigenesis

As mentioned previously, several studies strongly indicate that GRIM-19 loss or deregulation is advantageous to cancer development. Therefore, it is now relevant to consider the mechanisms underlying GRIM-19 function. To achieve this, we will discuss the proteins known to interact with GRIM-19 and their roles in tumorigenesis.

3.1. STAT3

GRIM-19 directly interacts with STAT3, inhibiting its gene stimulatory function (Lufei et al., 2003; Zhang et al., 2003). STAT3 is constitutively active in a number of human cancers either by autocrine growth factors or activated oncogenes (Buettner et al., 2002). Activated STAT3 induces the expression of a number of cellular proto-oncogenes, including c-myc, c-fos and c-met (Yang et al., 2005); cell cycle-regulating proteins, such as cyclin D1, cyclin B1 and CDK1/cdc2 (Bromberg et al., 1999); and anti-apoptotic proteins, such as B-cell lymphoma protein 2 (Bcl-2), myeloid cell leukemia sequence 1 (mcl-1) and Bcl-X_L (Buettner et al., 2002). All of these are known to promote tumor growth. Zhang et al. (2003) showed that STAT3 bound to GRIM-19 in unstimulated cells and that the amount of STAT3 coimmunoprecipitated with GRIM-19 increased after IFN-β/RA treatment. Remarkably, this interaction is restricted to STAT3, as experiments performed failed to detect any interaction between GRIM-19 and STAT1, STAT2 or STAT5, despite their abundant expression in the cells used. The authors further demonstrate that GRIM-19 inhibited STAT3-induced gene expression, but not its activation or ability to bind to DNA. By mutation analysis, the authors were able to map the transactivation domain (TAD) as the region on STAT3 targeted by GRIM-19, and that phosphorylation of a serine residue at position 727 (S727), within the TAD, was essential for binding. Considering the known role of activated STAT3 in tumor growth, it is tempting to predict that GRIM19 inhibition of STAT3 is anti-oncogenic. Another study, by Lufei et al. (2003), also found that GRIM-19 bound to STAT3 inhibiting it. However, the authors propose that such inhibition of STAT3 occurs by impeding its translocation to the nucleus. It remains to be clarified exactly how GRIM-19 inhibits STAT3 function.

Later, two studies by Kalakonda et al. (2007a, 2007b), explored in more detail the tumor suppressive role of GRIM-19 through interaction with STAT3. In one of these studies, the authors examined GRIM-19 function in the presence of constitutively active STAT3 (Kalakonda et al., 2007b). Chronic tyrosyl phosphorylation of STAT3, rendering the protein constitutively active, is sufficient to induce oncogenic transformation and has been described in a number of human tumors and tumor cell lines (Bromberg et al., 1999; Buettner et al., 2002). The authors showed that GRIM-19 counteracted constitutive STAT3-induced cellular transformation and suppressed the expression of genes involved in cell proliferation (Kalakonda et al., 2007b). In the other study, it was shown that GRIM-19 was able to suppress src-induced cellular transformation (Kalakonda et al., 2007a). The src family of tyrosine kinases is known to control several cellular activities, including motility and invasion (Martin, 2001). Moreover, src was the first proto-oncogene to be described in the vertebrate genome (Martin, 2001). In the presence of GRIM-19, the number of src-transformed soft-agar colonies was significantly decreased and these were much smaller as well. GRIM-19 was also able to inhibit src-induced cell motility and growth *in vitro*, and tumor formation *in vivo*. The authors demonstrated that GRIM-19 inhibition of src-induced cellular transformation was mediated by downregulation of a number of STAT3-dependent genes. However, not all of the GRIM-19 effects observed were dependent on STAT3, as GRIM-19 inhibition of src-induced phosphorylation of cellular proteins still occurred even when STAT3 was knocked-down. Actually, Sun et al. (2009) demonstrate that GRIM-19 dramatically suppresses src-induced tyrosyl phosphorylation of cortactin, an F-actin-bundling protein that localizes to podosomes and lamellipodia, which may explain the suppressive role of GRIM-19 on src-induced cell motility (Sun et al., 2009). These studies highlight that GRIM-19 function as a tumor suppressor seems to occur at multiple levels and that the mechanisms underlying these are still far from clear.

Interestingly, it was also reported that STAT3 regulates a metabolic function in the mitochondria as a modulator of mitochondrial respiration (Wegrzyn et al., 2009). It was observed that STAT3 was present in the mitochondria of cultured cells and primary tissues, although in a smaller amount than in the cytosol. Importantly, mitochondrial STAT3 was shown to regulate complexes I and II, as the activities of these were significantly decreased in STAT3 knock-out cells. These roles were dependent on STAT3 targeting to mitochondria and phosphorylation of S727, but had no relationship with its classical function in the nucleus (Wegrzyn et al., 2009). Another study showed that this mitochondrial STAT3 is also essential for Ras-induced cellular transformation (Gough et al., 2009). Expression of oncogenic Ras (H-RasV12) conferred to cells the ability to grow into colonies in soft-agar, which was impaired without STAT3. Noticeably, STAT3 function was dependent on S727 but not on phosphorylation of a tyrosine residue at position 705 (T705) or DNA-binding domains. These results were also verified for the other members of the Ras family, N and K-Ras. Mitochondrial STAT3 was also essential for tumor growth *in vivo* and seemed to be involved in the metabolic shift (Warburg effect) characteristic of cancer cells.

Recently, another study brought new insights into how GRIM-19 restrains cell growth via STAT3 inhibition (Nallar et al., 2010). It was found that a motif in the N terminus of GRIM-19 protein was essential for its function as a tumor suppressor. This motif is formed by the four amino acids glutamic acid, aspartate, methionine and proline (QDMP) and exhibits structural similarities with some viral RNA proteins. Point mutations in the DMP residues strongly impaired the ability of GRIM-19 to suppress colony formation in soft-agar in comparison to the wild-type protein. Mutation in the Q residue also caused loss of the ability to suppress anchorage-independent growth, but the results were not as dramatic as those obtained with the other mutants. In addition, it was previously reported that GRIM-19 inhibits cell motility (Kalakonda et al., 2007a), a very prominent feature of cancer cells that is required for metastasis. However, all mutants lost the ability to suppress cell motility as assessed by wound-healing assays in which a scratch-wound is made in a confluent cell monolayer. It was also demonstrated that, unlike the wild-type protein, these mutants were incapable of restraining cell growth. These results clearly reveal that the tumor suppressive function of GRIM-19 occurs in different cellular processes. Furthermore, the results obtained with the mutants cannot be explained by altered localization of these within the cells, since immunofluorescence and cell fractionation experiments revealed that they were present in the nucleus, mitochondria and cytoplasm just like the wild-type protein. Remarkably, a tumor-derived mutation in the N terminus, which was previously described by our group (Maximo et al., 2005) and results in a lysine to asparagine substitution at residue 5 (K5N), also led to the failure of GRIM-19 to inhibit colony formation in soft-agar and limit cell growth (Nallar et al., 2010). The *in vitro* data was further supported by *in vivo* experiments in which it was shown that mutant-expressing tumors grew significantly faster than those expressing the empty vector or wild-type GRIM-19. To explore in more detail the mechanisms on the basis of the observations for the mutant proteins, the authors analyzed their ability to suppress STAT3-dependent gene expression. As expected, while the wild-type protein clearly inhibited the expression of STAT3-responsive genes, this anti-STAT3 activity was dramatically reduced in some of the mutants. This anti-STAT3 activity was determined not only through real-time PCR and reporter gene assays but also by expressing a constitutively active STAT3 in cells and then evaluating the effect of the mutants in STAT3- induced gene expression. The authors performed an additional experiment where the effect of the

Please cite this article as: Moreira, S., et al., GRIM-19 function in cancer development, Mitochondrion (2011), doi:10.1016/j.mito.2011.05.011

selected mutants was assessed on cellular transformation induced by src, a known STAT3 activator. As anticipated, the mutant lacking the N-terminus completely lost the anti-transforming activity observed with wild-type GRIM-19. Immunoprecipitation experiments demonstrated that this loss was due to their inability to interact with STAT3.

3.2. GW112 (or Olfactomedin 4, OLFM4)

A protein previously found to be overexpressed in tumors of the digestive system – GW112 – has been shown to interact with GRIM-19 reducing its ability to mediate apoptotic cell death (Zhang et al., 2004). It was shown that GW112/OLFM4 is expressed at relatively low levels in normal tissues, including prostate, colon, breast and pancreas. However, its expression was dramatically higher in pancreatic, stomach and colon cancer tissues. Gene reporter experiments revealed that GW112/OLFM4 localized mainly in the cytoplasm but some foci could be observed also in the nucleus. Interestingly, most of the cytoplasmic GW112/OLFM4 colocalized with a mitochondrial marker. Since GW112/OLFM4 was found to interact with GRIM19 in yeast two-hybrid assay, the authors then explored its role in induced apoptotic cell death. Indeed, GW112/OLFM4 overexpression was sufficient to reduce hydrogen peroxide and IFN-β/RA-induced apoptosis and apoptotic gene expression. They also demonstrated that overexpression of GW112/OLFM4 was capable of promoting tumor growth *in vivo*, as assessed by injecting mice with slow growing TRAMP-C1 prostate cancer cells expressing GW112/OLFM4 or control vector. These results were further corroborated by another study that compared GW112/OLFM4 mRNA expression levels in colon, breast and lung cancer tissues with those of matched non-cancerous tissue (Koshida et al., 2007). Sample comparison uncovered that GW112/OLFM4 mRNA levels were increased in 90%, 68.8% and 84.6% of the cases analyzed for colon, breast and lung cancer tissues, respectively. For colon and breast cancer tissues, high mRNA GW112/OLFM4 expression levels were present even in the early stages of disease. In the case of lung specimens, it was shown that GW112/OLFM4 levels were significantly higher in squamous cell carcinomas than in adenocarcinomas. *In vitro* experiments showed that in SBC-1 lung cancer cells, GW112/OLFM4 knock-down by siRNA dramatically decreased their growth capacity.

A recent study explored more carefully the link between GRIM-19 and GW112/OLFM4, and their effects on tumor cell invasion and metastasis (Huang et al., 2010). In human gastric cancer SGC-7901 cells, GRIM-19 upregulation suppressed the expression of GW112/OLFM4 and decreased nuclear factor-κB (NF-κB) binding activity. NF-κB was previously shown to bind to the GW112/OLFM4 promoter and to regulate its expression (Chin et al., 2008). In the study by Huang et al. (2010), *in vitro* assays revealed that when GRIM-19 was upregulated, the cells' ability to adhere to Matrigel was significantly decreased. Additionally, the number of migratory cells as well as of those with the ability to invade through Matrigel and a membrane in a Matrigel-coated invasion chamber was decreased as well. Metastatic assays in nude mice clearly demonstrated that SGC-7901 cells overexpressing GRIM-19 gave rise to fewer visible liver metastases than those expressing the control vector. As cell invasion and metastasis are dependent on the cells' capacity to degrade extracellular matrix, the authors analyzed the effect of GRIM-19 in the expression of matrix metalloproteinase (MMP)-2, MMP-9, urokinase-type plasminogen activator (u-PA) and vascular endothelial growth factor (VEGF), which are known to mediate this process (Hooper et al., 2005; Jin et al., 2007; Pahl, 1999). The authors observed that when GRIM-19 was upregulated, the cells secreted less MMP-2, MMP-9, u-PA and VEGF, leading them to propose that the inhibitory effect of GRIM-19 in gastric cancer metastasis is, at least in part, achieved through downregulation of these proteins.

It is worth to mention that in PANC-1 cells, OLFM4 expression was found to be especially elevated during early S phase of the cell cycle (Kobayashi et al., 2007). OLFM4 seems to be particularly important for G2/M transition and thus has a direct effect on the cells' ability to proliferate. Notably, OLFM4 inhibition by siRNA led only to a small increase in apoptosis, which is considerably different from what was observed in STAT3 knock-down experiments. Thus, OLFM4 interplay with GRIM-19 may be STAT3-independent (Kalvakolanu et al., 2010).

3.3. $p16^{Ink4a}$

Using a proteomic analysis, Sun et al. (2010) discovered that GRIM-19 also interacts with the cell cycle inhibitor CDKN2A ($p16^{Ink4a}$). P16 is a tumor suppressor, and mutations in its gene sequence or epigenetic repression of its expression have been described in a number of tumors (Ruas and Peters, 1998). CDK activity can be blocked by CDK inhibitors, which fall within the two protein families Kip/Cip and Inhibitor of CDK kinase (INK). The INK4 family is composed of four proteins p15, p16, p18 and p19, which have been shown to interact with CDK4/6 in order to suppress cyclin-dependent phosphorylation of the retinoblastoma (RB) protein (Ruas and Peters, 1998; Sherr and Roberts, 1995). RB is a very well characterized tumor suppressor and is known to inhibit the expression of proliferation-associated genes through binding to the transcription factor E2F1 (Dyson, 1998). Using MCF-7 cells, which lack endogenous p16, the authors showed that exogenous p16 expression led to significant repression of genes required in S-phase (Sun et al., 2010). This seems to occur because p16 prevents cyclin D1 association with CDK4 and subsequent expression of E2F1-responsive genes. Indeed, in the presence of GRIM-19, the association of p16 with CDK4 was high and caused a decrease in cyclin D1-bound CDK4. This effect was reverted by GRIM-19 depletion. Importantly, GRIM-19 and p16 coexpression synergistically suppressed E2F1-dependent gene expression resulting in cell cycle arrest. The physiological relevance of this interaction is further corroborated by *in vivo* experiments where p16 and GRIM-19 coexpression resulted in a dramatic reduction of tumor size. However, as expression of GRIM-19 alone suppressed E2F1-driven transcription, it is possible that GRIM-19 is a novel E2F1 inhibitor. Nonetheless, the mechanism underlying this inhibition is yet to be defined. It was unclear to date how genetic alterations in the fourth ankyrin-like repeat of p16 identified in various tumor types were responsible for its inactivation (Ruas and Peters, 1998). In this study, the authors showed that deletion of the fourth ankyrin-like repeat or introduction of clinically observed mutations, abolished p16 interaction with GRIM-19 and its ability to synergistically repress E2F1-driven transcription and tumor growth. This was the first report to identify a function for GRIM-19 in cell cycle control and to propose a functional interaction between two unrelated tumor suppressors.

4. Are we in the presence of a paradox?

The studies described above indicate that GRIM-19 loss or deregulation provides growth advantage to cancer cells. However, it is also known that GRIM-19 is a component of complex I and that its deletion results in embryonic lethality. Therefore, how do tumor cells survive? This apparent paradox can be explained by the so-called Warburg effect. In the 50s, Otto Warburg discovered that tumor cells undergo a metabolic shift from aerobic respiration, which relies on OXPHOS, to aerobic glycolysis, even in the presence of oxygen (Warburg, 1956). Among the metabolic changes reported in tumor cells were upregulation of glycolytic enzymes, downregulation of OXPHOS components and upregulation of glucose transporters in the plasma membrane (Gatenby and Gillies, 2004; Hsu and Sabatini, 2008). The shift to aerobic glycolysis leads to the generation of lactic acid and pyruvate and it is known that the pH of the microenvironment in a number of tumors is highly acidic (Gatenby and Gillies, 2004).

The Warburg effect has been demonstrated in several studies and is considered a hallmark feature of cancer cells (Vander Heiden et al., 2009). Some evidence suggests that tumor suppressor genes may contribute to this effect; moreover, an increasing number of studies describe mutations in enzymes involved in the Krebs cycle and

Please cite this article as: Moreira, S., et al., GRIM-19 function in cancer development, Mitochondrion (2011), doi:10.1016/j.mito.2011.05.011

OXPHOS in human tumors (DeBerardinis, 2008; Gatenby and Gillies, 2004; Maximo et al., 2009). For instance, previous studies by our group have identified somatic and germline mutations in complex I genes that have been associated with malignant thyroid tumors (Maximo et al., 2002). Also, loss of function mutations in the Krebs cycle and OXPHOS enzyme succinate dehydrogenase (SDH) were reported in sporadic and hereditary forms of paragangliomas (PGL) (Baysal et al., 2000; Lima et al., 2007). Mutations in a different enzyme of the Krebs cycle, fumarate hydratase, were described in RCC, uterine fibroids and hereditary leiomyomatosis (Tomlinson et al., 2002). Despite the fact that the Warburg effect has been described decades ago and being such a prominent feature of tumor cells, the molecular mechanisms underlying it as well as its putative interest in cancer therapy still remain to be explored.

5. Conclusion

The initial discovery of GRIM-19 as a growth suppressor raised the hypothesis that it could be a target for oncogenic events. The studies performed to date fit with this initial assumption but the picture concerning the role of GRIM-19 and/or GRIM-19-dependent pathways in the context of malignant transformation is still very incomplete. To the best of our knowledge, there is only one published study directly assessing GRIM-19 function in induced oncogenic transformation (Kalakonda et al., 2007a). In this study, the authors investigated whether GRIM-19 expression would be sufficient for reverting cellular transformation induced by src. The experiments performed strongly support that GRIM-19 suppresses src-induced transformation *in vitro* and *in vivo* by downregulating STAT3-dependent genes (Kalakonda et al., 2007a). Additionally, the data obtained from *in vivo* experiments makes it tempting to speculate that GRIM-19 may be a novel therapy target. For instance, it has been shown that coexpression of GRIM-19 with STAT3-specific shRNA synergistically suppressed prostate tumor growth and metastasis in mice injected with PC-3M cells (Zhang et al., 2008). Just recently, it was reported that targeted delivery of GRIM-19 into the cytoplasm of cells with constitutively active STAT3, resulted in a significant reduction of STAT3-dependent transcription *in vitro* (Okamoto et al., 2010). This targeting was achieved through the use of a protein carrier called nona-arginine (R9)-protein transduction domain (R9-PTD) fused with GRIM-19 (rR9–GRIM-19). In addition to the *in vitro* observations, it was also shown that intratumoral injections of rR9-GRIM-19 in mice dramatically inhibited the growth of tumors produced by constitutively active STAT3. Although preliminary, these results are encouraging as they reinforce the hypothesis that GRIM-19 can become a therapeutic target. As we began to fully understand GRIM-19 function in carcinogenesis, we may get closer to transferring the results obtained in the lab into the clinic.

References

Alchanati, I., Nallar, S.C., Sun, P., Gao, L., Hu, J., Stein, A., Yakirevich, E., Konforty, D., Alroy, I., Zhao, X., Reddy, S.P., Resnick, M.B., Kalvakolanu, D.V., 2006. A proteomic analysis reveals the loss of expression of the cell death regulatory gene GRIM-19 in human renal cell carcinomas. Oncogene 25, 7138–7147.

Altucci, L., Gronemeyer, H., 2001. The promise of retinoids to fight against cancer. Nat. Rev. Cancer 1, 181–193.

Angell, J.E., Lindner, D.J., Shapiro, P.S., Hofmann, E.R., Kalvakolanu, D.V., 2000. Identification of GRIM-19, a novel cell death-regulatory gene induced by the interferon-beta and retinoic acid combination, using a genetic approach. J. Biol. Chem. 275, 33416–33426.

Attardi, G., Yoneda, M., Chomyn, A., 1995. Complementation and segregation behavior of disease-causing mitochondrial DNA mutations in cellular model systems. Biochim. Biophys. Acta 1271, 241–248.

Barnich, N., Hisamatsu, T., Aguirre, J.E., Xavier, R., Reinecker, H.C., Podolsky, D.K., 2005. GRIM-19 interacts with nucleotide oligomerization domain 2 and serves as downstream effector of anti-bacterial function in intestinal epithelial cells. J. Biol. Chem. 280, 19021–19026.

Baysal, B.E., Ferrell, R.E., Willett-Brozick, J.E., Lawrence, E.C., Myssiorek, D., Bosch, A., van der Mey, A., Taschner, P.E., Rubinstein, W.S., Myers, E.N., Richard 3rd, C.W., Cornelisse, C.J., Devilee, P., Devlin, B., 2000. Mutations in SDHD, a mitochondrial complex II gene, in hereditary paraganglioma. Science 287, 848–851.

Bromberg, J.F., Wrzeszczynska, M.H., Devgan, G., Zhao, Y., Pestell, R.G., Albanese, C., Darnell, J.E., 1999. Stat3 as an oncogene. Cell 98, 295–303.

Buettner, R., Mora, L.B., Jove, R., 2002. Activated STAT signaling in human tumors provides novel molecular targets for therapeutic intervention. Clin. Cancer Res. 8, 945–954.

Canzian, F., Amati, P., Harach, H.R., Kraimps, J.L., Lesueur, F., Barbier, J., Levillain, P., Romeo, G., Bonneau, D., 1998. A gene predisposing to familial thyroid tumors with cell oxyphilia maps to chromosome 19p13.2. Am. J. Hum. Genet. 63, 1743–1748.

Chidambaram, N.V., Angell, J.E., Ling, W., Hofmann, E.R., Kalvakolanu, D.V., 2000. Chromosomal localization of human GRIM-19, a novel IFN-beta and retinoic acid-activated regulator of cell death. J. Interferon Cytokine Res. 20, 661–665.

Chin, K.L., Aerbajinai, W., Zhu, J., Drew, L., Chen, L., Liu, W., Rodgers, G.P., 2008. The regulation of OLFM4 expression in myeloid precursor cells relies on NF-kappaB transcription factor. Br. J. Haematol. 143, 421–432.

DeBerardinis, R.J., 2008. Is cancer a disease of abnormal cellular metabolism? New angles on an old idea. Genet. Med. 10, 767–777.

Dyson, N., 1998. The regulation of E2F by pRB-family proteins. Genes Dev. 12, 2245–2262.

Fearnley, I.M., Carroll, J., Shannon, R.J., Runswick, M.J., Walker, J.E., Hirst, J., 2001. GRIM-19, a cell death regulatory gene product, is a subunit of bovine mitochondrial NADH: ubiquinone oxidoreductase (complex I). J. Biol. Chem. 276, 38345–38348.

Gatenby, R.A., Gillies, R.J., 2004. Why do cancers have high aerobic glycolysis? Nat. Rev. Cancer 4, 891–899.

Gong, L.B., Luo, X.L., Liu, S.Y., Tao, D.D., Gong, J.P., Hu, J.B., 2007. Correlations of GRIM-19 and its target gene product STAT3 to malignancy of human colorectal carcinoma. Ai Zheng 26, 683–687.

Gough, D.J., Corlett, A., Schlessinger, K., Wegrzyn, J., Larner, A.C., Levy, D.E., 2009. Mitochondrial STAT3 supports Ras-dependent oncogenic transformation. Science 324, 1713–1716.

Gresser, I., Belardelli, F., 2002. Endogenous type I interferons as a defense against tumors. Cytokine Growth Factor Rev. 13, 111–118.

Guerra, S., Lopez-Fernandez, L.A., Pascual-Montano, A., Munoz, M., Harshman, K., Esteban, M., 2003. Cellular gene expression survey of vaccinia virus infection of human HeLa cells. J. Virol. 77, 6493–6506.

Hooper, A.T., Akiri, G., Jin, D., Shmelkov, S.V., Chuang, E., Shin, S.J., Wu, Y., Hicklin, D.J., Rafii, S., Vahdat, L.T., 2005. VEGF receptor expression on reactive breast cancer stroma: paving the way for tumor invasion. ASCO Meeting Abstracts, 23, p. 9642.

Hsu, P.P., Sabatini, D.M., 2008. Cancer cell metabolism: Warburg and beyond. Cell 134, 703–707.

Hu, J., Angell, J.E., Zhang, J., Ma, X., Seo, T., Raha, A., Hayashi, J., Choe, J., Kalvakolanu, D.V., 2002. Characterization of monoclonal antibodies against GRIM-19, a novel IFN-beta and retinoic acid-activated regulator of cell death. J. Interferon Cytokine Res. 22, 1017–1026.

Huang, G., Lu, H., Hao, A., Ng, D.C.H., Ponniah, S., Guo, K., Lufei, C., Zeng, Q., Cao, X., 2004. GRIM-19, a cell death regulatory protein, is essential for assembly and function of mitochondrial complex I. Mol. Cell. Biol. 24, 8447–8456.

Huang, Y., Yang, M., Yang, H., Zeng, Z., 2010. Upregulation of the GRIM-19 gene suppresses invasion and metastasis of human gastric cancer SGC-7901 cell line. Exp. Cell Res. 316, 2061–2070.

Ikeda, H., Old, L.J., Schreiber, R.D., 2002. The roles of IFN gamma in protection against tumor development and cancer immunoediting. Cytokine Growth Factor Rev. 13, 95–109.

Jin, H., Pan, Y., He, L., Zhai, H., Li, X., Zhao, L., Sun, L., Liu, J., Hong, L., Song, J., Xie, H., Gao, J., Han, S., Li, Y., Fan, D., 2007. p75 neurotrophin receptor inhibits invasion and metastasis of gastric cancer. Mol. Cancer Res. 5, 423–433. doi:10.1158/1541-7786.MCR-06-0407.

Kalakonda, S., Nallar, S.C., Gong, P., Lindner, D.J., Goldblum, S.E., Reddy, S.P., Kalvakolanu, D.V., 2007a. Tumor suppressive protein gene associated with retinoid-interferon-induced mortality (GRIM)-19 inhibits src-induced oncogenic transformation at multiple levels. Am. J. Pathol. 171, 1352–1368.

Kalakonda, S., Nallar, S.C., Lindner, D.J., Hu, J., Reddy, S.P., Kalvakolanu, D.V., 2007b. Tumor-suppressive activity of the cell death activator GRIM-19 on a constitutively active signal transducer and activator of transcription 3. Cancer Res. 67, 6212–6220.

Kalvakolanu, D.V., Nallar, S.C., Kalakonda, S., 2010. Cytokine-induced tumor suppressors: a GRIM story. Cytokine 52, 128–142.

Katoh, R., Harach, H.R., Williams, E.D., 1998. Solitary, multiple, and familial oxyphil tumours of the thyroid gland. J. Pathol. 186, 292–299.

Kobayashi, D., Koshida, S., Moriai, R., Tsuji, N., Watanabe, N., 2007. Olfactomedin 4 promotes S-phase transition in proliferation of pancreatic cancer cells. Cancer Sci. 98, 334–340.

Koshida, S., Kobayashi, D., Moriai, R., Tsuji, N., Watanabe, N., 2007. Specific overexpression of OLFM4(GW112/HGC-1) mRNA in colon, breast and lung cancer tissues detected using quantitative analysis. Cancer Sci. 98, 315–320.

Lima, J., Feijao, T., Ferreira da Silva, A., Pereira-Castro, I., Fernandez-Ballester, G., Maximo, V., Herrero, A., Serrano, L., Sobrinho-Simoes, M., Garcia-Rostan, G., 2007. High frequency of germline succinate dehydrogenase mutations in sporadic cervical paragangliomas in northern Spain: mitochondrial succinate dehydrogenase structure–function relationships and clinical–pathological correlations. J. Clin. Endocrinol. Metab. 92, 4853–4864.

Lufei, C., Ma, J., Huang, G., Zhang, T., Novotny-Diermayr, V., Ong, C.T., Cao, X., 2003. GRIM-19, a death-regulatory gene product, suppresses Stat3 activity via functional interaction. EMBO J. 22, 1325–1335.

Martin, G.S., 2001. The hunting of the Src. Nat. Rev. Mol. Cell Biol. 2, 467–475.

Maximo, V., Soares, P., Lima, J., Cameselle-Teijeiro, J., Sobrinho-Simoes, M., 2002. Mitochondrial DNA somatic mutations (point mutations and large deletions) and mitochondrial DNA variants in human thyroid pathology: a study with emphasis on Hurthle cell tumors. Am. J. Pathol. 160, 1857–1865.

Please cite this article as: Moreira, S., et al., GRIM-19 function in cancer development, Mitochondrion (2011), doi:10.1016/j.mito.2011.05.011

Maximo, V., Botelho, T., Capela, J., Soares, P., Lima, J., Taveira, A., Amaro, T., Barbosa, A.P., Preto, A., Harach, H.R., Williams, D., Sobrinho-Simoes, M., 2005. Somatic and germline mutation in GRIM-19, a dual function gene involved in mitochondrial metabolism and cell death, is linked to mitochondrion-rich (Hurthle cell) tumours of the thyroid. Br. J. Cancer 92, 1892–1898.

Maximo, V., Lima, J., Soares, P., Silva, A., Bento, I., Sobrinho-Simoes, M., 2008. GRIM-19 in health and disease. Adv. Anat. Pathol. 15, 46–53.

Maximo, V., Lima, J., Soares, P., Sobrinho-Simoes, M., 2009. Mitochondria and cancer. Virchows Arch. 454, 481–495.

Murray, J., Zhang, B., Taylor, S.W., Oglesbee, D., Fahy, E., Marusich, M.F., Ghosh, S.S., Capaldi, R.A., 2003. The subunit composition of the human NADH dehydrogenase obtained by rapid one-step immunopurification. J. Biol. Chem. 278, 13619–13622.

Nallar, S.C., Kalakonda, S., Sun, P., Ohmori, Y., Hiroi, M., Mori, K., Lindner, D.J., Kalvakolanu, D.V., 2010. Identification of a structural motif in the tumor-suppressive protein GRIM-19 required for its antitumor activity. Am. J. Pathol. 177, 896–907.

Okamoto, T., Inozume, T., Mitsui, H., Kanzaki, M., Harada, K., Shibagaki, N., Shimada, S., 2010. Overexpression of GRIM-19 in cancer cells suppresses STAT3-mediated signal transduction and cancer growth. Mol. Cancer Ther. 9, 2333–2343.

Pahl, H.L., 1999. Activators and target genes of Rel/NF-kappaB transcription factors. Oncogene 18, 6853–6866.

Prazeres, H., Rodrigues, F., Soares, P., Naidenov, P., Figueiredo, P., Campos, B., Lacerda, M., Martins, T., 2008. Loss of heterozygosity at 19p13.2 and 2q21 in tumours from familial clusters of non-medullary thyroid carcinoma. Fam. Cancer 7, 141–149.

Reeves, M.B., Davies, A.A., McSharry, B.P., Wilkinson, G.W., Sinclair, J.H., 2007. Complex I binding by a virally encoded RNA regulates mitochondria-induced cell death. Science 316, 1345–1348.

Ruas, M., Peters, G., 1998. The p16INK4a/CDKN2A tumor suppressor and its relatives. Biochim. Biophys. Acta 1378, F115–F177.

Seo, T., Lee, D., Shim, Y.S., Angell, J.E., Chidambaram, N.V., Kalvakolanu, D.V., Choe, J., 2002. Viral interferon regulatory factor 1 of Kaposi's sarcoma-associated herpes-virus interacts with a cell death regulator, GRIM19, and inhibits interferon/retinoic acid-induced cell death. J. Virol. 76, 8797–8807.

Sherr, C.J., Roberts, J.M., 1995. Inhibitors of mammalian G1 cyclin-dependent kinases. Genes Dev. 9, 1149–1163.

Stankov, K., Pastore, A., Toschi, L., McKay, J., Lesueur, F., Kraimps, J., Bonneau, D., Gibelin, H., Levillain, P., Volante, M., Papotti, M., Romeo, G., 2004. Allelic loss on chromosomes 2q21 and 19p 13.2 in oxyphilic thyroid tumors. Int. J. Cancer 111, 463–467.

Sun, P., Nallar, S.C., Kalakonda, S., Lindner, D.J., Martin, S.S., Kalvakolanu, D.V., 2009. GRIM-19 inhibits v-Src-induced cell motility by interfering with cytoskeletal restructuring. Oncogene 28, 1339–1347.

Sun, P., Nallar, S.C., Raha, A., Kalakonda, S., Velalar, C.N., Reddy, S.P., Kalvakolanu, D.V., 2010. GRIM-19 and p16INK4a synergistically regulate cell cycle progression and E2F1-responsive gene expression. J. Biol. Chem. 285, 27545–27552.

Tomlinson, I.P., Alam, N.A., Rowan, A.J., Barclay, E., Jaeger, E.E., Kelsell, D., Leigh, I., Gorman, P., Lamlum, H., Rahman, S., Roylance, R.R., Olpin, S., Bevan, S., Barker, K., Hearle, N., Houlston, R.S., Kiuru, M., Lehtonen, R., Karhu, A., Vilkki, S., Laiho, P., Eklund, C., Vierimaa, O., Aittomaki, K., Hietala, M., Sistonen, P., Paetau, A., Salovaara, R., Herva, R., Launonen, V., Aaltonen, L.A., 2002. Germline mutations in FH predispose to dominantly inherited uterine fibroids, skin leiomyomata and papillary renal cell cancer. Nat. Genet. 30, 406–410.

Tripathy, M.K., Ahmed, Z., Ladha, J.S., Mitra, D., 2010. The cell death regulator GRIM-19 is involved in HIV-1 induced T-cell apoptosis. Apoptosis 15, 1453–1460.

Vander Heiden, M.G., Cantley, L.C., Thompson, C.B., 2009. Understanding the Warburg effect: the metabolic requirements of cell proliferation. Science 324, 1029–1033.

Warburg, O., 1956. On the origin of cancer cells. Science 123, 309–314.

Wegrzyn, J., Potla, R., Chwae, Y.-J., Sepuri, N.B.V., Zhang, Q., Koeck, T., Derecka, M., Szczepanek, K., Szelag, M., Gornicka, A., Moh, A., Moghaddas, S., Chen, Q., Bobbili, S., Cichy, J., Dulak, J., Baker, D.P., Wolfman, A., Stuehr, D., Hassan, M.O., Fu, X.-Y., Avadhani, N., Drake, J.I., Fawcett, P., Lesnefsky, E.J., Larner, A.C., 2009. Function of mitochondrial Stat3 in cellular respiration. Science 323, 793–797.

Yang, J., Chatterjee-Kishore, M., Staugaitis, S.M., Nguyen, H., Schlessinger, K., Levy, D.E., Stark, G.R., 2005. Novel roles of unphosphorylated STAT3 in oncogenesis and transcriptional regulation. Cancer Res. 65, 939–947.

Yeo, W.M., Isegawa, Y., Chow, V.T., 2008. The U95 protein of human herpesvirus 6B interacts with human GRIM-19: silencing of U95 expression reduces viral load and abrogates loss of mitochondrial membrane potential. J. Virol. 82, 1011–1020.

Zhang, J., Yang, J., Roy, S.K., Tininini, S., Hu, J., Bromberg, J.F., Poli, V., Stark, G.R., Kalvakolanu, D.V., 2003. The cell death regulator GRIM-19 is an inhibitor of signal transducer and activator of transcription 3. PNAS 100, 9342–9347.

Zhang, X., Huang, Q., Yang, Z., Li, Y., Li, C.-Y., 2004. GW112, a novel antiapoptotic protein that promotes tumor growth. Cancer Res. 64, 2474–2481.

Zhang, L., Gao, L., Li, Y., Lin, G., Shao, Y., Ji, K., Yu, H., Hu, J., Kalvakolanu, D.V., Kopecko, D.J., Zhao, X., Xu, D.-Q., 2008. Effects of plasmid-based Stat3-specific short hairpin RNA and GRIM-19 on PC-3M tumor cell growth. Clin. Cancer Res. 14, 559–568.

Zhou, Q., Amar, S., 2006. Identification of proteins differentially expressed in human monocytes exposed to *Porphyromonas gingivalis* and its purified components by high-throughput immunoblotting. Infect. Immun. 74, 1204–1214.

Zhou, Y., Li, M., Wei, Y., Feng, D., Peng, C., Weng, H., Ma, Y., Bao, L., Nallar, S., Kalakonda, S., Xiao, W., Kalvakolanu, D.V., Ling, B., 2009. Down-regulation of GRIM-19 expression is associated with hyperactivation of STAT3-induced gene expression and tumor growth in human cervical cancers. J. Interferon Cytokine Res. 29, 695–703.

Please cite this article as: Moreira, S., et al., GRIM-19 function in cancer development, Mitochondrion (2011), doi:10.1016/j.mito.2011.05.011